



DIONE PEREIRA CARDOSO

**RAINFALL EROSIVITY ESTIMATION VIA SEVERAL
METHODS, AND WATER EROSION MODELING AT PEIXE
ANGICAL RESERVOIR-TO**

LAVRAS - MG

2021

DIONE PEREIRA CARDOSO

**RAINFALL EROSIVITY ESTIMATION VIA SEVERAL METHODS, AND WATER
EROSION MODELING AT PEIXE ANGICAL RESERVOIR-TO**

Thesis presented to the Federal University of Lavras, as part of the requirements of the Postgraduate Program in Soil Science, area of concentration in Environmental Resources and Land Use, to obtain the title of Doctor.

Prof. Dr. Junior Cesar Avanzi

Advisor

Prof. Ph.D. Nilton Curi

Co-advisor

LAVRAS - MG

2021

**Ficha catalográfica elaborada pelo Sistema de Geração de Ficha Catalográfica da Biblioteca
Universitária da UFLA, com dados informados pelo(a) próprio(a) autor(a).**

Cardoso, Dione Pereira.

Rainfall erosivity estimation via several methods, and water erosion modeling at Peixe Angical Reservoir-TO / Dione Pereira

Cardoso. - 2021.

105 p. : il.

Orientador(a): Junior Cesar Avanzi.

Coorientador(a): Nilton Curi.

Tese (doutorado) - Universidade Federal de Lavras, 2021.

Bibliografia.

1. Rainfall erosivity. 2. Modified Fournier. 3. Soil losses. I. Avanzi, Junior Cesar. II. Curi, Nilton. III. Título.

DIONE PEREIRA CARDOSO

**RAINFALL EROSIVITY ESTIMATION VIA SEVERAL METHODS, AND WATER
EROSION MODELING AT PEIXE ANGICAL RESERVOIR-TO**

Thesis presented to the Federal University of Lavras, as part of the requirements of the Postgraduate Program in Soil Science, area of concentration in Environmental Resources and Land Use, to obtain the title of Doctor.

APPROVED in 30 April 2021.

Dr. Fábio Ribeiro Pires	CEUNES/UFES
Dr. Ronaldo Luiz Mincato	ICN/UNIFAL
Ph.D. Salvador Francisco Acuña Guzman	DFI/UFLA
Dr. Marx Leandro Naves Silva	DCS/UFLA

Dr. Junior Cesar Avanzi
Advisor

LAVRAS - MG

2021

*À minha querida mãe, Elvira Pereira Cardoso,
e avó, Luzia Pereira de Carvalho (in memoriam).*

DEDICO

A Deus,
OFEREÇO

AGRADECIMENTOS

A *DEUS*, o criador da vida e dos recursos naturais.

“Tudo posso naquele que me fortalece.” (Fp 4:13)

O presente trabalho foi realizado com apoio da Coordenação de Aperfeiçoamento de Pessoal de Nível Superior – Brasil (CAPES) – Código de Financiamento 001. E as agências de fomento Conselho Nacional de Desenvolvimento Científico e Tecnológico (CNPq) e Fundação de Amparo à Pesquisa do Estado de Minas Gerais (Fapemig) pelo apoio financeiro nos projetos de pesquisa. Ao apoio técnico da Agência Nacional de Águas e Saneamento Básico (ANA), ao Instituto Nacional de Meteorologia (INMET), ao Banco de Dados Meteorológico do INMET (BDMEP), ao Centro Nacional de Monitoramento e Alertas de Desastres Naturais (CEMADEN), ao Projeto de Mapeamento Anual da Cobertura e Uso do Solo no Brasil (MapBiomass), a Enerpeixe S.A., a Embrapa, unidade Solos, e unidade Pesca e Aquicultura.

A banca examinadora, aos professores Dr. Fábio Ribeiro Pires, Dr. Marx Leandro Naves Silva, Dr. Ronaldo Luiz Mincato e Ph.D. Salvador Francisco Acuña Guzman pela disponibilidade na avaliação desse trabalho. Aos suplentes Dr. Marcelo Ribeiro Viola e Dr. Eduardo da Costa Severiano. Ao orientador Dr. Junior Cesar Avanzi e coorientador Ph.D. Nilton Curi pela orientação, correções, sugestões para realização desse trabalho. Aos demais autores dos artigos dessa tese, Dr. Edilson Marcelino Silva e MSc. Mariana Neves Merlo e aos professores Dr. Joel Augusto Muniz, Dr. Daniel Ferreira, Dr. Fausto Weimar Arcebi Júnior e Dr. Sérgio Henrique Godinho Silva.

Aos colegas da pós-graduação, em especial, aos amigos da Sala de Conservação Adnane Beniaich, Danielle Guimarães, Diego Amorim, Evens Robert, Fábio Avalos e Warley Santos, e também, da Fertilidade do Solo, a Patriciani Cipriano. Aos professores, laboratoristas e demais funcionários do Departamento de Ciência do Solo. Aqueles que direta ou indiretamente contribuíram para a realização desse trabalho. Aos amigos dos Programas de Pós-Graduação em Estatística (Edilson Silva e Henrique Alves), Engenharia Florestal (Bruna Almeida), Fitopatologia (Mário Colares) e Ciências Veterinárias (Mirian Braz).

Em especial, a dedicação da minha mãe Elvira, presente em todos os momentos. É meu alicerce e minha inspiração. O meu muito obrigada!

Obrigada a todos!

*“O Senhor é a minha força
e o meu escudo;
nele o meu coração confia,
nele fui socorrido;
por isso, o meu coração exulta,
e com o meu cântico o louvarei.”*

Sl. 28:7

RESUMO GERAL

O processo de erosão sofre modificações à medida que o uso da terra e a cobertura do solo se alteram por meio da conversão da floresta em pastagem e/ou em culturas agrícolas. Além da cobertura vegetal, outros fatores como a erosividade da chuva –que é o potencial da chuva em causar erosão–, são indispensáveis na modelagem da erosão. Esta tese foi dividida em capítulos, onde no primeiro capítulo foi desenvolvido o pacote *RainfallErosivityFactor* dentro da linguagem de programação R, e posteriormente disponibilizado no CRAN do R. Este pacote é uma ferramenta para analisar dados de chuva, como precipitação total, volume e número de chuvas erosivas e não erosivas e determinar a erosividade da chuva, tendo saídas mensais e anuais. Deste modo, o fator erosividade da chuva é calculado com exatidão e eficácia. Um exemplo foi fornecido para Pirassununga, SP, Brasil, usando um conjunto de dados de chuva de 7 anos com intervalo de 10 minutos entre as medições. Os resultados poderão ser processados no próprio ambiente R para análise estatística, construção de gráficos, ou aplicação de geostatística. A erosividade média da chuva para Pirassununga foi de $9.512,9 \text{ MJ mm ha}^{-1} \text{ h}^{-1} \text{ ano}^{-1}$. Diante do exposto, práticas conservacionistas devem ser adotadas para minimizar os impactos do processo erosivo. No segundo capítulo, o método de determinação da erosividade da chuva proposto por Wischmeier e Smith foi comparado com outros métodos utilizados em diversas partes do mundo para estimar a erosividade da chuva, visando selecionar um método consistente para substituir o método de Wischmeier e Smith para condições tropicais sem considerar a intensidade da chuva. Os métodos testados incluíram: Fournier modificado, MF; Fournier modificado por Zhang, MF-Z; Fournier modificado por Men, MF-M; Desagregação de chuva, RD; Satélite TRMM com coeficiente de Fournier modificado, TRMM-F; e Satélite TRMM com precipitação mensal, TRMM-M. As análises foram realizadas de acordo com o modelo *Additive Main Effects and Multiplicative Interaction* (AMMI) e testes de agrupamentos Scott-Knott. Os métodos avaliados se comportaram de forma diferente para os períodos chuvoso, seco, mensal e anual. O método MF mostrou-se capaz de substituir de forma consistente o método de Wischmeier e Smith. Destaca-se que os métodos baseados no satélite TRMM podem ser uma alternativa plausível para locais sem informações de precipitação. Finalmente, no terceiro capítulo, o objetivo foi modelar as perdas de solo na bacia de drenagem do reservatório do Peixe Angical, Brasil, além de avaliar o nível de importância dos fatores da RUSLE. Os valores de exportação de sedimentos também foram calculados para identificar áreas onde as práticas de conservação do solo eram necessárias. Para estimar as perdas de solo para o cenário cronológico de 1990, 2000, 2010 e 2017, o modelo RUSLE foi acoplado a ferramentas GIS. A avaliação do nível de importância de cada fator RUSLE foi realizada usando um algoritmo de aprendizado de máquina não paramétrico, Floresta Aleatória. O nível de importância dos fatores RUSLE foi avaliado na seguinte ordem: $C > K > LS > R$. A erosão hídrica na bacia de drenagem do reservatório Peixe Angical aumentou ao longo dos anos devido a mudanças no uso do solo, embora perdas de solo na maior parte da bacia foram classificadas como muito baixa ($< 2,5 \text{ Mg ha}^{-1} \text{ ano}^{-1}$). O impacto da mudança no uso do solo deve ser minimizado com práticas de conservação do solo, possibilitando o desenvolvimento sustentável.

Palavras-chave: Erosividade da chuva. Fournier Modificado. Desagregação de chuva. TRMM. Perdas de solo. Exportação de sedimentos.

GENERAL ABSTRACT

The erosion process undergoes changes as land use and land cover change through the conversion of the forest to pasture and / or agricultural crops. In addition to vegetation cover, other factors such as rainfall erosivity –which is the potential of rain to cause erosion– are indispensable in erosion modeling. This thesis was divided into chapters, where in the first chapter the package `RainfallErosivityFactor` was developed within the programming language R, and later made available on CRAN of R. This package is a tool to analyze rain data, such as total precipitation, depth and number of erosive and non-erosive rains, and to determine the rainfall erosivity, with monthly and annual outputs. In this way, the rainfall erosivity factor is calculated accurately and effectively. An example was provided for Pirassununga, SP, Brazil, using a 7-year rainfall data set with an interval of 10 minutes between measurements. The results can be processed in the R environment itself for statistical analysis, construction of graphs, or application of geostatistics. The average rainfall erosivity for Pirassununga was $9,512.9 \text{ MJ mm ha}^{-1} \text{ h}^{-1} \text{ year}^{-1}$. In view of the above, conservationist practices must be adopted to minimize the impacts of the erosion process. In the second chapter, the method of determining rainfall erosivity proposed by Wischmeier and Smith was compared with other methods used in different parts of the world to estimate rainfall erosivity, in order to select a consistent method to replace the Wischmeier and Smith method for conditions without considering the intensity of the rain. The tested methods included: Modified Fournier, MF; Modified Fournier by Zhang, MF-Z; Modified Fournier by Men, MF-M; Rainfall Disaggregation, RD; TRMM satellite with modified Fournier coefficient, TRMM-F; and TRMM Satellite with monthly precipitation, TRMM-M. The analyzes were performed according to the Additive Main Effects and Multiplicative Interaction (AMMI) model and Scott-Knott cluster tests. The evaluated methods behaved differently for the rainy, dry, monthly and annual periods. The MF method proved to be able to consistently replace the Wischmeier and Smith method. It is emphasized that the methods based on the TRMM satellite can be a plausible alternative for locations without precipitation information. Finally, in the third chapter, the objective was to model soil losses in the drainage basin of the Peixe Angical Reservoir, Brazil, in addition to assessing the level of importance of the RUSLE factors. The sediment export values were also calculated to identify areas where soil conservation practices were needed. To estimate soil losses for the 1990, 2000, 2010 and 2017 chronological scenario, the RUSLE model was coupled with GIS. The evaluation of the level of importance of each RUSLE factor was carried out using a non-parametric machine learning algorithm, Random Forest. The level of importance of the RUSLE factors was assessed in the following order: C > K > LS > R. Water erosion in the drainage basin of the Peixe Angical Reservoir has increased over the years due to changes in land use, although soil losses in most of the basin were classified as very low ($<2.5 \text{ Mg ha}^{-1} \text{ year}^{-1}$). The impact of change in land use must be minimized with soil conservation practices, enabling sustainable development.

Keywords: Rainfall erosivity. Modified Fournier. Rainfall Disaggregation. TRMM. Soil losses. Sediment export.

LIST OF FIGURES

Article I

- Fig. 1.** Location of Pirassununga, State of São Paulo, Brazil. 30
- Fig. 2.** Minimum, average, and maximum values for: (a) rainfall, mm; (b) amount of erosive rainfall, mm; (c) amount of non-erosive rainfall, mm; and (d) rainfall erosivity, $\text{MJ mm ha}^{-1} \text{h}^{-1} \text{month}^{-1}$ 32

Article II

- Fig. 1.** Location map of the municipality of Pirassununga, in the State of São Paulo, Brazil. 46
- Fig. 2.** Map of co-occurrence network referring to rainfall erosivity, based on the Scopus survey (02/12/2020), and elaborated in VOSviewer. 47
- Fig. 3.** Average monthly rainfall amount of erosive events, and average number of erosive rains, from 2009 to 2015, at Pirassununga, State of São Paulo, Brazil. 50
- Fig. 4.** Rasters referring to monthly average rainfall data (from 2009 to 2015) extracted the TRMM satellite, for Pirassununga, State of São Paulo, Brazil. 52
- Fig. 5.** Comparison between standard (WS) and other estimated rainfall erosivity (EI_{30}) methods. WS: Wischmeier and Smith; MF: modified Fournier; MF-Z: modified Fournier by Zhang; MF-M: modified Fournier by Men; RD: Rainfall Disaggregation; TRMM-F: TRMM-M Satellite. 56
- Fig. 6.** The univariate grouping of methods of estimation of the monthly rainfall erosivity indexes (January to June), by Scott and Knott (1974), with a Chi-squared significance level of 5%. 59
- Fig. 7.** The univariate grouping of methods for estimation of the monthly rainfall erosivity indexes (July to December), by Scott and Knott (1974), with a Chi-squared significance level of 5%. 61
- Fig. 8.** The univariate grouping of methods for estimation of the rainfall erosivity (R Factor), by Scott and Knott (1974), with a Chi-squared significance level of 5%. 63

Article III

- Fig. 1.** Location of the Peixe Angical Reservoir drainage basin (PARDB). 73
- Fig. 2.** Digital Elevation Model (a), and slope steepness categories (%) of the Tocantins River upstream from Peixe Angical Reservoir drainage basin (PARDB). 74

Fig. 3. Location of the gauging station inside and around the Peixe Angical Reservoir drainage basin (PARDB).....	75
Fig. 4. Annual average rainfall erosivity ($\text{MJ mm ha}^{-1} \text{ h}^{-1} \text{ yr}^{-1}$) from 1990 to 2017 in the Peixe Angical Reservoir drainage basin (PARDB).....	83
Fig. 5. Soil classes distribution in the Peixe Angical Reservoir drainage basin (PARDB).	84
Fig. 6. Spatial distribution of topographic factor - LS (dimensionless) in the Peixe Angical Reservoir drainage basin (PARDB).	85
Fig. 7. Map of land use for the Peixe Angical Reservoir drainage basin (PARDB) in the years of 1990, 2000, 2010, and 217. (Adapted from MapBiomias).	86
Fig. 8. Map of soil loss rate ($\text{Mg ha}^{-1} \text{ yr}^{-1}$) for the Peixe Angical Reservoir drainage basin (PARDB) in the years of 1990, 2000, 2010, and 2017.....	88
Fig. 9. Identification of explanatory variables of soil losses by Random Forest algorithm. Factors C and K were assessed as the most important variables for soil loss prediction using RUSLE at the Peixe Angical Reservoir drainage basin (PARDB) in the years of 1990, 2000, 2010, and 2017.	90
Fig. 10. Spatial distribution of exported sediments ($\text{Mg ha}^{-1} \text{ year}^{-1}$) and percentage classification for the Peixe Angical Reservoir drainage basin (PARDB).	92

LIST OF TABLES

Article I

Table 1. Monthly rainfall, erosive rainfall, and rainfall erosivity obtained through the RainfallErosivityFactor package, for Pirassununga, SP, Brazil. (continue...)	34
--	----

Article II

Table 1. Adjusted equations, coefficients of determination, critical points, and rainfall erosivity indexes (EI_{30} , $MJ\ mm\ ha^{-1}\ h^{-1}$) corresponding to critical point for the evaluated methods	55
--	----

Table 2. Percentages of the sum of total squares (methods x months) associated to each main axis, being the individual and accumulated values according to AMMI analysis for the standard method (WS) and the other methods (MF, MF-Z, MF-M, RD, TRMM-F, and TRMM-M) use to estimate the rainfall erosivity of Pirassununga-SP	57
---	----

Table 3. Summary of the analysis of variance and mean squares associated with the effect of the interaction between methods and months, referring to the rainfall erosivity of Pirassununga-SP	58
---	----

Article III

Table 1. Soil classification according to the FAO-World Reference Base (WRB) and the Brazilian Soil Classification System (SiBCS), their respective geographical expression within the Peixe Angical Reservoir drainage basin (PARDB), and soil erodibility factor values	77
--	----

Table 2. Land use and the respective values for the C factor	78
---	----

Table 3. The input data, format, variation, spatial resolution (m) and references used in the InVEST SDR model, version 3.8.2	81
--	----

Table 4. Change in the percentage of erosion risk classes from 1990 to 2000, from 2000 to 2010, and from 2010 to 2017, which corresponds to the complete chronological scenario, in a time span of 28 years	89
--	----

LIST OF ABBREVIATIONS

Article I

Ec = Kinetic Energy

EI₃₀ = Rainfall Erosivity Index

R-factor = Rainfall Erosivity factor

Article II

Cemaden = Centre for Monitoring and Early Warnings of Natural Disasters

MF = Modified Fournier

MF-M = Modified Fournier by Men

MF-Z = Modified Fournier by Zhang

RD = Rainfall Disaggregation

TRMM-F = TRMM Satellite with Modified Fournier Coefficient

TRMM-M = TRMM Satellite with Monthly Rainfall

WS = Standard Model

Article III

A = Annual Soil Loss

C = Cover Management

e = Code referring to soil structure

IC = Index of Connectivity

K = Soil Erodibility

K factor = Soil Erodibility factor

LS factor = Topographic factor

LS= Slope length and steepness

M = Percentage of modified silt, *i.e.*, percentage of silt plus very fine sand

MSE_{OOB} = Mean squared error

OOB = Methodology out-of-bag

p = Code referring to soil permeability

P = Support practices

R = Rainfall Erosivity

R factor = Rainfall Erosivity factor

Var_{ex} = Explained variance percent

LIST OF ACRONYMS

Article I

CLIGEN = Stochastic Weather Generator

CRAN = Comprehensive R Archive Network

GIS = Geographic Information System

GPL = General Public License

RIST = Rainfall Intensity Summarization Tool

RUSLE = Revised Universal Soil Loss Equation

RUSLE2 = Revised Universal Soil Loss Equation2

USLE = Universal Soil Loss Equation

USPWS = University of São Paulo Weather Station

WEPP = Water Erosion Prediction Project

WERM = Web Erosivity Module

Article II

AMMI = Additive Main effects and Multiplicative Interaction

ANA = National Water and Sanitation Agency

EI₃₀ = Rainfall erosivity index

INMET = National Institute of Meteorology

MSDE = Mean Squared Deviation Error

PCA = Principal Component Analysis

RMSE = Root Mean Square Error

TRMM = Tropical Rainfall Measurement Mission

USLE = Universal Soil Loss Equation

USP = University of São Paulo

Article III

ANA = National Water and Sanitation Agency

DEM = Digital Elevation Model

GIS = Geographic Information System

HPP = Hydroelectric Power Plant

InVEST = Integrated Valuation of Ecosystem Services and Tradeoffs

PARDB = Peixe Angical Reservoir Drainage Basin

Rc = Rainfall Coefficient

RF = Random Forest

RUSLE = Revised Universal Soil Loss Equation

SAGA = System for Automated Geoscientific Analyses

SDR = Sediment Delivery Rate

SI = International System of Units

SiBCS = Brazilian Soil Classification System

SRTM = Shuttle Radar Topography Mission

USDA = United States Department of Agriculture

WRB = World Reference Base

SUMMARY

RESUMO GERAL	8
GENERAL ABSTRACT	9
FIRST PART	19
1 INTRODUÇÃO GERAL	19
REFERÊNCIAS	22
SECOND PART – Articles	26
Article I - RainfallErosivityFactor: An R package for rainfall erosivity (R-factor) determination	26
Abstract	26
1. Introduction	26
2. Methods	28
2.1. <i>Structure of the package RainfallErosivityFactor</i>	28
2.2. <i>Documentation of the package RainfallErosivityFactor</i>	28
2.3 <i>Version of the software R</i>	29
2.4. <i>Use of the package RainfallErosivityFactor for scientific research</i>	29
2.4.1. <i>Site description</i>	29
2.4.2. <i>Source and characteristics of the rainfall data</i>	31
3. Results	31
3.1. <i>Package performance</i>	31
3.2. <i>Weather station from Pirassununga</i>	31
4. Discussion	33
4.1 <i>Rainfall erosivity</i>	33
4.2. <i>Comparison with other programs</i>	36
4.3. <i>Limitations of R factor</i>	37
4.4. <i>Landscape scale application</i>	37
5. Conclusions	38
References	38
Article II - Rainfall Erosivity Estimation: A comparison and statistical assessment among methods using data from Southeastern Brazil	43
Abstract	43
1. Introduction	43
2. Materials and Methods	45
2.1. <i>Characterization of the study area</i>	45
2.2. <i>Methods for determining rainfall erosivity</i>	46
2.2.1. <i>Wischmeier and Smith, WS</i>	47

2.3. <i>Methods estimating rainfall erosivity</i>	48
2.3.1. <i>Modified Fournier Index, MF</i>	48
2.3.2. <i>Modified Fournier by Zhang, MF-Z</i>	48
2.3.3. <i>Modified Fournier by Men, MF-M</i>	49
2.3.4. <i>Rainfall Disaggregation, RD</i>	49
2.3.5. <i>TRMM Satellite with modified Fournier coefficient, TRMM-F</i>	51
2.3.6. <i>TRMM Satellite with monthly rainfall, TRMM-M</i>	53
2.4. <i>Statistical assessment of the methods</i>	53
3. Results	54
3.1. <i>Rainfall Erosivity Estimations</i>	54
3.2. <i>Statistical Comparion of Methods</i>	57
4. Discussion	63
5. Conclusions	65
References	66
Article III - Machine Learning Assessment of the Soil Erosion Modeling using RUSLE: A case study in a sub-basin on the Upper Tocantins River, Brazil	70
Abstract	70
1. Introduction	70
2. Materials and Methods	72
2.1. <i>Study area</i>	72
2.2. <i>RUSLE Model</i>	74
2.2.1. <i>Rainfall erosivity factor (R factor)</i>	74
2.2.2. <i>Soil erodibility factor (K factor)</i>	76
2.2.3. <i>Topographic factor (LS factor)</i>	78
2.2.4. <i>Cover management factor (C factor)</i>	78
2.2.5. <i>Support practices factor (P factor)</i>	79
2.3. <i>Soil losses</i>	79
2.4. <i>Level of importance of each RUSLE factor</i>	79
2.5. <i>Sediment analysis</i>	80
2.5.1. <i>Sediment Delivery Ratio (SDR)</i>	80
2.5.2. <i>Sediment Export</i>	82
2.6. <i>Calibration and Validation of the models</i>	82
3. Results	83
3.1. <i>Soil erosion factors</i>	83
3.2. <i>Soil loss potential</i>	87
3.3. <i>Analysis of soil erosion risk</i>	88

3.4. <i>Evaluation of the R, K, LS, and C factors, through Random Forest</i>	89
3.5. <i>Sediment export</i>	91
4. Discussion	92
5. Conclusions	96
References	96
APPENDICES	103

FIRST PART

1 INTRODUÇÃO GERAL

O uso e ocupação do solo, quando realizada de maneira inadequada, contribui para aceleração da degradação do solo. Esta é ocasionada pela erosão que é um problema mundial, com consequências não desejadas ao meio ambiente, afetando também a sociedade e o setor econômico. O processo de erosão do solo é modificado pelo ambiente biofísico composto por clima, solo, relevo, cobertura do solo e a interação entre eles (GANASRI; RAMESH, 2016). Nas condições tropicais, como no Brasil, os efeitos negativos relacionados aos solos são impulsionados pelo impacto da chuva sobre a superfície, desagregando o solo e propiciando o escoamento superficial, ou seja, a erosão hídrica do solo. De acordo com Chen et al. (2021), a erosividade da chuva descreve o efeito de várias características da chuva como duração, quantidade e intensidade. E isto, corresponde ao índice de erosividade (EI_{30}) que é o produto da energia cinética das chuvas e a intensidade máxima contínua de 30 minutos no evento de chuvas (WISCHMEIER; SMITH, 1978). A forma atual como se determina a erosividade da chuva torna o desempenho da pesquisa mais trabalhoso e, conseqüentemente, a modelagem da erosão hídrica e/ou a distribuição espacial e temporal da erosividade tem sido menos reportado do que poderia. Portanto, desenvolver um programa ou pacote eficiente nessa questão, tornou-se de suma importância para obter um resultado rápido e com exatidão.

Por causa da alta variabilidade temporal e espacial da erosividade da chuva, registros precisos com longas séries de dados são requeridos (ANGULO-MARTÍNEZ; BEGUERÍA, 2009), bem como dados com alta resolução temporal, que são informações presentes em estações instaladas em várias partes do mundo. Por isso, a estimativa da erosividade por métodos com aplicação de baixa resolução temporal, como dados anuais, mensais, diários e horários, tornou-se uma alternativa viável para substituir os métodos de determinação com dados de alta resolução temporal (WISCHMEIER; SMITH, 1965, 1978; RENARD et al., 1997; McCOOL et al., 2004), que utilizam dados sub-horários no cálculo da energia cinética.

Com a escassez de dados de pluviógrafos, ou estações automatizadas com alta resolução temporal, restringe-se a determinação da erosividade da chuva, por isso, avaliar e selecionar um método confiável estatisticamente para estimar este fator torna-se essencial nos estudos de conservação do solo. Como nem sempre há dados de precipitação de alta resolução, alternativas para estimar a erosividade da chuva precisam ser melhor analisadas. Deste modo, alguns métodos de estimativa da erosividade foram testados (com resolução horária, mensais e anuais), utilizando os dados de precipitação disponíveis do município de Pirassununga-SP para,

futuramente, embasar a estimativa da erosividade para outras localidades tropicais, como na bacia de Peixe Angical-TO, nos estados do TO, GO e DF, Brasil.

A modelagem da erosão é de suma importância para mitigar os efeitos negativos do processo erosivo sobre os recursos naturais, como o solo e a água, sendo uma das etapas utilizadas para a identificação dos pontos críticos de erosão e o planejamento conservacionista visando a proteção do solo (BEZAK et al., 2021). Quanto maior o grau de severidade destes pontos, mais prioritárias estas áreas serão para a conservação do solo, visando sua redução das perdas de solo para níveis toleráveis. A intervenção antrópica é necessária para o desenvolvimento do País, desde que o uso do solo seja de acordo com sua capacidade de exploração. Assim, a implementação das melhores técnicas de manejo e conservação do solo e da água deve ser analisada, independentemente de ser área protegida por lei ou não.

Devido à importância deste tema, vários pesquisadores têm contribuído para o aprimoramento do estudo sobre a modelagem da erosão hídrica, mediante informações mais detalhadas a respeito dos programas aplicados para estimativa das perdas de solo (BATISTA et al., 2019; BEZAK et al., 2021; BORRELLI et al., 2021; PANDEY et al., 2021). Dos modelos para predição das perdas de solo, têm-se a *Universal Soil Loss Equation*, USLE (WISCHMEIER; SMITH, 1965, 1978) e suas versões revisadas, RUSLE (RENARD et al., 1997) e RUSLE2 (McCOOL et al., 2004). Recentemente, estes modelos têm sido acoplado para valoração dos serviços ecossistêmicos, citando o modelo *Integrated Valuation of Ecosystem Services and Tradeoffs*, InVEST (SHARP et al., 2020), sendo o componente *Sediment Delivery Ratio* – SDR (HAMEL et al., 2015), utilizado para estimar a produção de sedimentos em uma bacia hidrográfica.

Dentre estes, o modelo Revised Universal Soil Loss Equation – RUSLE, desenvolvido nos Estados Unidos (RENARD et al., 1997), tem sido amplamente aplicado no Brasil para os biomas Amazônia (CRUZ et al., 2019), Cerrado (GALDINO et al., 2016; BATISTA et al., 2017; CUNHA; BACANI; PANACHUKI, 2017; GOMES et al., 2017; SALIS; COSTA; VIANA, 2019), Mata Atlântica (OLIVEIRA; VIEIRA, 2017) e Pampa (STEINMETZ et al., 2018; NACHTIGALL et al., 2020). E também, em outros países como Índia (GANASRI; RAMESH, 2016), Etiópia (GELAGAY; MINALE, 2016), Malásia (VIJITH; HURMAIN; DODGE-WAN, 2018), Etiópia (ZERIHUN et al., 2018) e Sri Lanka (FAYAS et al., 2019), entre outros. No entanto, este modelo não estima a taxa de entrega de sedimento, *Sediment Delivery Ratio*-SDR, informação necessária para analisar a quantidade que realmente atinge os cursos de água. O InVEST SDR, com relatos de aplicação em países como Tunísia, Sri Lanka, China e Etiópia (BOUGUERRA; JEBARI, 2017; DIAS et al., 2019; ZHOU et al., 2019;

ANESEYEE et al., 2020). De acordo com Morgan e Nearing (2011), estudar todos os locais da superfície terrestre não é viável, por isso, ferramentas de avaliação e predição precisam ser aplicadas para avaliar os problemas atuais, prever tendências futuras e fornece uma base científica para decisões de política e de gestão. Os modelos de erosão podem cumprir esta função, desde que usados corretamente e sejam robustos (MORGAN; NEARING, 2011). Deste modo, o modelo RUSLE foi selecionado para modelagem das perdas de solo na bacia de Peixe Angical. Além do modelo InVEST SDR para estimativa da taxa de entrega de sedimentos pela bacia.

Os modelos de perdas de solo necessitam de uma avaliação quanto as suas incertezas, de acordo com Batista et al. (2019) há diversas formas de avaliar estes modelos conforme a escala e finalidade da aplicação, como por imagens aéreas de alta resolução utilizada na avaliação qualitativa e semiquantitativa. No entanto, a avaliação visual não é válida para a taxa de transporte de sedimentos (BATISTA et al., 2021). Nesse caso, torna-se necessário a comparação entre dados observados e preditos. Uma vez que, a estimativa da exportação de sedimentos é o produto da perda de solo pela taxa de entrega de sedimentos. Neste sentido, presume-se que a avaliação das incertezas da exportação de sedimentos seja suficiente para verificar a eficiência de toda a modelagem da erosão, desde as perdas de solo até a taxa de entrega de sedimentos.

No primeiro artigo, os objetivos foram desenvolver um pacote no ambiente R para determinar a erosividade da chuva a partir de dados sub-horários. O pacote foi desenvolvido e encontra-se disponível para *download* desde novembro de 2018, com o nome RainfallErosivityFactor. Este pacote tem como resultados os valores de erosividade da chuva mensal, anual e a média do período, também, a precipitação total, volume e número de chuvas (erosivas e não erosivas) mensal e anual. Para validar o pacote utilizou-se um banco de dados abertos referente ao município de Pirassununga-SP.

No segundo artigo, visto que, nem sempre os dados sub-horários estão disponíveis, o objetivo foi selecionar um método alternativo ao considerado padrão, Wischmeier e Smith, visando uma substituição em caso de ausência de dados sub-horários. Para isso foi aplicado a técnica *Additive Main Effects and Multiplicative Interaction* (AMMI) para avaliar a interação entre métodos e meses. Quando a interação foi significativa aplicou-se o agrupamento Scott-Knott, o qual visou verificar, qual método foi estatisticamente semelhante ao método padrão.

No terceiro artigo, os objetivos foram estimar as perdas de solo e sedimentos exportados pela bacia de drenagem do reservatório de Peixe Angical, localizada nos estados de Tocantins, Goiás e Distrito Federal. Após estimar as perdas de solo, esta foi classificada como

muito baixa a extremamente alta, sendo um parâmetro para definir as áreas prioridades para conservação do solo, contribuindo para tomada de decisões quanto ao planejamento da aplicação das práticas conservacionistas. Além disso, verificar entre os fatores do modelo RUSLE –fatores R, K, LS e C–, aquele de maior importância para a modelagem da erosão hídrica. A bacia do reservatório de Peixe Angical está inserida no bioma Cerrado, o qual vem sofrendo intensas modificações de uso. Assim, a avaliação dos recursos ambientais, analisando o passado e o presente, de uma sequência cronológica (1990, 2000, 2010 e 2017) e o futuro, tornam-se essenciais para o monitoramento da bacia de Peixe Angical, propiciando a qualidade e quantidade dos seus recursos hídricos.

REFERÊNCIAS

- ANESEYEE, A. B.; ELIAS, E.; SOROMESSA, T.; FEYISA, G. L. Land use/land cover change effect on soil erosion and sediment delivery in the Winike watershed, Omo Gibe Basin, Ethiopia. **Science of the Total Environment**, Amsterdam, v. 728, n. 138776, p. 1–16, Aug 2020. doi: 10.1016/j.scitotenv.2020.138776.
- ANGULO-MARTÍNEZ, M.; BEGUERÍA, S. Estimating rainfall erosivity from daily precipitation records: A comparison among methods using data from the Ebro Basin (NE Spain). **Journal of Hydrology**, Amsterdam, v. 379, n. 1–2, p. 111–121, Dec 2009. doi: 10.1016/j.jhydrol.2009.09.051.
- BATISTA, P. V. G.; DAVIES, J.; SILVA, M. L. N.; QUINTON, J. N. On the evaluation of soil erosion models: Are we doing enough? **Earth-Science Reviews**, Amsterdam, v. 197, p. 102898, Oct 2019. doi: 10.1016/j.earscirev.2019.102898.
- BATISTA, P. V. G.; LACEBY, J. P.; DAVIES, J.; CARVALHO, T. S.; TASSINARI, D.; SILVA, M. L. N.; CURTI, N.; QUINTON, J. N. A framework for testing large-scale distributed soil erosion and sediment delivery models: Dealing with uncertainty in models and the observational data. **Environmental Modelling and Software**, Oxford, v. 137, p. 104961, Mar 2021. doi: 10.1016/j.envsoft.2021.104961.
- BATISTA, P. V. G.; SILVA, M. L. N.; SILVA, B. P. C.; CURTI, N.; BUENO, I. T.; JÚNIOR, F. W. A.; DAVIES, J.; QUINTON, J. Modelling spatially distributed soil losses and sediment yield in the upper Grande River Basin - Brazil. **Catena**, Amsterdam, v. 157, p. 139–150, Oct 2017. doi: 10.1016/j.catena.2017.05.025.
- BEZAK, N.; MIKOŠ, M.; BORRELLI, P.; ALEWELL, C.; ALVAREZ, P.; AYACH ANACHE, J. A.; BAARTMAN, J.; BALLABIO, C.; BIDDOCCU, M.; CERDÀ, A.; CHALISE, D.; CHEN, S.; CHEN, W.; DE GIROLAMO, A. M.; GESSESSE, G. D.; DEUMLICH, D.; DIODATO, N.; EFTHIMIOU, N.; ERPUL, G.; FIENER, P.; FREPPAZ, M.; GENTILE, F.; GERICKE, A.; HAREGEWEYN, N.; HU, B.; JEANNEAU, A.; KAFFAS, K.; KIANI-HARCHEGANI, M.; VILLUENDAS, I. L.; LI, C.; LOMBARDO, L.; LÓPEZ-VICENTE, M.; LUCAS-BORJA, M. E.; MÄRKER, M.; MIAO, C.; MODUGNO, S.; MÖLLER, M.; NAIPAL, V.; NEARING, M.; OWUSU, S.; PANDAY, D.; PATAULT, E.; PATRICHE, C. V.; POGGIO, L.; PORTES, R.; QUIJANO, L.; RAHDARI, M. R.; RENIMA, M.; RICCI, G. F.; RODRIGO-COMINO, J.; SAIA, S.; SAMANI, A. N.;

- SCHILLACI, C.; SYRRIS, V.; KIM, H. S.; SPINOLA, D. N.; OLIVEIRA, P. T.; TENG, H.; THAPA, R.; VANTAS, K.; VIEIRA, D.; YANG, J. E.; YIN, S.; ZEMA, D. A.; ZHAO, G.; PANAGOS, P. Soil erosion modelling: A bibliometric analysis. **Environmental Research**, San Diego, v. 197, p. 111087, Jun 2021. doi: 10.1016/j.envres.2021.111087.
- BORRELLI, P.; ALEWELL, C.; ALVAREZ, P.; ANACHE, J. A. A.; BAARTMAN, J.; BALLABIO, C.; BEZAK, N.; BIDDOCCU, M.; CERDÀ, A.; CHALISE, D.; CHEN, S.; CHEN, W.; DE GIROLAMO, A. M.; GESSESSE, G. D.; DEUMLICH, D.; DIODATO, N.; EFTHIMIOU, N.; ERPUL, G.; FIENER, P.; FREPPAZ, M.; GENTILE, F.; GERICKE, A.; HAREGEWEYN, N.; HU, B.; JEANNEAU, A.; KAFFAS, K.; KIANI-HARCHEGANI, M.; VILLUENDAS, I. L.; LI, C.; LOMBARDO, L.; LÓPEZ-VICENTE, M.; LUCAS-BORJA, M. E.; MÄRKER, M.; MATTHEWS, F.; MIAO, C.; MIKOŠ, M.; MODUGNO, S.; MÖLLER, M.; NAIPAL, V.; NEARING, M.; OWUSU, S.; PANDAY, D.; PATAULT, E.; PATRICHE, C. V.; POGGIO, L.; PORTES, R.; QUIJANO, L.; RAHDARI, M. R.; RENIMA, M.; RICCI, G. F.; RODRIGO-COMINO, J.; SAIA, S.; SAMANI, A. N.; SCHILLACI, C.; SYRRIS, V.; KIM, H. S.; SPINOLA, D. N.; OLIVEIRA, P. T.; TENG, H.; THAPA, R.; VANTAS, K.; VIEIRA, D.; YANG, J. E.; YIN, S.; ZEMA, D. A.; ZHAO, G.; PANAGOS, P. Soil erosion modelling: A global review and statistical analysis. **Science of the Total Environment**, Amsterdam, v. 780, p. 146494, Aug 2021. doi: 10.1016/j.scitotenv.2021.146494.
- BOUGUERRA, S.; JEBARI, S. Identification and prioritization of sub-watersheds for land and water management using InVEST SDR model: Rmelriver basin, Tunisia. **Arabian Journal of Geosciences**, Osaka, v. 10, n. 15, p. 1–9, Aug 2017. doi: 10.1007/s12517-017-3104-z.
- CHEN, Y.; XU, M.; WANG, Z.; GAO, P.; LAI, C. Applicability of two satellite-based precipitation products for assessing rainfall erosivity in China. **Science of the Total Environment**, Amsterdam, v. 757, p. 143975, Feb 2021. doi: 10.1016/j.scitotenv.2020.143975.
- CRUZ, D. C. da; BENAYAS, J. M. R.; FERREIRA, G. C.; MONTEIRO, A. L.; SCHWARTZ, G. Evaluation of soil erosion process and conservation practices in the Paragominas-Pa municipality (Brazil). **Geographia Technica**, Cluj-Napoca, v. 14, n. 1, p. 14–35, Mar 2019. doi: 10.21163/GT.
- CUNHA, E. R. da; BACANI, V. M.; PANACHUKI, E. Modeling soil erosion using RUSLE and GIS in a watershed occupied by rural settlement in the Brazilian Cerrado. **Natural Hazards**, Dordrecht, v. 85, n. 2, p. 851–868, Jan 2017. doi: 10.1007/s11069-016-2607-3.
- DIAS, B. A. R. H.; UDAYAKUMARA, E. P. N.; JAYAWARDANA, J. M. C. K.; MALAVIPATHIRANA, S.; DISSANAYAKE, D. A. T. W. K. Assessment of soil erosion in Uma Oya catchment, Sri Lanka. **Journal of Environmental Professionals Sri Lanka**, Sri Lanka, v. 8, n. 1, p. 39–51, Mar 2019. doi: 10.4038/jeps1.v8i1.7875.
- FAYAS, C. M.; ABEYSINGHA, N. S.; NIRMANEE, K. G. S.; SAMARATUNGA, D.; MALLAWATANTRI, A. Soil loss estimation using RUSLE model to prioritize erosion control in KELANI river basin in Sri Lanka. **International Soil and Water Conservation Research**, China, v. 7, n. 2, p. 130–137, Jun 2019. doi: 10.1016/j.iswcr.2019.01.003.
- GALDINO, S.; SANO, E. E.; ANDRADE, R. G.; GREGO, C. R.; NOGUEIRA, S. F.; BRAGANTINI, C.; FLOSI, A. H. G. Large-scale modeling of soil erosion with RUSLE for conservationist planning of degraded cultivated Brazilian Pastures. **Land Degradation & Development**, Chichester, v. 27, n. 3, p. 773–784, Aug 2016. doi: 10.1002/ldr.2414.

- GANASRI, B. P.; RAMESH, H. Assessment of soil erosion by RUSLE model using remote sensing and GIS - A case study of Nethravathi Basin. **Geoscience Frontiers**, Pequim, v. 7, n. 6, p. 953–961, Nov 2016. doi: 10.1016/j.gsf.2015.10.007.
- GELAGAY, H. S.; MINALE, A. S. Soil loss estimation using GIS and Remote sensing techniques: A case of Koga watershed, Northwestern Ethiopia. **International Soil and Water Conservation Research**, China, v. 4, n. 2, p. 126–136, Jun 2016. doi: 10.1016/j.iswcr.2016.01.002.
- GOMES, L.; SIMÕES, S. J. C.; FORTI, M. C.; OMETTO, J. P. H. B.; NORA, E. L. D. Using Geotechnology to Estimate Annual Soil Loss Rate in the Brazilian Cerrado. **Journal of Geographic Information System**, v. 9, p. 420–439, 2017. doi: 10.4236/jgis.2017.94026.
- HAMEL, P.; CHAPLIN-KRAMER, R.; SIM, S.; MUELLER, C. A new approach to modeling the sediment retention service (InVEST 3.0): Case study of the Cape Fear catchment, North Carolina, USA. **Science of The Total Environment**, Amsterdam, v. 524–525, n. 15, p. 166–177, Aug 2015. doi: 10.1016/j.scitotenv.2015.04.027.
- McCOOL, D. K.; FOSTER, G. R.; YODER, D. C.; WEESIES, G. A.; MCGREGOR, K. C.; BINGNER, R. L. The revised universal soil loss equation, Version 2. In: International Soil Conservation Organization Conference Proceedings, **Anais...2004**.
- MORGAN, R. P. C.; NEARING, M. A. (Ed.). **Handbook of erosion modelling**. West Sussex: Wiley-Blackwell, 2011.
- NACHTIGALL, S. D.; NUNES, M. C. M.; MOURA-BUENO, J. M.; LIMA, C. L. R. de; MIGUEL, P.; BESKOW, S.; SILVA, T. P. Modelagem espacial da erosão hídrica do solo associada à sazonalidade agroclimática na região sul do Rio Grande do Sul, Brasil. **Engenharia Sanitária e Ambiental**, Rio de Janeiro, v. 25, n. 6, p. 933–946, dez. 2020. doi: 10.1590/s1413-4152202020190136.
- OLIVEIRA, N. G.; VIEIRA, C. V. Soil loss estimate in the Cubatão do norte river hydrographic basin , northeast of Santa Catarina , Brazil. **International Journal of Development Research**, v. 7, n. 7, p. 13887–13895, Jul 2017.
- PANDEY, S.; KUMAR, P.; ZLATIC, M.; NAUTIYAL, R.; PANWAR, V. P. Recent advances in assessment of soil erosion vulnerability in a watershed. **International Soil and Water Conservation Research**, China, Mar 2021. doi: 10.1016/j.iswcr.2021.03.001.
- RENARD, K. G.; FOSTER, G. R.; WEESIES, G. A.; McCOOL, D. K.; YODER, D. C. **Predicting soil erosion by water: A guide to conservation planning with the Revised Universal Soil Loss Equation (RUSLE)**. Washington:USDA, 1997. 385p (Agriculture Handbook, 703).
- SALIS, H. H. C. de; COSTA, A. M. da; VIANA, J. H. M. Estimativa da perda anual de solos na bacia hidrográfica do Córrego Marinheiro, Sete Lagoas – MG, por meio da RUSLE. **Boletim de Geografia**, Maringá, v. 37, n. 1, p. 101–115, May 2019. doi: 10.4025/bolgeogr.v37i1.37213.
- SHARP, R.; DOUGLASS, J.; WOLNY, S.; ARKEMA, K.; BERNHARDT, J.; BIERBOWER, W.; CHAUMONT, N.; DENU, D.; FISHER, D.; GLOWINSKI, K.; GRIFFIN, R.; GUANNEL, G.; GUERRY, A.; JOHNSON, J.; HAMEL, P.; KENNEDY, C.; KIM, C. K.; LACAYO, M.; LONSDORF, E.; MANDLE, L.; ROGERS, L.; SILVER, J.; TOFT, J.; VERUTES, G.; VOGL, A. L.; WOOD, S.; WYATT, K. **InVEST 3.9.0.post150+ug.ga885d58.d20210525 User’s Guide**. The Natural Capital Project, Stanford

University, University of Minnesota, The Nature Conservancy, and World Wildlife Fund. Disponível em: < <https://invest-userguide.readthedocs.io/en/latest/>>. Acesso em: 1 dez. 2019.

STEINMETZ, A. A.; CASSALHO, F.; CALDEIRA, T. L.; OLIVEIRA, V. A. de; BESKOW, S.; TIMM, L. C. Assessment of soil loss vulnerability in data-scarce watersheds in southern Brazil. **Ciência & Agrotecnologia**, Lavras, v. 42, n. 6, p. 575–587, Nov-Dec 2018. doi: 10.1590/1413-70542018426022818.

VIJITH, H.; HURMAIN, A.; DODGE-WAN, D. Impacts of land use changes and land cover alteration on soil erosion rates and vulnerability of tropical mountain ranges in Borneo. **Remote Sensing Applications: Society and Environment**, v. 12, p. 57–69, 2018. doi: 10.1016/j.rsase.2018.09.003.

WISCHMEIER, W. H.; SMITH, D. D. **Predicting rainfall-erosion losses from cropland east of the rocky mountains**: Guide for selection of practices for soil and water conservation. 1. ed. Washington:USDA, 1965. 47p. (Agricultural Handbook, 282).

WISCHMEIER, W. H.; SMITH, D. D. **Predicting rainfall erosion losses**: A guide to conservation planning. 2. ed. Washington:USDA, 1978. 58p. (Agricultural Handbook, 537).

ZERIHUN, M.; MOHAMMEDYASIN, M. S.; SEWNET, D.; ADEM, A. A.; LAKEW, M. Assessment of soil erosion using RUSLE, GIS and remote sensing in NW Ethiopia. **Geoderma Regional**, Amsterdam, v. 12, p. 83–90, Mar 2018. doi: 10.1016/j.geodrs.2018.01.002.

ZHOU, M.; DENG, J.; LIN, Y.; BELETE, M.; WANG, K.; COMBER, A.; HUANG, L.; GAN, M. Identifying the effects of land use change on sediment export: Integrating sediment source and sediment delivery in the Qiantang River Basin, China. **Science of the Total Environment**, Amsterdam, v. 686, p. 38–49, Oct 2019. doi: 10.1016/j.scitotenv.2019.05.336.

SECOND PART – Articles

Article I - RainfallErosivityFactor: An R package for rainfall erosivity (R-factor) determination

(Article published in Catena, <https://doi.org/10.1016/j.catena.2020.104509>)

Abstract

RainfallErosivityFactor is an R package developed as a tool for the analysis of rainfall data and the calculation of the R-factor, a relevant parameter for soil loss prediction due to water erosion. The package consists of a user-friendly routine for loading large rainfall datasets into the R software environment and classifying data into erosive and non-erosive events. Erosive rainfall events are then used to compute rainfall erosivity values. This paper explains the development of the package with the purpose of showing how rainfall data can be analyzed accurately, fast and efficiently. An example is provided for Pirassununga, SP, Brazil, using a 7-year rainfall dataset with 10-minute interval between measurements. This package proved to be an efficient and fast tool for the determination of rainfall erosivity, which can be subsequently used to predict soil erosion. Considerations for future developments may come in the form of feedback, such as the need for more options of time interval.

Keywords: decision making tool; rainfall data analysis; water erosion; R software environment; erosion model prediction.

1. Introduction

The R-factor –rainfall erosivity– is defined as the capacity of rainfall to cause soil loss by water. The R-factor is one of the six factors in the Universal Soil Loss Equation-USLE (Wischmeier and Smith, 1978) and its revised versions. Due to the irregular distribution of precipitation, in time and space, rainfall erosivity (R-factor) can be computed and mapped (Nearing et al., 2017). Thus, the R-factor is an important soil conservation tool for decision making and proper selection of best management practices for anthropogenic activities such as agriculture, urban development, barrage construction, among others (Wischmeier, 1959; Wischmeier and Smith, 1978).

Rainfall erosivity has been widely studied worldwide (Nearing et al., 2017). A survey with the term “Rainfall Erosivity” was performed recently (February 2020) using the Scopus database. Results of this search showed 1265 records, 86.2% of which were associated with scientific papers.

Nowadays there are only a few computer programs capable to assist on the computation of rainfall erosivity: Chuveros, NetErosividade, Climate Generator (CLIGEN), Rainfall Intensity Summarization Tool (RIST), and Web ERosivity Module (WERM). In Brazil, Chuveros was used in only a few regional research projects in the State of Rio Grande do Sul (Bazzano et al., 2007; 2010). NetErosividade usage has been reported in the scientific literature for several studies in the Brazilian states of São Paulo, Minas Gerais, Espírito Santo, and Rio Grande do Sul (Moreira et al., 2006; 2008; 2012; 2016), whereas CLIGEN is a weather generator used by the Water Erosion Prediction Project (WEPP) for the modeling of soil loss (Lobo et al., 2015; Kinnell, 2019). The other two recently reported tools for the prediction of rainfall erosivity include RIST (Araujo et al., 2018) and WERM (Risal et al., 2016; 2018).

Rainfall erosivity can be calculated using datasets from automated weather stations or even pluviograms. However, in both cases, data processing begins by entering values manually into spreadsheets. A challenge in computing the R-factor refers to the vast rainfall input data required for a reliable calculation; *e.g.* it is recommended to use historical precipitation series of ≥ 20 years (Renard and Freimund, 1994; Vantas et al., 2019). Even for smaller datasets, calculation of rainfall erosivity becomes time-consuming. Thus, the determination of R-factor becomes an exhaustive process for reliable predictions, requiring a lot of attention or automation to avoid errors. For rather long historical series, the manual procedure increases the chances of failed calculations or cumulative errors.

An easy-to-adopt software package was developed to avoid errors during the computation of erosivity values, as well as to make its determination process faster and straightforward. This software package can be used as a tool, *ad-hoc* to the vertiginous technological and scientific times, to facilitate the scientific and extensionist work in the area of soil and water conservation. The R-project is an open source and collaborative free environment for advanced statistics, data management, graphic generation, and predictive analytics (R Core Team, 2018). Thus, the first objective was to develop a package to be run at the R software environment to calculate rainfall erosivity accurately, fast, and efficiently. Once the R package: RainfallErosivityFactor for R-factor determination was developed, the second objective was to validate it using a robust public database from Pirassununga, State of São Paulo, Brazil.

2. Methods

2.1. Structure of the package *RainfallErosivityFactor*

The *RainfallErosivityFactor* package was developed and created using the R software environment (R Core Team, 2018). The package became available at the Comprehensive R Archive Network (CRAN) on the 18th of November of 2018. The *RainfallErosivityFactor* package was developed accordingly to the procedure described by Wischmeier (1959); Wischmeier and Smith (1978). The package first identifies single rainfall events. A single rainfall event refers to an interruption in rain in an interval of 6 h with precipitation ≤ 1 mm. Then, the kinetic energy is determined using: $E = 0.119 + 0.0873 * \text{Log}_{10}I$ ($\text{MJ ha}^{-1} \text{mm}^{-1}$). Subsequently, rainfall erosivity (EI_{30} , $\text{MJ mm h}^{-1} \text{ha}^{-1} \text{year}^{-1}$) is computed according to Wischmeier (1959), considering the total kinetic energy of a storm in a maximum of 30-minute intensity (EI_{30}). The sum of these products corresponds to the R-factor of the USLE (Wischmeier and Smith, 1978).

The *RainfallErosivityFactor* package differentiates non-erosive from erosive rainfall events. Erosive rainfall events are computed based on the following criteria: i) the cumulative rainfall of an event is greater than 10 mm; ii) the intensity in 10 minutes (I_{10}) is greater than 24 mm h^{-1} ; and iii) the kinetic energy is greater than 3.6 MJ ha^{-1} . Conversely, when these criteria are not met, the rainfall event is considered non-erosive.

The outputs provided by the *RainfallErosivityFactor* package are the monthly values of precipitation, rainfall erosivity, number of erosive rainfall events, number of non-erosive rainfall events, sum of erosive rains, and sum of non-erosive rains, as well as annual values. Finally, the *RainfallErosivityFactor* package delivers the annual average value of rainfall erosivity for the period evaluated. The slowest runtime analysis for a 7-year period database was 56 s using a Windows-based computer.

2.2. Documentation of the package *RainfallErosivityFactor*

The *RainfallErosivityFactor* package was developed using the R software environment. The package is currently available for installation at the CRAN public repository <https://CRAN.R-project.org/package=RainfallErosivityFactor>, which is free to access worldwide. The *RainfallErosivityFactor* package is documented in the R software through the standard package documentation systems established by CRAN. The documentation contains a manual divided into four reports: Description; *RainfallErosivity Factor* (The Rainfall Erosivity Factor); *RainFallExample* (dataset to perform an example of Rainfall Erosivity Factor); and

RFactor (The R-Factor function - Computes Rainfall Erosivity Factor). For more information, see the supplementary data.

As part of the RainfallErosivityFactor package validation process -for the package to be approved and made available at <https://cran.r-project.org/web/packages/RainfallErosivityFactor/index.html>-, the data were presented, the results verified by the maintenance team, and evaluated by CRAN.

To use the package, it is necessary to install it by the command line:

```
install.package (RainfallErosivityFactor)
```

Immediately after installation, the library of the package should be loaded; *viz.* the installation of the library by command line:

```
library (RainfallErosivityFactor)
```

To run the function, from a dataset:

```
data (RainFallExample, package="RainfallErosivityFactor")
RFactor (Data, initialmonth, months, registration, nyear).
```

The report “RainFallExample” shows the way the database must be organized for the package to recognize the serial data.

The report “RFactor” displays the details of the main function of the program. The main function of the library is executed by the following command line:

```
RFactor(Data, initialmonth, months, registration, nyear).
```

2.3 Version of the software R

The RainfallErosivityFactor package was developed using versions of R 3.4.3 and 1.0.136 - © 2009-2016 RStudio, Inc. Therefore, versions equal to or greater than those utilized in creating the package must be used for correct performance. The license used to create the package was the GPL General Public License Version equal to or greater than 2.

2.4. Use of the package RainfallErosivityFactor for scientific research

2.4.1. Site description

Brazil is a country of continental proportions and one of the world’s leading producers of sugar, soybeans, beef, poultry, coffee, citrus, and corn (IBGE, 2018; Miranda and Fonseca,

2020). Correspondingly, the State of São Paulo remains the main producer of sugarcane (Veiga et al., 2018; Miranda and Fonseca, 2020), and citrus (AGRIANUAL, 2016; IBGE, 2018) in Brazil. The city of Pirassununga is located in the State of São Paulo (SP), at the geographical coordinates $21^{\circ}59'46''$ S and $47^{\circ}25'33''$ WGr (Fig. 1). Regarding Pirassununga, typical farming systems comprehend crop production, pastures for cattle, and installations for poultry and other small species (Godoi, 2018). According to the Köppen classification, the climate is Cwb (Alvares et al., 2013), *i.e.* humid subtropical climate, with dry winters and mild summers. Precipitation information was obtained from the University of São Paulo Weather Station (USPWS) located at the Fernando Costa campus in Pirassununga. This referred university campus includes rural and agricultural areas devoted to experimental research and productive farming, well concealed by the surrounding areas of pasture for livestock, and farmland for citrus and sugarcane production (Godoi, 2018). This weather station was selected due to the importance of the region for agricultural production, and because precipitation data is open access and readily available on-line.

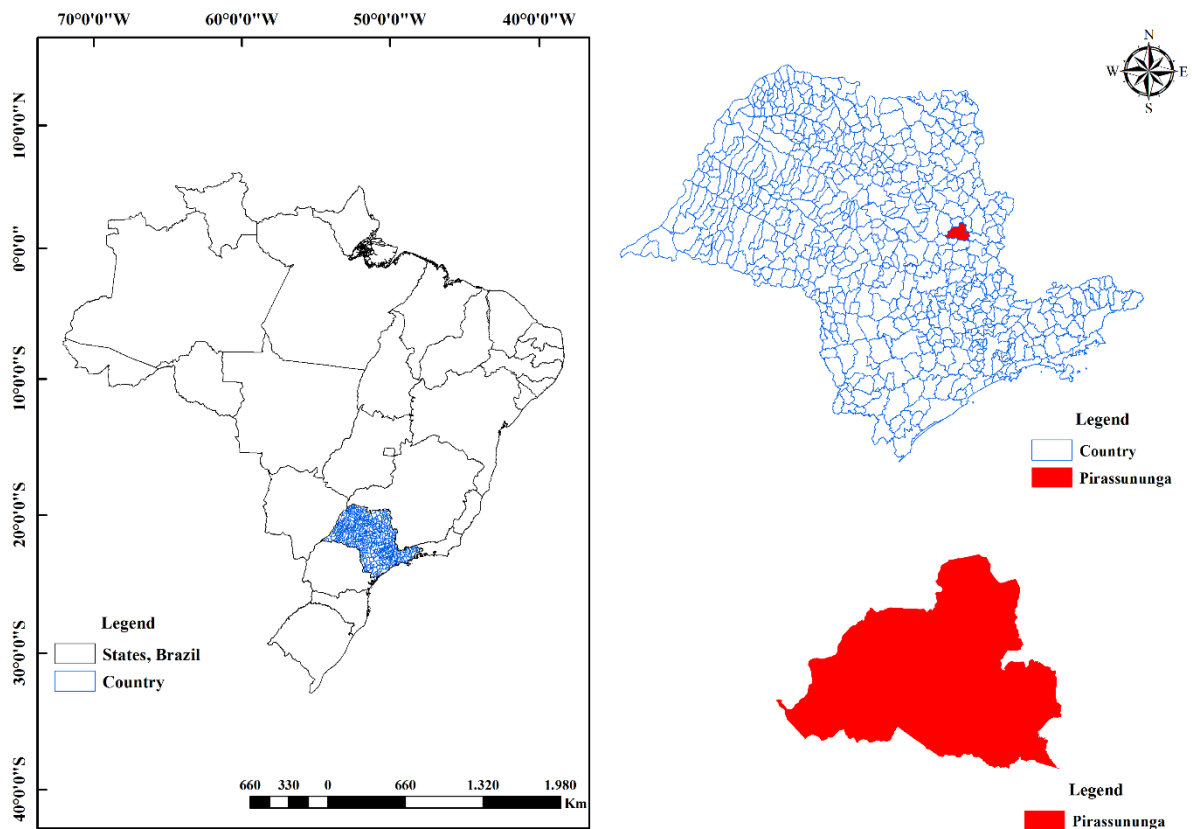


Fig. 1. Location of Pirassununga, State of São Paulo, Brazil.

2.4.2. Source and characteristics of the rainfall data

The USPWS rainfall dataset comprises the period from 2009 to 2015. Data were recorded in automatic rain gauges every 10 min with accuracy of 0.1 mm. These data were used to calculate rainfall erosivity using the RainfallErosivityFactor package.

3. Results

3.1. Package performance

The RainfallErosivityFactor package computed –with no errors– rainfall erosivity, monthly and total annual rainfall, and number of erosive and non-erosive events. Therefore, the RainfallErosivityFactor package revealed to be accurate, fast, and effective in calculating the R-factor. It is important to acknowledge that the computed R-factor was the average rainfall erosivity for the studied period.

Additionally to the package being open access, there is no limitation regarding the dataset size to be analyzed by it. These characteristics are very advantageous since the package is already available and operational worldwide.

3.2. Weather station from Pirassununga

The studied area has a well-defined wet season (Table 1), being concentrated during the months of November to April. In terms of annual amount, there is a large variation of rainfall, directly proportional to the rainfall erosive potential.

Regarding to rainfall amount, 2014 was an atypical year with water deficit in many parts of Brazil, especially in the study region. Santos et al. (2017) compared the hydrological year of 2013-2014 to the rain distribution of the previous 21 years and found out rainfall indexes significantly below average, with irregular distribution of precipitation during the rainy season. Marengo et al. (2015) reported that the main cause leading to this heavy lack of rain was an intense, persistent and anomalous high pressure system blocking moisture flow from the Amazon and cold front systems in the South Atlantic Convergence Zone. Although 2014 was the year with the lowest total rainfall accumulation rainfall, the smallest rainfall erosivity value was computed for 2012. These results showed rainfall erosivity relates more to rainfall intensity than to total accumulation.

The R-factor for Pirassununga ranged from 6983.6 to 13236.4 MJ mm ha⁻¹ h⁻¹ year⁻¹ (Table 1), being the smallest for year 2012 and the most erosive for 2009. The average rainfall erosivity for the period corresponds to 9512.9 MJ mm ha⁻¹ h⁻¹ year⁻¹, being classified as medium-high erosivity, according to Foster et al. (1981).

Fig. 2 depicts the minimum, average, and maximum values of each of the output data for Pirassununga, SP, Brazil. One can observe the large variability of the data, thus the importance of using as input a large rainfall dataset for predicting a reliable R-factor.

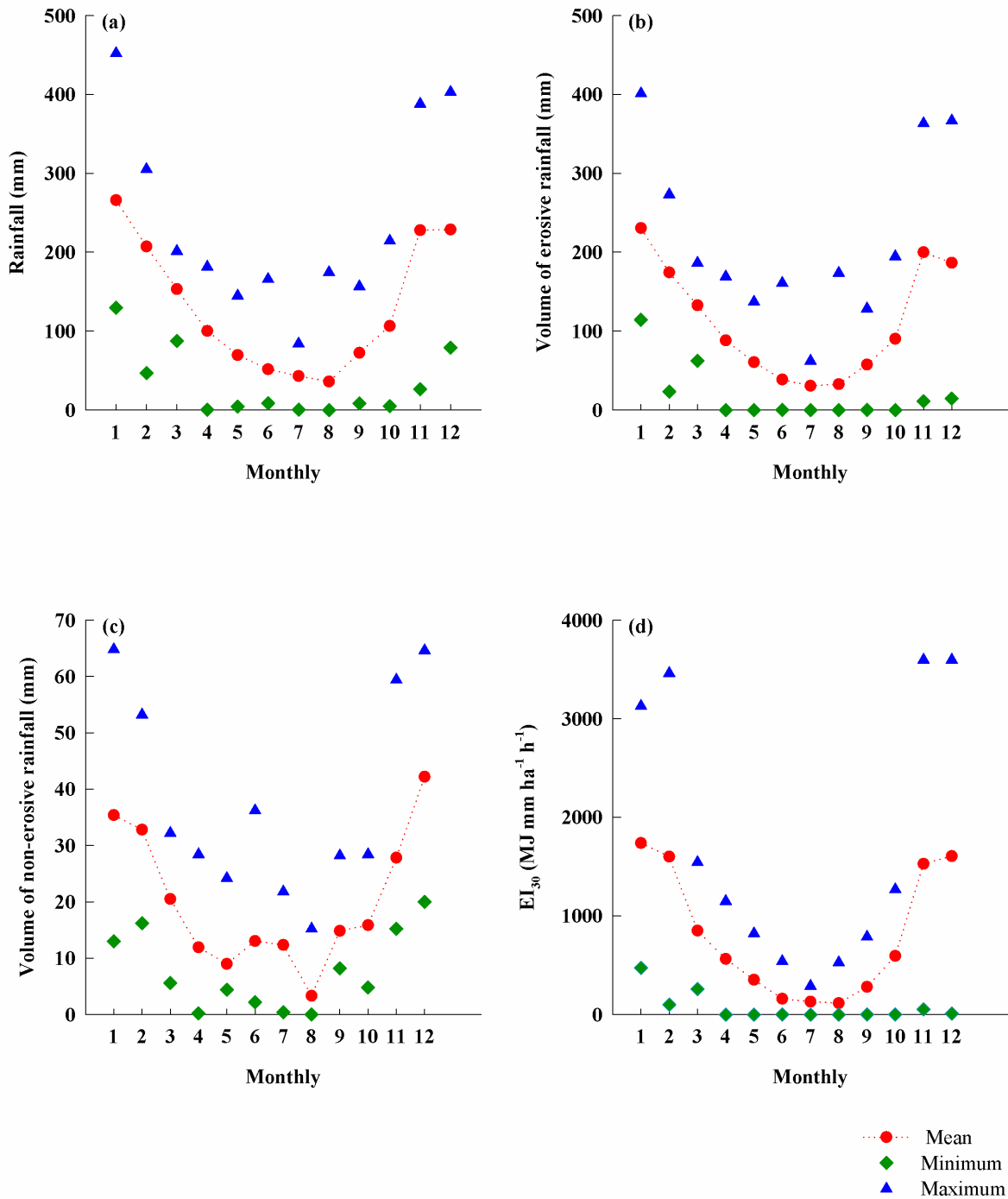


Fig. 2. Minimum, average, and maximum values for: (a) rainfall, mm; (b) amount of erosive rainfall, mm; (c) amount of non-erosive rainfall, mm; and (d) rainfall erosivity, $MJ\ mm\ ha^{-1}\ h^{-1}\ month^{-1}$.

4. Discussion

4.1 Rainfall erosivity

Average rainfall erosivity for Pirassununga was 9512.9 MJ mm ha⁻¹ h⁻¹ year⁻¹. This value was higher than those reported by Oliveira et al. (2012); Oliveira et al. (2015); Trindade et al. (2016). They computed rainfall erosivity values ranging from 6000 to 8000 MJ mm ha⁻¹ h⁻¹ year⁻¹.

A more global perspective can be perceived by comparing these values to other parts of the world. Hoyos et al. (2005) reported an R-factor of 13,192 MJ mm ha⁻¹ h⁻¹ year⁻¹ for the Andes of Colombia, a greater value compared to Pirassununga. For Asia, Yu et al. (2001) reported rainfall erosivity values of 13,600 and 21,600 MJ mm ha⁻¹ h⁻¹ year⁻¹ for two locations of the Malaysian Peninsula. However, for the entire Peninsula, Leow et al. (2011) obtained values ranging from 7500 to 20,000 MJ mm ha⁻¹ h⁻¹ year⁻¹. For Japan, Shiono et al. (2013) reported a range from 700 to 15,000 MJ mm ha⁻¹ h⁻¹ year⁻¹. Higher rainfall erosivity values than those for Pirassununga were also observed for Cuba, where the R-factor ranged from 13,500 to 15,500 MJ mm ha⁻¹ h⁻¹ year⁻¹ (Schiettecatte et al., 2008). Lower values were registered for central Chile, which ranged from 71 to 4025 MJ mm ha⁻¹ h⁻¹ year⁻¹ (Bonilla and Vidal, 2011). For Europe, average rainfall erosivity values were lower than those determined for Pirassununga, as 871 MJ mm ha⁻¹ h⁻¹ year⁻¹ for Belgium (Verstraeten et al., 2006), 1715.2 MJ mm ha⁻¹ h⁻¹ year⁻¹ for Italy (Borrelli et al., 2016), and 849.6 MJ mm ha⁻¹ h⁻¹ year⁻¹ for Greece (Panagos et al., 2016). Rainfall erosivity values vary according to climate, largely associated to different types of rain, *i.e.* in terms of duration and intensity. Consequently, higher rainfall erosivity values are observed in South-eastern Asia (Cambodia, Indonesia, Malaysia, the Philippines, and Bangladesh), Central Africa (Congo, and Cameroon), South America (Brazil, Colombia, and Peru), Central America and the Caribbean. Conversely, lower rainfall erosivity values are commonly located in regions of Siberia, the Middle East, Northern Africa, Canada, and Northern Europe (Panagos et al., 2017).

Table 1. Monthly rainfall, erosive rainfall, and rainfall erosivity obtained through the RainfallErosivityFactor package, for Pirassununga, SP, Brazil. (continue...)

Year	Monthly												Annual Total
	January	February	March	April	May	June	July	August	September	October	November	December	
Rainfall (mm)													
2009	302.6	255.2	170.8	89.6	82.0	46.4	84.0	174.4	156.6	133.8	252.8	403.0	2151.2
2010	198.0	305.2	201.4	181.4	40.0	15.4	33.4	0.0	87.0	4.8	26.2	215.0	1307.8
2011	452.2	166.8	181.0	115.2	4.4	44.0	0.4	28.8	8.4	214.4	224.0	219.0	1658.6
2012	316.0	85.2	89.6	151.8	105.0	165.8	55.6	0.2	64.4	117.4	176.0	230.2	1557.2
2013	275.8	297.2	168.0	92.6	144.8	49.2	40.8	25.6	52.0	157.8	230.0	79.0	1612.8
2014	129.8	46.8	87.6	0.2	31.2	8.6	44.2	0.4	47.6	20.0	388.0	238.6	1043.0
2015	186.8	293.4	173.8	70.0	79.2	31.8	42.2	22.2	90.2	96.8	297.4	215.4	1599.2
Volume of erosive rainfall (mm)													
2009	264.2	239.0	165.2	80.6	57.8	10.2	62.2	173.6	128.4	105.4	232.6	366.8	1886.0
2010	133.2	273.2	186.4	169.0	34.8	12.8	32.4	0.0	70.0	0.0	11.0	195.0	1117.8
2011	401.2	128.0	172.0	106.0	0.0	41.8	0.0	13.6	0.0	194.6	198.2	179.0	1434.4
2012	279.0	60.8	63.2	141.6	97.8	161.0	35.0	0.0	51.4	108.0	147.6	173.2	1318.6
2013	247.8	244.0	135.8	78.6	137.0	22.0	22.8	23.4	42.2	135.6	209.0	14.4	1312.6
2014	114.4	23.2	62.2	0.0	25.0	0.0	41.0	0.0	28.4	0.0	363.2	201.2	858.6
2015	173.8	252.0	144.0	41.6	71.4	22.2	20.8	17.8	82.0	87.2	238.0	175.4	1326.2
Rainfall Erosivity (MJ mm ha ⁻¹ h ⁻¹)													

Table 1. (concluded)

2009	2679.9	1487.5	745.5	553.8	403.0	10.3	268.3	527.0	788.3	881.0	1294.6	3597.2	13236.4
2010	471.5	3462.0	1544.0	1150.0	316.6	26.7	289.2	0.0	156.1	0.0	52.7	1537.9	9006.7
2011	3128.3	876.1	679.8	907.4	0.0	210.7	0.0	19.9	0.0	936.1	2131.6	1968.8	10858.7
2012	1746.4	598.6	258.4	600.7	303.3	539.3	211.9	0.0	146.5	347.6	792.0	1438.9	6983.6
2013	1527.9	2889.1	820.5	407.5	821.5	29.2	28.1	239.7	92.2	1268.6	918.0	10.2	9052.5
2014	1135.2	100.0	1370.6	0.0	157.6	0.0	72.1	0.0	40.9	0.0	3596.9	1631.3	8104.6
2015	1484.9	1791.7	532.8	317.1	457.4	300.1	36.0	16.1	733.9	720.2	1900.8	1057.0	9348.0

According to Foster et al. (1981), the average rainfall erosivity of Pirassununga was classified as medium-high ($9512.9 \text{ MJ mm ha}^{-1} \text{ h}^{-1} \text{ year}^{-1}$). This value indicates soil and water conservation practices should be adopted to minimize the water erosion impacts in the area. In Brazil, water erosion of cropland areas results in soil loss rates of more than 600 million tons per year (Dechen et al., 2015). Regarding the State of São Paulo, 65% of the agricultural area requires some type of intervention to curtail soil losses (Medeiros et al., 2016). Nationwide, no-till cropping systems have been adopted in approximately 50% of annual crop cultivated areas; whereas in the State of São Paulo, no-till systems are much less common (only 11% of annual crop cultivated areas) (Llanillo et al., 2013). According to the computed rainfall erosivity values (Table 1), the region of study presents high soil erosion vulnerability during the months above the critical limit—more than $500 \text{ MJ mm ha}^{-1} \text{ h}^{-1} \text{ month}^{-1}$ (Rufino, 1986)—, adding up to about half of the year. Thus, Telles et al. (2019) suggest adequate soil conservation practices as no-till systems integrated with agricultural terracing, contour farming, intercropping, or crop rotation.

4.2. Comparison with other programs

Chuveros program runs on MS-DOS and the input file requires only erosive rainfall data in .DAT format. The process to separate only erosive events is arduous, time-consuming, and very susceptible to errors. Chuveros is no longer available for download. The NetErosividade program is available for download and it requires users to input the geographical coordinates. Thus, its calculations rely on an internal rainfall database limited to a few Brazilian States: Minas Gerais, São Paulo, Espírito Santo, and Rio Grande do Sul. The output results of rainfall erosivity are based on neural network analyzes. According to Moreira et al. (2006), the NetErosividade for the state of São Paulo makes it possible to obtain the annual erosivity value.

The other programs require a more sophisticated climatic information input (*e.g.* daily rainfall, storm duration, air temperature, solar radiation, and wind speed and direction). However, meteorological stations in developing countries, such as Brazil, usually lack this information. RIST accepts input data files in .TXT or .CSV formats. The intensity and time intervals should be checked (5, 10, 15, 30 and 60 min). Its outputs are precipitation (mm), duration (hours), maximum intensity (mm h^{-1}), kinetic energy (MJ ha^{-1}), and EI_{30} ($\text{MJ mm ha}^{-1} \text{ h}^{-1}$). RIST does not return the number of erosive rainfall events. Furthermore, it is necessary to divide the computed R-factor by the years of the dataset. The WERM outputs are precipitation,

maximum intensity in 30 minutes and R-factor, being these results expressed per event and month, and rain erosivity per year.

The RainfallErosivityFactor package is simple and can be employed for any rainfall dataset. An advantage of it is the input of data in any format acceptable by R software environment (.TXT, .CSV, XLSX, among others). Once the package is loaded into the R software library, descriptive analyses may be performed altogether.

4.3. Limitations of R factor

A common hurdle for engineers and scientists using USLE or its revised versions (RUSLE and RUSLE2), in various parts of the world, consists of a lack of continuous and fine temporal resolution rainfall data for the computation of the R-factor, since long term (≥ 20 years) precipitation records are required (Renard and Freimund, 1994; Vantas et al., 2019). The R-factor is usually computed for time periods greater than 20 years to minimize any possible bias caused by unusual wet or dry rainfall periods (Vantas et al., 2019). Nevertheless, the developers of RUSLE2 (USDA-ARS, 2013) reported a rainfall record of 15 years sufficed for R-factor computation in Northern Mississippi.

Although for illustrative purposes we used a 7-year rainfall dataset, the region of study presented small amounts of precipitation during the wet seasons of years 2014 and 2016. This may underestimate rainfall erosivity (skewing R-factor). Thus, the accentuated importance of identifying a source of rainfall data with null or minimum latency, and appropriate temporal resolution.

Furthermore, Nearing et al. (2017) pointed out that the first version of USLE (Wischmeier and Smith, 1965) defined rainfall erosivity as an empirical function of rainfall intensity. Nevertheless, soil loss during interrill erosion is dominated by either splash detachment (correlated to rainfall intensity) or sheet-flow sediment transport (not correlated to rainfall intensity). Similarly, soil loss during rill or gully erosion is driven by runoff rate; *i.e.* it is not rainfall intensity dependent. Thus, depending on the physical conditions of the area of study, it may result in significantly underestimated erosivity.

4.4. Landscape scale application

Rainfall erosivity must be computed locally according to available historic rainfall datasets. Nevertheless, once proximal regions are analyzed, rainfall erosivity can be mapped using geostatistical tools for interpolation as means to achieve the spatial distribution of the R-

factor. Panagos et al. (2017) mapped the global rainfall erosivity to provide R-factor values around the globe. This information may be used to estimate current soil erosion rates under different land-use and vegetation cover conditions, or to estimate soil losses considering future climate change scenarios.

An adequate spatial interpolation can only be achieved by using precipitation data from various locations within or around the vicinity of the region of interest. The RainfallErosivityFactor package can assist to compute the rainfall erosivity at each individual locale. The results can be fed into any GIS software, or another package also available at CRAN to run the geostatistics.

5. Conclusions

The RainfallErosivityFactor package is robust in determining rainfall erosivity. No operational errors occurred, and no dataset size limit was detected. This showed to be a rather fast, efficient, and accurate process for the determination of the R-factor.

Currently, the RainfallErosivity package is in version 0.1.0. The need to calculate fast and accurately the rainfall erosivity using a large dataset motivated the development of this package. In developing countries, such as Brazil, there is little monitoring of climatic variables in some regions, thus a package to calculate rainfall erosivity based on simple rainfall historic data constitutes a very useful tool.

Future versions of the package may include considerations by users around the world in the form of feedback, such as the addition of more options for time interval.

References

- Agriannual, 2016. AGRIANUAL 2016: Anuário da agricultura brasileira. Inf. Econ. FNP, São Paulo.
- Alvares, C.A., Stape, J.L., Sentelhas, P.C., Gonçalves, J.L.M., Sparovek, G., 2013. Köppen's climate classification map for Brazil. *Meteorol. Z.* 22, 711–728. <https://doi.org/10.1127/0941-2948/2013/0507>.
- Araujo, T.F., Sone, J.S., Alves Sobrinho, T., Oliveira, P.T.S. de, 2018. Assessing rainfall erosivity in a tropical region using free software, in XIII Brazilian Meeting of Sediment Engineering. I Particles in the Americas. *Hydrossedimentology in the Nexus Context for a Sustainable Society*, pp. 1-8.
- Bazzano, M.G.P., Eltz, F.L.F., Cassol, E.A., 2007. Erosivity, rainfall coefficient and patterns and return period in Quarai, RS, Brazil. *Rev. Bras. Cienc. Solo* 31, 1205–1217. <http://dx.doi.org/10.1590/S0100-06832007000500036>.
- Bazzano, M.G.P., Eltz, F.L.F., Cassol, E.A., 2010. Erosivity and hydrological characteristics

- of rainfalls in Rio Grande (RS, Brazil). *Rev. Bras. Cienc. Solo* 34, 235–244. <http://dx.doi.org/10.1590/S0100-06832010000100024>.
- Bonilla, C.A., Vidal, K.L., 2011. Rainfall erosivity in Central Chile. *J. Hydrol.* 410, 126–133. <https://doi.org/10.1016/j.jhydrol.2011.09.022>.
- Borrelli, P., Diodato, N., Panagos, P., 2016. Rainfall erosivity in Italy: a national scale spatio-temporal assessment. *Int. J. Digit. Earth* 9, 835–850. <https://doi.org/10.1080/17538947.2016.1148203>.
- Dechen, S.C.F., Telles, T.S., Guimarães, M.F., De Maria I.C., 2015. Losses and costs associated with water erosion according to soil cover rate. *Bragantia* 74, 224–233. <http://dx.doi.org/10.1590/1678-4499.0363>.
- Foster, G.R., McCool, D.K., Renard, K.G., Moldenhauer, W.C., 1981. Conversion of the universal soil loss equation to SI metric units. *J. Soil Water Conserv.* 36, 355–359.
- Godoi, F.R.S., 2018. Prospects for University Territories: The Rural University of São Paulo in Pirassununga. In: Leal Filho, W., Frankenberger, F., Iglecias, P., Mülfarth, R. (eds) *Towards Green Campus Operations*, pp. 349–359. World Sustainability Series. Springer. https://doi.org/10.1007/978-3-319-76885-4_22.
- Hoyos, N., Waylen, P.R., Jaramillo, Á., 2005. Seasonal and spatial patterns of erosivity in a tropical watershed of the Colombian Andes. *J. Hydrol.* 314, 177–191. <https://doi.org/10.1016/j.jhydrol.2005.03.014>.
- IBGE, 2018. *Produção agrícola municipal: culturas temporárias e permanentes*. Instituto Brasileiro de Geografia e Estatística. Rio de Janeiro.
- Kinnell, P.I.A., 2019. CLIGEN as a weather generator for RUSLE2. *Catena* 172, 877–880. <https://doi.org/10.1016/j.catena.2018.09.016>.
- Leow, C.S., Ghani, A.A., Zakaria, N.A., Abidin, R.Z., 2011. Development of rainfall erosivity isohyet map for Peninsular Malaysia, in: *3rd International Conference on Managing Rivers in the 21st Century: Sustainable Solutions for Global Crisis of Flooding, Pollution and Water Scarcity*. pp. 748–756.
- Llanillo, R.F., Telles, T.S., Soares Júnior, D., Pelinni, T., 2013. Tillage systems on annual crops in Brazil: Figures from the 2006 Agricultural Census. *Semin. Cienc. Agrar.* 34, 3691–3698. <http://dx.doi.org/10.5433/1679-0359.2013v34n6Sup1p3691>.
- Lobo, G.P., Frankenberger, J.R., Flanagan, D.C., Bonilla, C.A., 2015. Evaluation and improvement of the CLIGEN model for storm and rainfall erosivity generation in Central Chile. *Catena* 127, 206–213. <https://doi.org/10.1016/j.catena.2015.01.002>.
- Marengo, J.A., Nobre, C.A., Seluchi, M.E., Cuartas, A., Alves, L.M., Mendiondo, E.M., Obregón, G., Sampaio, G., 2015. A seca e a crise hídrica de 2014-2015 em São Paulo. *Rev. USP* 31–44. <https://doi.org/10.11606/issn.2316-9036.v0i106p31-44>.
- Medeiros, G.O.R., Giarolla, A., Sampaio, G., Marinho, M.A., 2016. Diagnosis of the Accelerated Soil Erosion in São Paulo State (Brazil) by the Soil Lifetime Index Methodology. *Rev. Bras. Cienc. Solo* 40, e0150498, 1–15. <http://dx.doi.org/10.1590/18069657rbc20150498>.
- Miranda, E.E., Fonseca, M.F., 2020. Sugarcane: food production, energy, and environment. In: Santos, F., Rabelo, S.C., Matos, M., Eichler, P. (eds) *Sugarcane Biorefinery*,

- Technology and Perspectives, pp. 67–88. Academic Press. Elsevier.
<https://doi.org/10.1016/B978-0-12-814236-3.00004-4>.
- Moreira, M.C., Cecílio, R.A., Pezzopane, J.E.M., Pruski, F.F., Fukunaga, D.C., 2012. Programa computacional para estimativa da erosividade da chuva no Espírito Santo. *Eng. Agric.* 20, 350–356. <https://doi.org/10.13083/1414-3984.v20n04a07>.
- Moreira, M.C., Cecílio, R.A., Pinto, F. A. C., Lombardi Neto, F., Pruski, F.F., 2006. Programa computacional para estimativa da erosividade da chuva no estado de São Paulo utilizando redes neurais artificiais. *Eng. Agric.* 14, 88–92.
- Moreira, M.C., Oliveira, T.E.C., Cecílio, R.A., Pinto, F. A. C., Pruski, F.F., 2016. Spatial interpolation of rainfall erosivity using artificial neural networks for Southern Brazil conditions. *Rev. Bras. Cienc. Solo* 40, e0150132, 1–11.
<https://doi.org/10.1590/18069657rbc20150132>.
- Moreira, M.C., Pruski, F.F., Oliveira, T.E.C., Pinto, F. A. C., Silva, D.D., 2008. NetErosividade MG: Erosividade da chuva em Minas Gerais. *Rev. Bras. Cienc. Solo* 32, 1349–1353. <http://dx.doi.org/10.1590/S0100-06832008000300042>.
- Nearing, M.A., Yin, S., Borrelli, P., Polyakov, V.O., 2017. Rainfall erosivity: An historical review. *Catena* 157, 357–362. <https://doi.org/10.1016/j.catena.2017.06.004>.
- Oliveira, J.P.B., Cecílio, R.A., Pruski, F.F., Zanetti, S.S., 2015. Espacialização da erosividade das chuvas no Brasil a partir de séries sintéticas de precipitação. *Rev. Bras. Cienc. Agrar.* 10, 558–563. <https://doi.org/10.5039/agraria.v10i4a4998>.
- Oliveira, P.T.S., Wendland, E., Nearing, M.A., 2012. Rainfall erosivity in Brazil: A review. *Catena* 100, 139–147. <https://doi.org/10.1016/j.catena.2012.08.006>.
- Panagos, P., Ballabio, C., Borrelli, P., Meusburger, K., 2016. Spatio-temporal analysis of rainfall erosivity and erosivity density in Greece. *Catena* 137, 161–172.
<https://doi.org/10.1016/j.catena.2015.09.015>.
- Panagos, P., Borrelli, P., Meusburger, K., Yu, B., Klik, A., Lim, K. J., Yang, J.E., Ni, J., Miao, C., Chattopadhyay, N., Sadeghi, S.H., Hazbavi, Z., Zabihi, M., Larionov, G.A., Krasnov, S.F., Gorobets, A.V., Levi, Y., Erpul, G., Birkel, C., Hoyos, N., Naipal, V., Oliveira, P.T.S., Bonilla, C.A., Meddi, M., Nel, W., Al-Dashti, H., Boni, M., Diodato, N., Van Oost, K., Nearing, M., Ballabio, C., 2017. Global rainfall erosivity assessment based on high-temporal resolution rainfall records. *Sci. Rep.*, 7, 4175.
<https://doi.org/10.1038/s41598-017-04282-8>.
- R Core Team, 2018. R: language and environment for statistical. R Foundation for Statistical Computing, Vienna, Austria. Available online at. <https://www.R-project.org/> (verified 16 Dec. 2018).
- Renard, K.G., Freimund, J.R., 1994. Using monthly precipitation data to estimate the R-factor in the revised USLE. *J. Hydrol.* 157, 287–306.
- Risal, A., Bhattarai, R., Kum, D., Park, Y.S., Yang, J.E., Lim, K.J., 2016. Application of Web ERosivity Module (WERM) for estimation of annual and monthly R factor in Korea. *Catena* 147, 225–237. <https://doi.org/10.1016/j.catena.2016.07.017>.
- Risal, A., Lim, K.J., Bhattarai, R., Yang, J.E., Noh, H., Pathak, R., Kim, J., 2018. Development of web-based WERM-S module for estimating spatially distributed rainfall

- erosivity index (EI30) using RADAR rainfall data. *Catena* 161, 37–49.
<https://doi.org/10.1016/j.catena.2017.10.015>.
- Rufino, R.L., 1986. Avaliação do potencial erosivo da chuva para o Estado do Paraná: Segunda aproximação. *Rev. Bras. Cienc. Solo*, 10, 279–281.
- Santos, B.C. dos, Souza, P.H. de, Vecchia, F.A. da S., 2017. A caracterização da precipitação do ano hidrológico de 2013-2014 na região de São Carlos/SP e sua repercussão no espaço geográfico. *Rev. Bras. Climatol.* 21, 135–152.
<http://dx.doi.org/10.5380/abclima.v21i0.51505>.
- Schiettecatte, W., D'hondt, L., Cornelis, W.M., Acosta, M.L., Leal, Z., Lauwers, N., Almoza, Y., Alonso, G.R., Díaz, J., Ruíz, M., Gabriels, D., 2008. Influence of landuse on soil erosion risk in the Cuyaguaje watershed (Cuba). *Catena* 74, 1–12.
<https://doi.org/10.1016/j.catena.2007.12.003>.
- Shiono, T., Ogawa, S., Miyamoto, T., Kameyama, K., 2013. Expected impacts of climate change on rainfall erosivity of farmlands in Japan. *Ecol. Eng.* 61, Part C, 678–689.
<https://doi.org/10.1016/j.ecoleng.2013.03.002>.
- Telles, T.S., Lourenço, M.A.P., Oliveira, J.F., Costa, G.V., Barbosa, G.M.C., 2019. Soil conservation practices in a watershed in Southern Brazil. *An. Acad. Bras. Cienc.*, 91, e20180578, 1–10. <https://dx.doi.org/10.1590/0001-3765201920180578>.
- Trindade, A.L.F., Oliveira, P.T.S., Anache, J.A.A., Wendland, E., 2016. Variabilidade espacial da erosividade das chuvas no Brasil. *Pesq. Agropec. Bras.* 51, 1918–1928.
<https://doi.org/10.1590/s0100-204x2016001200002>.
- USDA-ARS. 2013. Science Documentation, Revised Universal Soil Loss Equation Version 2 (RUSLE2). USDA-Agricultural Research Service; 2013.
- Vantas, K., Sidiropoulos, E., Evangelides, C., 2019. Rainfall erosivity and its estimation: conventional and machine learning methods. In: Hrisanthou, V., Kaffas, K. (eds) *Soil Erosion - Rainfall Erosivity and Risk Assessment*. IntechOpen, p. 19.
<https://doi.org/10.5772/intechopen.85937>.
- Veiga, P.S., Malik, A., Lenzen M., Ferreira Filho, J.B.deS., Romanelli, T.L., 2018. Triple-bottom-line assessment of São Paulo state's sugarcane production based on a Brazilian multi-regional input-output matrix. *Renew. Sustain. Energy Rev.* 82, 666–680.
<https://doi.org/10.1016/j.rser.2017.09.075>.
- Verstraeten, G., Poesen, J., Demarée, G., Salles, C., 2006. Long-term (105 years) variability in rain erosivity as derived from 10-min rainfall depth data for Ukkel (Brussels, Belgium): Implications for assessing soil erosion rates. *J. Geophys. Res.* 111, D22109.
<https://doi.org/10.1029/2006JD007169>.
- Wischmeier, W.H., Smith, D.D., 1965. Predicting rainfall erosion losses from cropland east of the Rocky Mountains--guide for selection of practices for soil and water conservation. US Department of Agriculture, Washington.
- Wischmeier, W.H., 1959. A rainfall erosion index for a Universal Soil-Loss Equation. *Soil Sci. Soc. Am. J.* 23, 246–249.
<https://doi.org/10.2136/sssaj1959.03615995002300030027x>.
- Wischmeier, W.H., Smith, D.D., 1978. Predicting rainfall erosion losses: a guide to

conservation planning, Washington: USDA.

Yu, B., Hashim, G.M., Eusof, Z., 2001. Estimating the R-factor with limited rainfall data: a case study from peninsular Malaysia. *J. Soil Water Conserv.* 56, 101–105.

Article II - Rainfall Erosivity Estimation: A comparison and statistical assessment among methods using data from Southeastern Brazil

(Article elaborated according to standards of the Journal Catena, ISSN: 0341-8162)

Abstract

Rainfall erosivity is an indispensable factor in water erosion modeling. The search for alternatives to replace the Wischmeier and Smith method (standard) for determining rainfall erosivity becomes important due to the scarcity of detailed rain data from weather stations in many parts of the globe, with emphasis upon tropical regions. Thus, the objective of this study was to select a consistent method for such substitution in Brazilian conditions without access to rainfall intensity data. The tested methods included: modified Fournier, MF; modified Fournier by Zhang, MF-Z; modified Fournier by Men, MF-M; Rainfall Disaggregation, RD; TRMM Satellite with modified Fournier coefficient, TRMM-F; and TRMM Satellite with monthly rainfall, TRMM-M. The rainfall data were obtained from the USP Meteorological Station located on the Fernando Costa campus, with a time series of 7 years, referring to the period from 2009 to 2015. The analyses were performed according to the Additive Main effects and Multiplicative Interaction (AMMI) model and Scott-Knott statistical tests. Considering the 1:1 line, all methods had good adjustment, presenting similar behavior in relation to the standard method. The assessed methods behaved differently for rainy, dry, monthly, and annual periods. The MF method proved to be capable to consistently replace the standard method in all aforementioned situations. Considering the driest period, any method can be used. For annual rainfall erosivity estimation, the RD, MF, TRMM-F, and TRMM-M methods can be applied; highlighting that TRMM-based methods are optimal for locations without on-site rain gauges. Additionally, it was computed that the modified Fournier by Men and modified Fournier by Zhang underestimated and overestimated the rainfall erosivity, respectively.

Keywords: Modified Fournier; Rainfall Disaggregation; TRMM.

1. Introduction

The erosive potential of rainfall, defined as rainfall erosivity index, can be calculated using datasets from automated weather stations or even pluviograms. The rainfall erosivity index –also represented as the R factor of EI_{30} – is computed as the product of rainfall kinetic energy times its 30-minute maximum intensity (Wischmeier and Smith, 1978). The R factor is

one of the six factors in the Universal Soil Loss Equation (USLE) (Wischmeier and Smith, 1978) and its revised versions. However, in parts of the globe, there is insufficient trustworthy rainfall data for a reliable calculation (Trindade et al., 2016), since it is recommended to use historical precipitation series of ≥ 20 years (Renard and Freimund, 1994; Vantas et al., 2019), and the rainfall stations do not present homogeneity in their distribution (Moraes et al., 2015). Thus, the lack of good resolution rainfall data –mainly rainfall intensity– has driven researchers to develop alternative methods to estimate the rainfall erosivity such as the Fournier index (Fournier, 1960), Modified Fournier (Arnoldus, 1980) by the adjustment of potential equations, and considering erosivity per day in half a month (Zhang et al., 2002), among others (Diodato et al., 2013; Diodato and Bellocchi, 2010; Men et al., 2008).

Other methodologies, such as rainfall disaggregation (Silveira, 2000) –considering annual or monthly totals for hourly or shorter periods–, or techniques based on orbital remote sensing to estimate rainfall depth (Duarte and Silva Filho, 2019; Li et al., 2020; Moreira et al., 2020), can be used at locations with low density of rain gauge data points. Rainfall erosivity mapping for Africa utilizing Tropical Rainfall Measurement Mission (TRMM) based on TMPA 3B43 satellite data (precipitation data) coupled with the modified Fournier index, proved to be a reliable methodology (Vrieling et al., 2010). Although, there are regions where available databases and automated data collection systems –automatic rain gauges, and real-time data transfer– provide reliable hourly or daily rainfall records, even some with 5-, 10-, or 15-minute resolution (Angulo-Martínez and Beguería, 2009; Diodato et al., 2017; Porto, 2016; Todisco et al., 2019; Yue et al., 2020), this is not the case for less technologically advanced countries (Di Raimo et al., 2018; Waltrick et al., 2015).

In Brazil, a country of continental proportions and one of the world's leading crop producers (USDA, 2020), the most reliable rainfall datasets are available on the websites of the National Water Agency (ANA, 2019), the National Institute of Meteorology (INMET, 2019), and the Centre for Monitoring and Early Warnings of Natural Disasters (Cemaden, 2019). Nevertheless, there is still a gap in utilizing the correct method for the estimation of rainfall erosivity based on the specific characteristics of the area of study (Trindade et al., 2016).

Studies conducted by Angulo-Martínez and Beguería (2009) compared different methods to estimate rainfall erosivity (R factor) and assess each of them via RUSLE. They reported some of the methods could be applied in other regions, provided the availability of high-resolution rainfall data (pluviographic data). Nearing et al. (2017) reported estimations of rainfall erosivity resulted in underestimation of soil erosion using RUSLE. Additionally, Vantas

et al. (2019) presented the correlation between the R factor and annual precipitation for several countries in the world, using parametric equations and geostatistical models. With this temporal resolution, regression models based on annual precipitation (coarser resolution) to estimate the R factor were compared by Lee and Heo (2011) using rainfall erosivity data in Korea. Thus, these methodologies have proved to be useful for the estimation of rainfall erosivity in regions with insufficient rainfall data.

It is worthy to mention that studies comparing methodologies for the estimation of rainfall erosivity are sparse. In this sense, (Ma et al., 2014) compared three models for estimating the R factor, including those proposed by Zhang et al. (2002) and (Men et al., 2008). The different methods presented discrepancies over the months of the year. Thus, alternative methods should be evaluated for accuracy as compared to the standard method.

Although there are great advancements in having readily useful rainfall erosivity data in Brazil (Oliveira et al., 2013), there are still some regions that lack reliable instrumentation and data acquisition. For these regions, we focus on identifying the best alternatives of estimating rainfall erosivity from monthly, daily, or hourly precipitation data. The objective of this work was to statistically assess alternative methods for the estimation of the R factor, as proposed by Wischmeier and Smith (1978) (WS), via a comparison of estimations using: modified Fournier (MF); modified Fournier by Zhang (MF-Z); modified Fournier by Men (MF-M); rainfall disaggregation (RD); TRMM Satellite with modified Fournier coefficient (TRMM-F); and TRMM Satellite with monthly rainfall (TRMM-M). Although, Ma et al. (2014) results were associated to climate conditions of China, we opted to test the Modified Fournier equations of Zhang et al. (2002) and Men et al. (2008) to verify if they could be useful for Southeastern Brazil conditions. These computational tools for R factor estimation can benefit different stakeholders: engineers, extensionists, policy makers, and research groups across Brazil, South America, and other tropical regions around the world.

2. Materials and Methods

2.1. Characterization of the study area

The selected study area was the municipality of Pirassununga, located in the State of São Paulo, between the coordinates of 21°50' and 22°8' south latitude and between 47°10' and 47°40' longitude WGr (Figure 1). The climate of the municipality according to Köppen classification is Cwb, *i.e.*, humid subtropical climate with dry winters and rainy summers (Alvares et al., 2013).

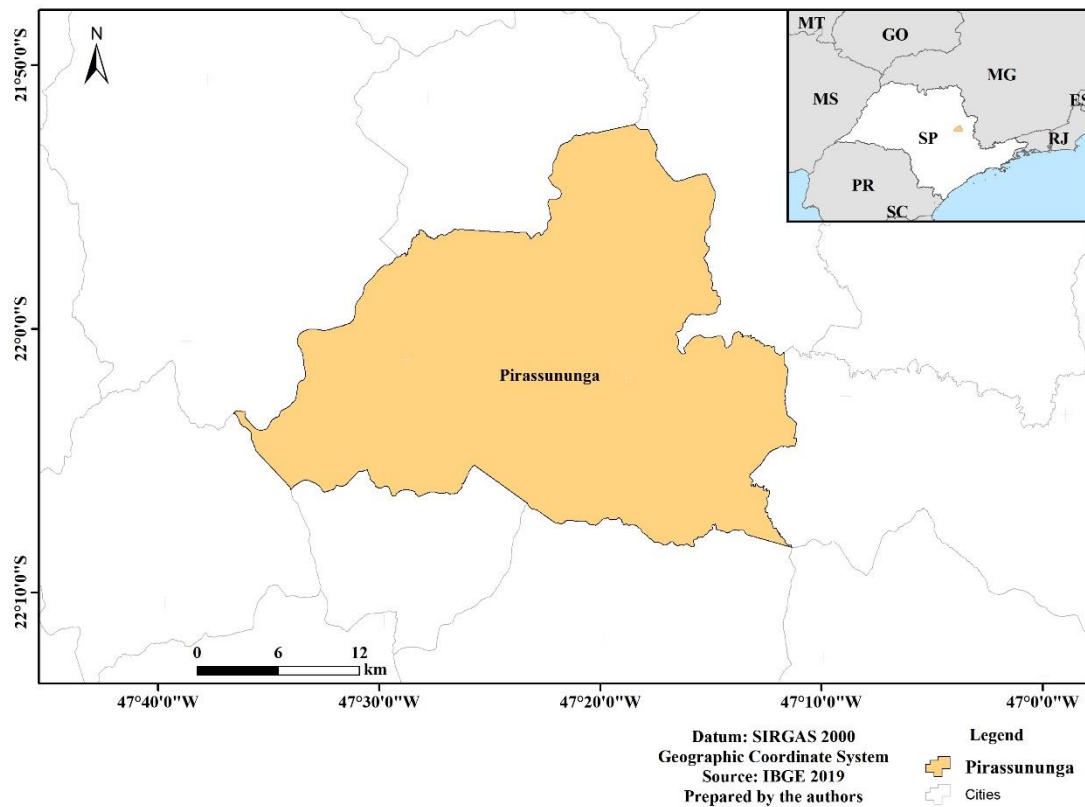


Fig. 1. Location map of the municipality of Pirassununga, in the State of São Paulo, Brazil.

The rainfall data were obtained from the Meteorological Station of the University of São Paulo (USP) located at the Fernando Costa campus, with a time series of 7 years, referring to the period from 2009 to 2015. The automatic rain gauge was configured to record frequency of rain every 10 minutes, with an accuracy of 0.1 mm.

2.2. Methods for determining rainfall erosivity

Rainfall erosivity is important for several studies (Figure 2), mainly for the area of environmental modeling, *i.e.* water erosion. This factor can be determined or estimated. Figure 2 highlights the determined EI_{30} (blue color) and estimated EI_{30} –represented by the original or modified Fournier index– (green color). Therefore, evaluating other methods for its estimation is essential to have method options for regions with a range of space-time rainfall information.

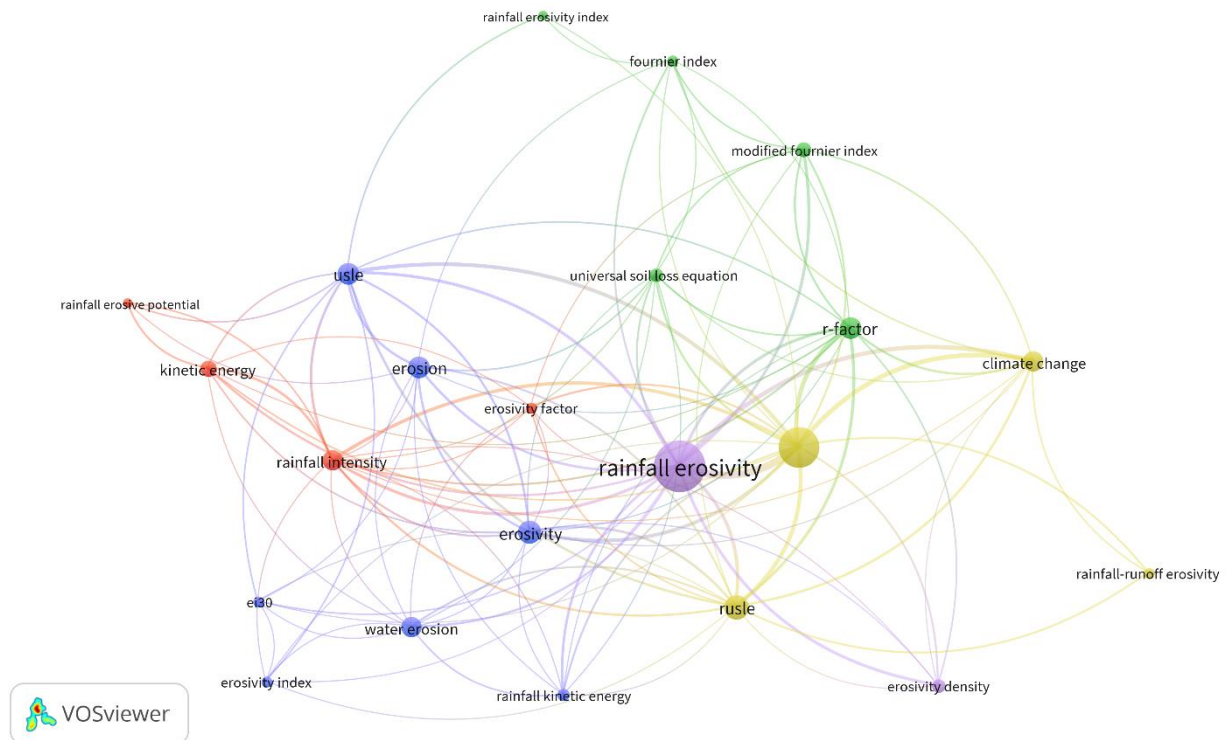


Fig. 2. Map of co-occurrence network referring to rainfall erosivity, based on the Scopus survey (02/12/2020), and elaborated in VOSviewer.

The rainfall erosivity index (R factor or EI_{30}) was estimated via a comparison of the following methods.

2.2.1. Wischmeier and Smith, WS

The methodology proposed by Wischmeier and Smith (1958), Wischmeier (1959), and Wischmeier and Smith (1978), is adopted as the standard method in this work according to studies conducted by Nearing et al. (2017). The method considers individualized events of rain, where the previous rain is separated from the subsequent one for at least 6 hours for rains up to 1 mm. The rainfall events are considered erosive for rain depths ≥ 10 mm, or rain duration ≥ 15 minutes and rain depths ≥ 6 mm (Wischmeier and Smith, 1958). The kinetic energy of rainfall was calculated by the following equation:

$$Ec = 0.119 + 0.0873 \times \log I \quad \text{Eq. 1}$$

where E_c is the kinetic energy ($\text{MJ ha}^{-1} \text{mm}^{-1}$); and I is the rainfall intensity (mm h^{-1}).

The rainfall erosivity index (EI_{30}) is the product of the kinetic energy of the rainfall event by the maximum intensity in 30 minutes (Brown and Foster, 1987).

$$EI_{30} = Ec \times I_{30} \quad \text{Eq. 2}$$

where EI_{30} is the erosivity index ($\text{MJ mm ha}^{-1} \text{ h}^{-1}$); Ec is the kinetic energy (MJ ha^{-1}); and I_{30} is the maximum intensity in 30 minutes (mm h^{-1}).

For this determination, the RainfallErosivityFactor package (Cardoso et al., 2020) was run in the R environment (R Core Team, 2020) to compute the R factor.

2.3. Methods estimating rainfall erosivity

2.3.1. Modified Fournier Index, MF

To estimate the rainfall erosivity, we first computed the rainfall coefficient of the modified Fournier index (Arnoldus, 1980) using Eq. 3.

$$MF = \sum_{i=1}^{12} \frac{p^2}{P} \quad \text{Eq. 3}$$

where MF is the rainfall coefficient (mm); p is the monthly average rainfall (mm); and P is the annual average rainfall (mm).

Subsequently, this rainfall coefficient was used to estimate the rainfall erosivity. The adjusted equation between rainfall erosivity index and rainfall coefficient for Pirassununga, SP, Brazil was calculated by Eq. 4.

$$EI_{30} = 128.39 \times MF^{0.7214} \quad \text{Eq. 4}$$

where EI_{30} is the rainfall erosivity index ($\text{MJ mm ha}^{-1} \text{ h}^{-1}$); and MF is the rainfall coefficient (mm).

2.3.2. Modified Fournier by Zhang, MF-Z

Rainfall erosivity index was obtained according to the methodology proposed by Zhang et al. (2002), with local calibrations of the parameters. The model uses daily rainfall amounts to estimate half-month rainfall erosivity. Thus, rainfall erosivity was estimated by equation 5.

$$M_i = \alpha \sum_{j=1}^k (D_j)^\beta \quad \text{Eq. 5}$$

where M_i is the half-month rainfall erosivity ($\text{MJ mm ha}^{-1} \text{ h}^{-1}$); D_j is the erosive rainfall for day j in half-month. D_j is equal to the actual rainfall, if the actual rainfall is greater than 12.7 mm, otherwise D_j is equal to zero; K is the number of days in half-month; β and α are empirical parameters adjusted locally, determined by the following equations:

$$\beta = 0.8363 + \frac{18.144}{P_{d12}} + \frac{24.455}{P_{y12}} \quad \text{Eq. 6}$$

$$\alpha = 21.586\beta^{-7.1891} \quad \text{Eq. 7}$$

where P_{d12} is the average daily rainfall greater than 12.7 mm; and P_{y12} is the annual average rainfall for days with rainfall greater than 12.7 mm.

2.3.3. Modified Fournier by Men, MF-M

In this method, Men et al. (2008) proposed an exponential equation to estimate the rainfall erosivity index by calculating the modified Fournier index (Eq. 8).

$$R_a = \alpha MF^\beta \quad \text{Eq. 8}$$

where R_a is the annual rainfall erosivity index ($\text{MJ mm ha}^{-1} \text{ h}^{-1}$); MF is the modified Fournier index calculated by Equation 3; α and β are empirical parameters. The β parameter was calculated by Equation 6, and α was determined by Equation 9.

$$\alpha = 10^{2.124 - 1.495\beta + 0.00214P_{dmax}} \quad \text{Eq. 9}$$

where P_{dmax} is the maximum daily rainfall in an average year.

2.3.4. Rainfall Disaggregation, RD

Silveira (2000) proposed disaggregation coefficients considering daily duration of rainfall totals for shorter durations (sub-event). So, to obtain daily rainfall amount, the number of erosive rains for the Pirassununga region was analyzed (Figure 3). The rainfall events are considered erosive if rain depths ≥ 10 mm, or if rain duration ≥ 15 minutes and rain depths ≥ 6 mm (Wischmeier and Smith, 1958).

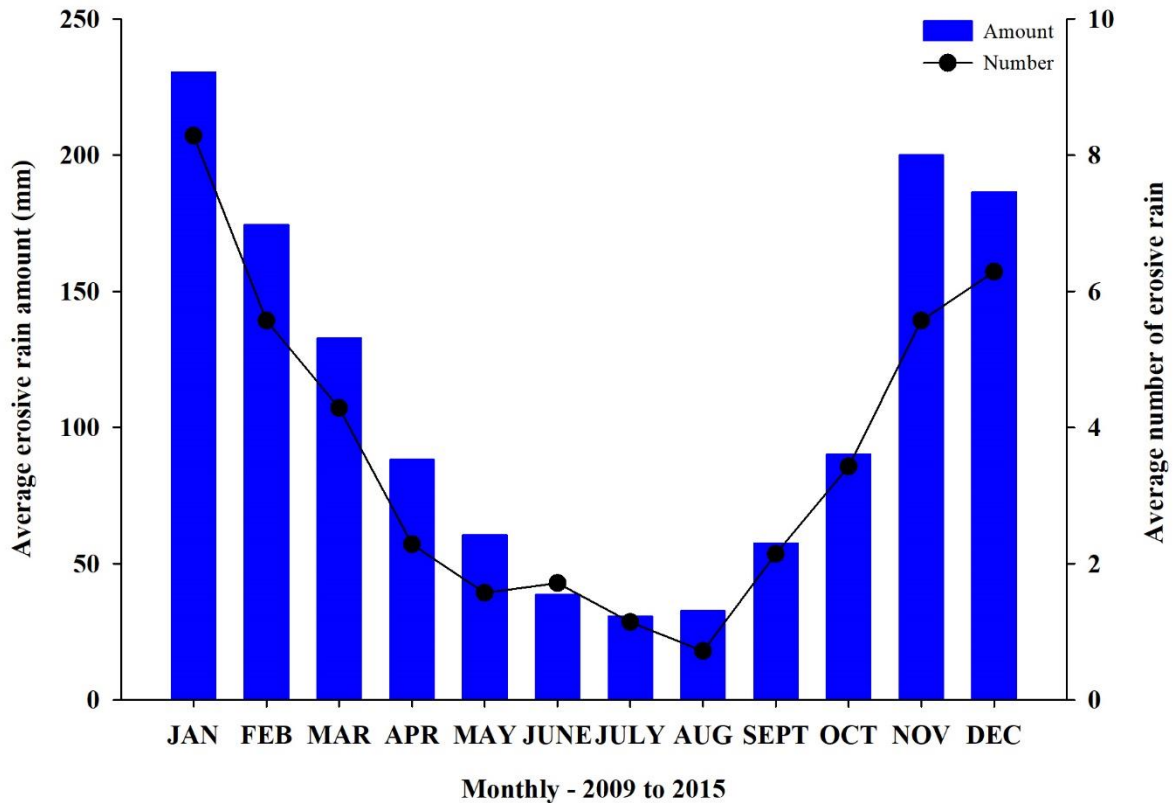


Fig. 3. Average monthly rainfall amount of erosive events, and average number of erosive rains, from 2009 to 2015, at Pirassununga, State of São Paulo, Brazil.

For months during dry season (Figure 3), the average number of rainfall events ranged from one to two events per month. Considering the rainiest months are the ones with the greatest erosion, the number of rainfall events between November and March were evaluated. Thus, six rainfall events were adopted as the average number of erosive rainfalls per month. Then, daily rainfall was computed by dividing monthly rainfall by 6. For the application of the Wischmeier and Smith (1978) methodology, the daily precipitation was disaggregated using coefficients obtained by Silveira (2000) for Brazilian rainfall characteristics. Disaggregation coefficients of 0.17 for 10-minute duration, and 0.31 for 30-minute duration were used to estimate the rainfall amount as input for equations 1 and 2, respectively (Silveira, 2000). After estimating the rainfall erosivity for such rainfall event, the value was multiplied by 6 rain events to obtain the monthly rainfall erosivity value.

2.3.5. TRMM Satellite with modified Fournier coefficient, TRMM-F

For this methodology, monthly average rainfall data (Figure 4) for Pirassununga, from 2009 to 2015, were obtained from the Tropical Rainfall Measuring Mission (TRMM) satellite. This information is available on the Giovanni platform of the National Aeronautics and Space Administration (NASA, 2019). These monthly data were transformed into 90-m spatial resolution (Figure 4).

Using the raster calculator tool of the ArcGIS 10.3 software (ESRI, 2014), the average monthly and the annual rainfall were extracted. Then, equations 3 and 4 were applied to estimate the rainfall erosivity.

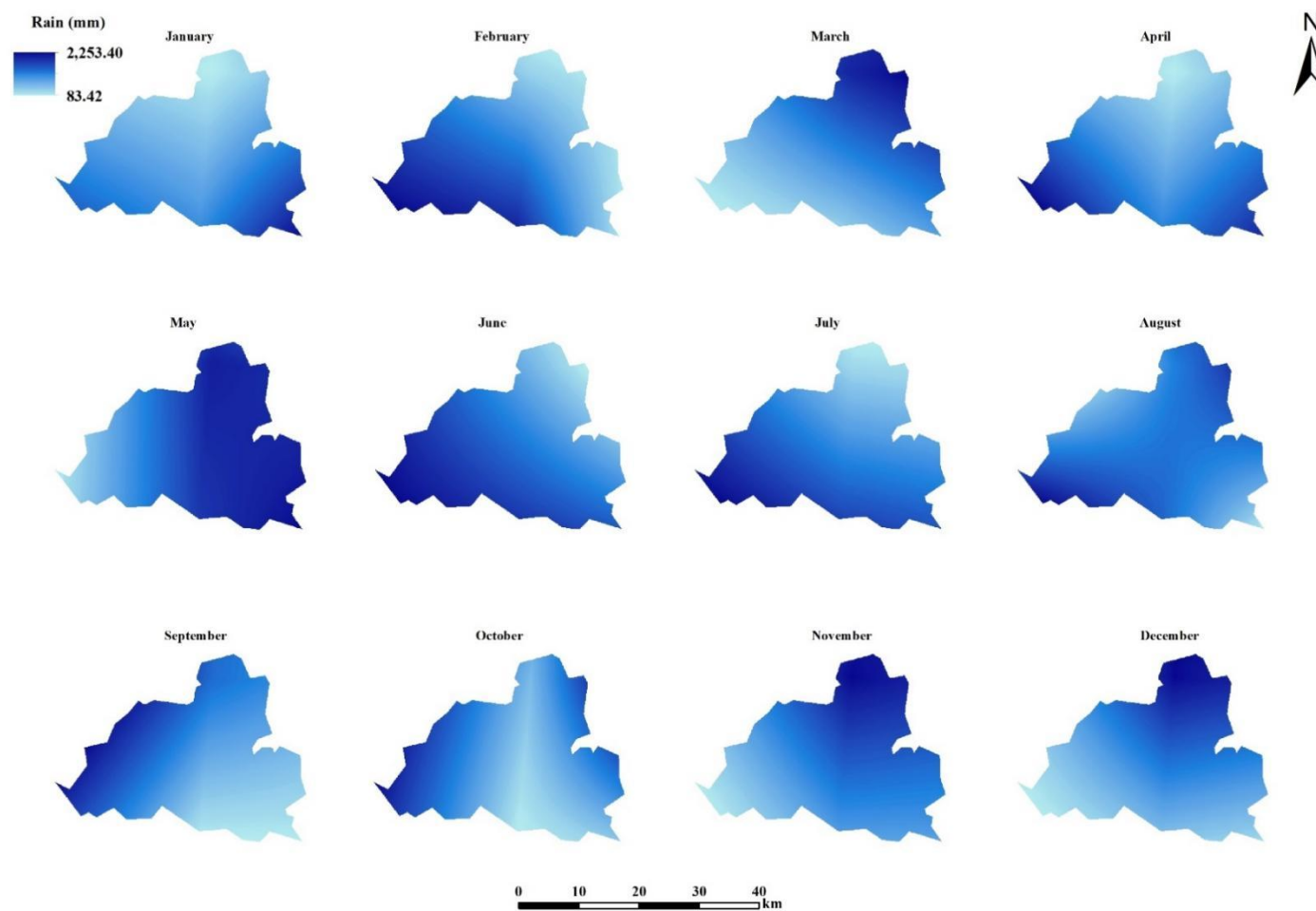


Fig. 4. Rasters referring to monthly average rainfall data (from 2009 to 2015) extracted the TRMM satellite, for Pirassununga, State of São Paulo, Brazil.

2.3.6. TRMM Satellite with monthly rainfall, TRMM-M

The average monthly rainfall amount was obtained according to the previous method, by Tropical Rainfall Measuring Mission (TRMM) satellite (Figure 4). However, rainfall erosivity was estimated by Eq. 10, which is calibrated for Pirassununga, SP and based on rainfall erosivity and average monthly rainfall.

$$EI_{30} = 7.7255 \times p - 213.75 \quad \text{Eq. 10}$$

where p is the average monthly rainfall.

2.4. Statistical assessment of the methods

After estimation of rainfall erosivity index by all different methods, a statistical assessment of these methods was performed using the Additive Main effects and Multiplicative Interaction (AMMI) model. The AMMI is a hybrid analysis that incorporates both, the additive and multiplicative, components of the two-way data structure. The AMMI model uses analysis of variance (ANOVA) followed by the principal component analysis (PCA) applied to the sums of squares allocated by the ANOVA to analyze the two factor interaction effects (Sabaghpour et al., 2012). In this work, the different methods tested correspond to the one factor and the month was the second factor. When the interaction was significant, the Scott-Knott test was performed at a 5% significance level to compare methods in each month.

The modified equation of Perkins and Jinks (1968) was applied aiming to analyze the behavior of the different methods in the estimation of the monthly rainfall erosivity over a 5-year period.

$$Y_{ij} = \mu + Me_i + Mo_j + (MeMo)_{ij} \quad \text{Eq. 11}$$

where Y_{ij} is the observation of the i -th method and j -th month; μ is the general average; Me_i is the effect of the i -th method; Mo_j is the effect of the j -th month; and $(MeMo)_{ij}$ is the effect of the interaction of the i -th method and j -th month.

The Principal Component Analysis (PCA) was applied to describe the structure of the interaction of methods and months, based on the method of least squares, allowing the experimental error to be estimated from the effect of the interaction and the application of the statistical tests. According to Hirai (2019) equation, it is possible to separate the deterministic part, given by $k=1, 2, \dots, K$ eigenvalues containing the highest variability of the interaction effect (methods x months), from the residual part (noise) $k = K+1, K+2, \dots, n$ eigenvalues with the lowest variability of the interaction effect:

$$(\widehat{ge})_{ij} = \sum_{k=1}^K \lambda_k \gamma_{ik} \delta_{jk} + \sum_{k=K+1}^n \lambda_k \gamma_{ik} \delta_{jk} = \sum_{k=1}^K \lambda_k \gamma_{ik} \delta_{jk} + \rho_{ij} \quad \text{Eq. 12}$$

where λ_k is the square root of the k -th eigenvalues of interaction (k -th singular value); γ_{ik} is the i -th element of the column vector $\overline{\gamma}_k$ associated with λ_k ; and δ_{jk} is the j -th element of the line vector $\overline{\delta}_k$ associated with λ_k .

Thus, the final AMMI model is expressed as:

$$Y_{ij} = \mu + Me_i + Mo_j + \sum_{k=1}^K \lambda_k \gamma_{Meik} \delta_{Mok} + \rho_{ij} \quad \text{Eq. 13}$$

where Y_{ij} is the response of the i -th method and j -th month; μ : general average; Me_i is the effect of the i -th method; Mo_j is the effect of the j -th month; λ_k is the square root of the k -th eigenvalues of the matrix methods x months; γ_{ik} is the i -th element of the column vector $\overline{\gamma}_k$ associated with λ_k ; δ_{jk} is the j -th element of the line vector $\overline{\delta}_k$ associated with λ_k ; and ρ_{ij} is the noise from the multiplicative part used as an error, being $\rho_{ij} \sim N(0, \sigma^2)$ considered the experimental error.

The analysis was carried out according to the AMMI model (Crossa, 1990), through the Stability Program. The Scott-Knott test was performed using the Mapgen computer program developed by Ferreira and Zambalde (1997).

3. Results

3.1. Rainfall Erosivity Estimations

According to the coefficient of determination (Table 1), all models had a good adjustment. The critical point (x -critical) of the standard model (WS) occurred at 6.99 months. This point corresponds to the derivative of the adjusted equation. In practical terms, corresponds to the lowest value of the rainfall erosivity (EI_{30}), consequently, it refers to the change in rainfall erosivity behavior. For all models tested, the inversion point occurred between the end of June and the beginning of July.

Considering the critical point for the WS (6.99 months; EI_{30} equal to 106.83 MJ mm ha⁻¹ h⁻¹), the rainfall erosivity in such point, obtained by interpolation, for the other methods, corresponded to 88.90 MJ mm ha⁻¹ h⁻¹, 53.58 MJ mm ha⁻¹ h⁻¹, 0.0 MJ mm ha⁻¹ h⁻¹, 0.0 MJ mm ha⁻¹ h⁻¹, 41.43 MJ mm ha⁻¹ h⁻¹ and 75.75 MJ mm ha⁻¹ h⁻¹ for MF, MF-Z, MF-M, RD, TRMM-F, and TRMM-M, respectively. However, the evaluation of the critical points and the respective minimum rainfall erosivity values (Table 1) revealed that the methods presented minimum

rainfall erosivity values lower than the WS, pointing out to an underestimation of such values for the peak of the dry season.

Table 1. Adjusted equations, coefficients of determination, critical points, and rainfall erosivity indexes (EI_{30} , $MJ\ mm\ ha^{-1}\ h^{-1}$) corresponding to critical point for the evaluated methods.

Methods	Equation	R^2	x-critical	EI_{30}
WS	$y = 1.6826x^3 + 23.55x^2 - 576.45x + 2410.09$	0.94	6.99	106.83
MF	$y = 0.3189x^3 + 53.512x^2 - 765.81x + 2718.40$	0.95	6.75	85.40
MF-Z	$y = 4.4793x^3 - 15.664x^2 - 481.43x + 2654.30$	0.93	7.26	47.54
MF-M	$y = -1.4409x^3 + 86.812x^2 - 938.73x + 2682.50$	0.93	6.44	0.00
RD	$y = -1.3976x^3 + 95.109x^2 - 1053.3x + 3156.6$	0.93	6.46	0.00
TRMM-F	$y = 1.7507x^3 + 29.567x^2 - 677.43x + 2734.10$	0.98	7.05	41.22
TRMM-M	$y = 2.1909x^3 + 16.871x^2 - 574.21x + 2516.90$	0.98	7.13	74.58

y = rainfall erosivity indexes; and x = months.

The fit plots (Figure 5) presented high values of coefficient of determination, varying from 0.8908 (TRMM-F method) to 0.9747 (MF method). Besides a better determination coefficient, the MF best fitted to the WS, presenting little dispersion around the 1:1 line.

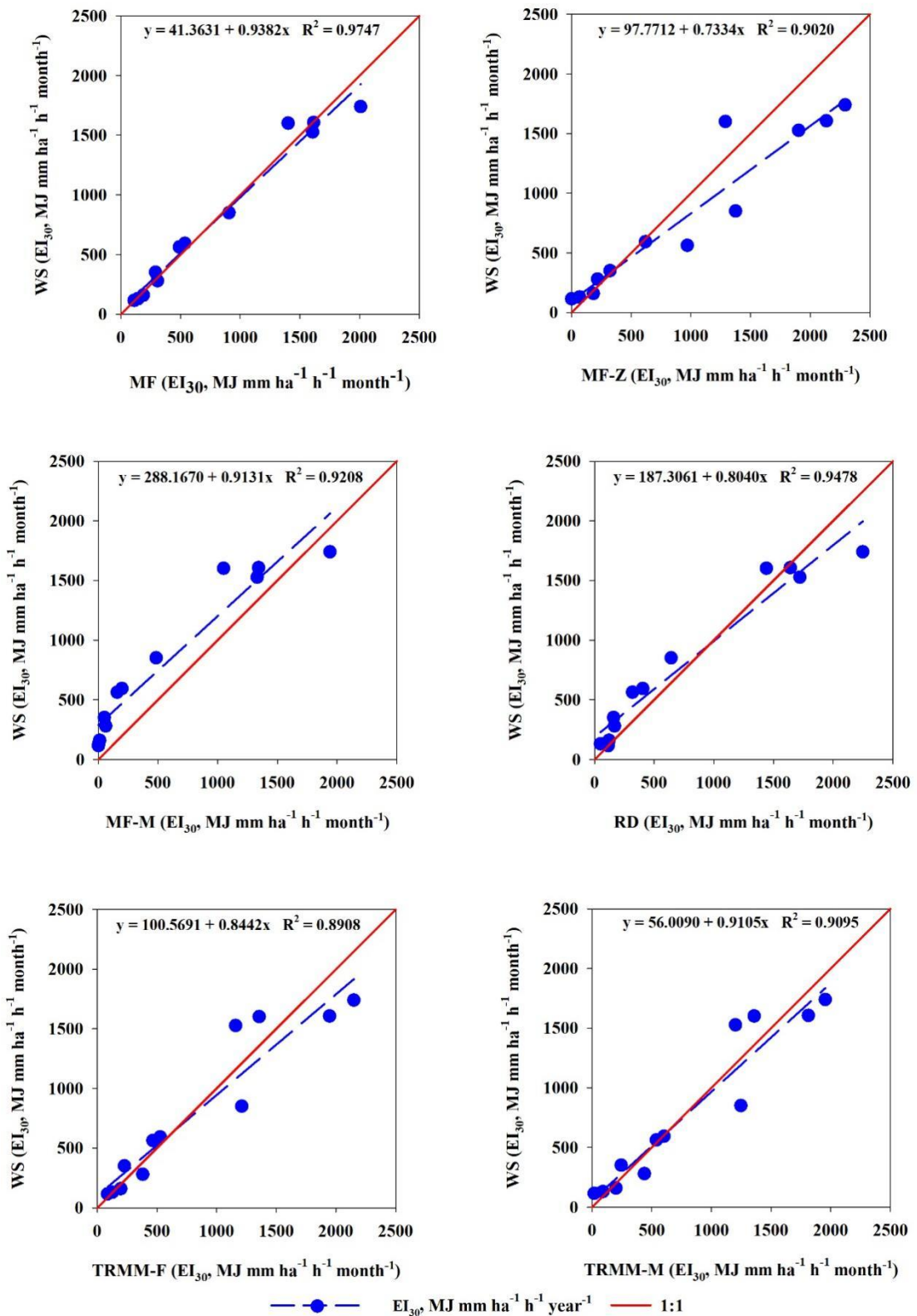


Fig. 5. Comparison between standard (WS) and other estimated rainfall erosivity (EI₃₀) methods. WS: Wischmeier and Smith; MF: modified Fournier; MF-Z: modified Fournier by Zhang; MF-M: modified Fournier by Men; RD: Rainfall Disaggregation; TRMM-F: TRMM-M Satellite.

The method MF-Z showed overestimation of the rainfall erosivity values (Figure 5) when compared to the WS, particularly for higher rainfall erosivity values, which are of paramount importance to predict water erosion. Conversely, the MF-M underestimated the rainfall erosivity, it is noteworthy that the method shifted the adjustment above to the 1:1 line, underestimating the rainfall erosivity values, but maintaining the same proportion, both for higher and lower EI₃₀ values.

The methods based on obtaining rainfall data by satellite or by disaggregation, also showed good adjustments (Figure 5). However, compared to the MF method, the rainfall erosivity estimation showed greater dispersion around the 1:1 line. In these cases, both methods (RD, TRMM-F and TRMM-M) may be inaccurate for the most extreme rainfall erosivity values.

3.2. Statistical Comparison of Methods

The selected methods were further classified by grouping, through the principal component analysis (Table 2) for rainfall erosivity and the Scott-Knott test –AMMI technique. The interaction of the methods with the months was significant at the 5% level (Table 3). Therefore, the methods responded differently for the analyzed months.

Table 2. Percentages of the sum of total squares (methods x months) associated to each main axis, being the individual and accumulated values according to AMMI analysis for the standard method (WS) and the other methods (MF, MF-Z, MF-M, RD, TRMM-F, and TRMM-M) use to estimate the rainfall erosivity of Pirassununga-SP.

Principal component	% Explanation	% Accumulated explanation
PC1	47.44	47.44
PC2	32.43	79.87
PC3	15.73	95.60
PC4	3.48	99.08
PC5	0.86	99.94
PC6	0.06	100.00

Table 3. Summary of the analysis of variance and mean squares associated with the effect of the interaction between methods and months, referring to the rainfall erosivity of Pirassununga-SP.

Source	GL	QM	Fc	Pr>Fc
Methods	6	167056.6107	55.23	0.00*
Monthly	11	3491670.0616	1154.36	0.00*
Methods x Monthly	42	37554.72892	12.42	1.00e ⁻⁸ *
Residual	24	3024.7772		

The principal components, PC1, and PC2, explained together 79.87% of the variation in rainfall erosivity, being 47.44% and 32.43% explained by PC1 and PC2, respectively (Table 2).

The AMMI technique provides a joint analysis of ANOVA and principal component analysis. In this way, the level of significance of the parameters was separated from the interaction between them, in this case, utilized methods and months. The formed groups indicated that the methods belong to the same group and are statistically equal, *i.e.*, they do not differ from each other. In this work, for all the methods compared, the WS method was considered the baseline –blue color– (Figures 6, 7, and 8), this way the compared methods were grouped as 1) statistically equal, 2) methods that underestimate, or 3) methods that overestimate.

Considering the month of January (Figure 6), the methods were divided into 3 groups. The method considered standard (WS) was the only one in group 1. Thus, all methods assessed overestimated the rainfall erosivity, being statistically grouped into Group 2: MF-M, TRMM-M, and MF methods; and Group 3: TRMM-F, RD, and MF-Z –greater overestimation than Group 2– methods.

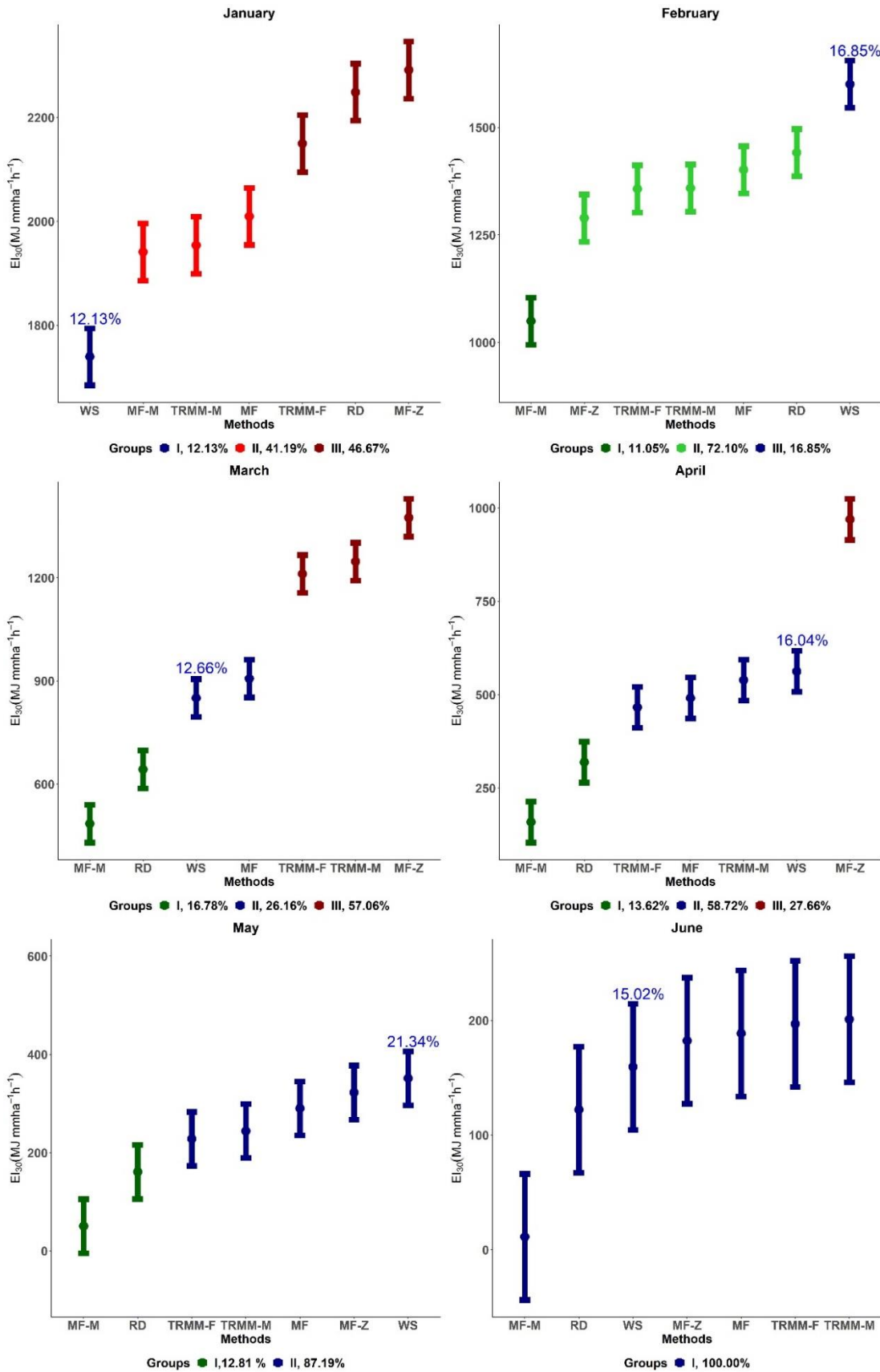


Fig. 6. The univariate grouping of methods of estimation of the monthly rainfall erosivity indexes (January to June), by Scott and Knott (1974), with a Chi-squared significance level of 5%.

Considering the month of February (Figure 6), methods were statistically grouped into Group 1: MF-M –greatest underestimation–; Group 2: MF-Z, TRMM-F, TRMM-M, MF, and RD; and Group 3: WS-standard method. Conversely to January, for this month all methods underestimated the rainfall erosivity indexes.

Taking into account the March month (Figure 6), the methods were separated into three groups. The first group underestimated the EI_{30} (MF-M and RD), the second group was statistically equal (WS and MF) and the third one overestimated the rainfall erosivity indexes (TRMM-F, TRMM-M and MF-Z).

As well as March, for the month of April (Figure 6), the methods were also classified into three groups. Group 1 (MF-M and RD), Group 2 (TRMM-F, MF, TRMM-M, and WS) and Group 3 (MF-Z). For this month, the MF-M and RD methods underestimated, and the MF-Z method overestimated the rainfall erosivity index values.

Concerning to May (Figure 6), the methods were stratified by only two groups (Figure 5), with underestimating rainfall erosivity values in Group 1 (MF-M and RD), and considered equal values for Group 2 (TRMM-F, TRMM-M, MF, MF-Z, and WS).

For the driest period of the year –June (Figure 6), July and August (Figure 7)–, there was no statistical difference between the methods evaluated and the standard one (WS).

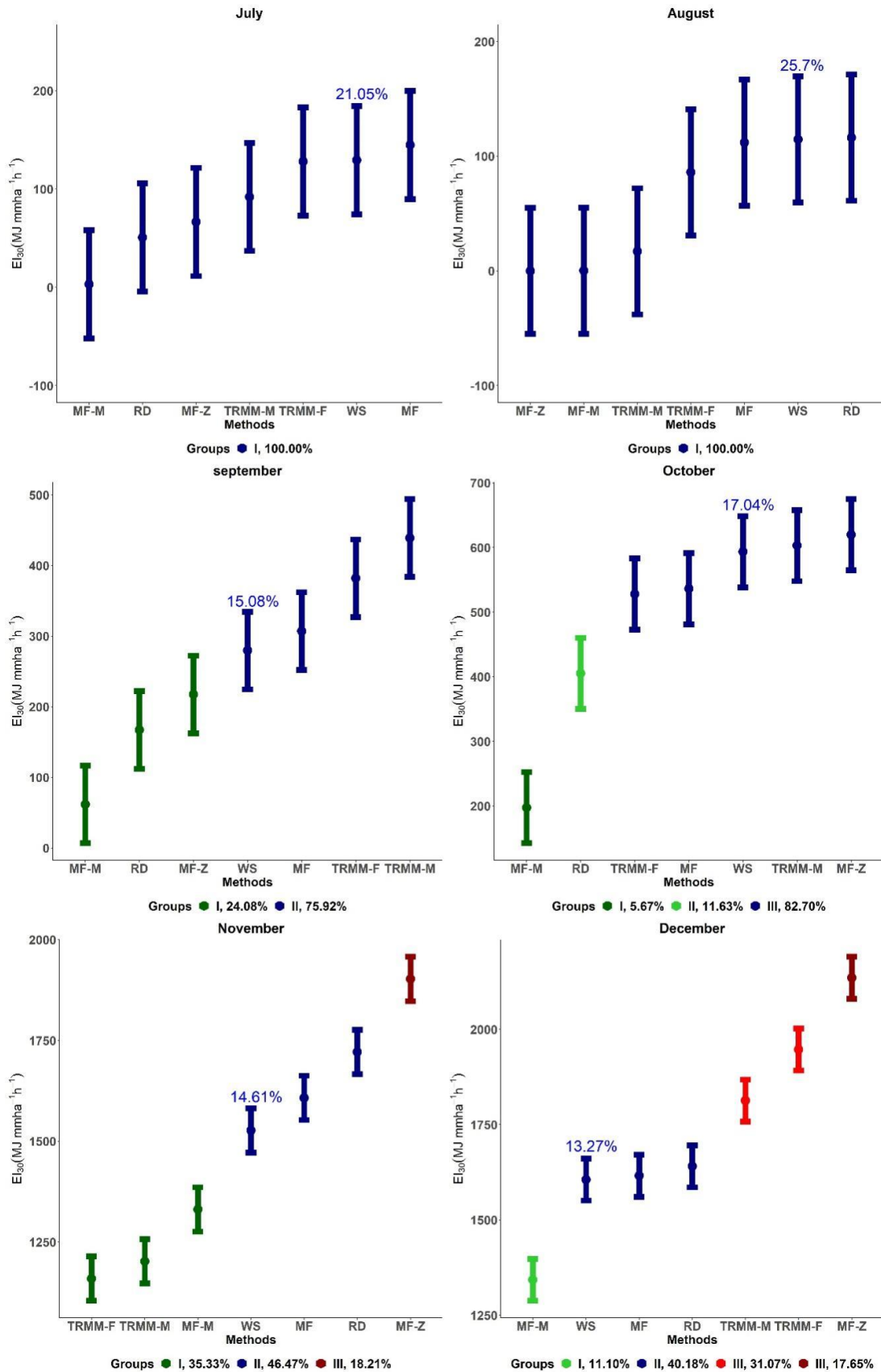


Fig. 7. The univariate grouping of methods for estimation of the monthly rainfall erosivity indexes (July to December), by Scott and Knott (1974), with a Chi-squared significance level of 5%.

For the month of September (Figure 7), the MF-M, RD, and MF-Z methods (Group 1) underestimated the EI_{30} , while the other methods (MF, TRMM-F, and TRMM-M) showed to be equal to the WS.

Considering the month of October (Figure 7), there were three groups. The methods TRMM-F, MF, TRMM-M, and MF-Z (Group 3) were equal to the WS. The methods MF-M (Group 1) and RD (Group 2) underestimated the rainfall erosivity index values.

For November (Figure 7), the groups were classified as 1 (TRMM-F, TRMM-M, and MF-M), 2 (WS, MF, and RD), and 3 (MF-Z). The WS belongs to group 2, therefore group 1 underestimated and group 3 overestimated the rainfall erosivity values.

Finally, for December (Figure 7), the methods were classified in Group 1 (MF-M), Group 2 (WS, MF, and RD), Group 3 (TRMM-F and TRMM-M) and Group 4 (MF-Z), being the values of the rainfall erosivity index underestimated by Group 1 and overestimated by Groups 3 and 4 in comparison to the WS method.

For the rainy season (November to March), the MF method was statistically equal or grouped very close to the WS (Figures 6 and 7), reflecting the adequate fit between them (Figure 5). Therefore, in this period, with a lack of more detailed rainfall data –short intervals–, the MF method can replace the WS with accuracy. For the dry season, methods did not differ from WS.

The annual rainfall erosivity or R Factor was classified into 2 groups (Figure 8), with Group 1 represented by the MF-M method, and Group 2 represented by the RD, WS, MF, TRMM-M, TRMM-F, and MF-Z methods. Group 1 underestimated the rainfall erosivity values in relation to the WS. By analyzing the 1:1 fitting line (Figure 5), the predictions were parallel to the line. However, for the other methods (Figure 5), the estimates always crossed the 1:1 line, which means under or overestimation according to higher or lower rainfall erosivity values.

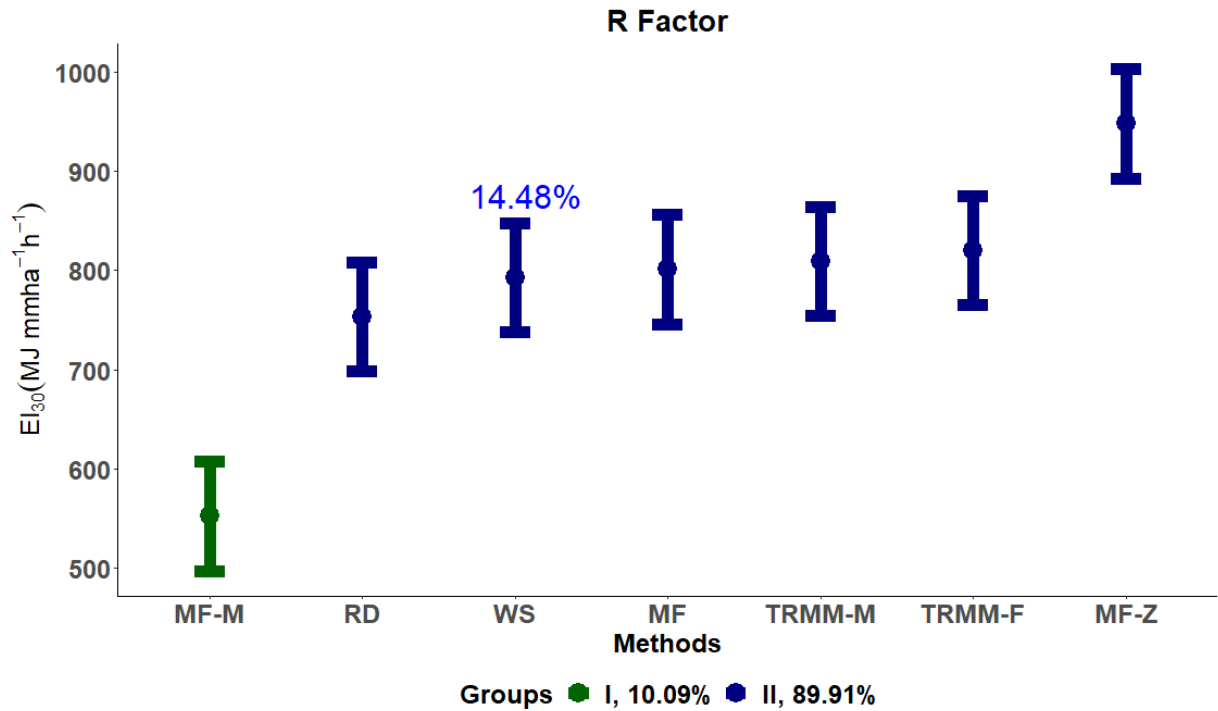


Fig. 8. The univariate grouping of methods for estimation of the rainfall erosivity (R Factor), by Scott and Knott (1974), with a Chi-squared significance level of 5%.

In general, regardless of the estimated rainfall erosivity values (monthly or annual) (Figures 6, 7, and 8), the MF-M and MF-Z methods underestimated and overestimated EI₃₀ values in relation to the WS method, respectively. The MF method showed to be always closer to the standard method (Figures 6, 7, and 8).

4. Discussion

According to our results, rainfall erosivity estimates are a reliable alternative to the product of kinetic energy and intensity of the rain. Regardless of the way employed, R factor and its estimates were low between June and August, these months corresponded to the dry season. Additionally, coarse temporal resolution of the data, such as monthly data in relation to the sub-event intervals, can result in low estimated values for rainfall erosivity. The monthly evaluation of rainfall erosivity index is important for the planning of farmers' activities on a small-time scale, while the total annual soil and water losses estimation is crucial to assess the impacts of the cultivations for the correct management and adoption of conservation practices.

The irregular distribution of weather stations, lack of maintenance and failure of older stations, together with little automated data acquisition systems in place are some problems which can be easily overcome by using precipitation data from TRMM 3B42-v7 (Galvão et al.,

2020). These authors compared rainfall stations data –only the ones with continuous rainfall data– to the data extracted from the TRMM; they found these data could be reliable and useful in regions with no pluviometric stations installed. Similarly, we found the usage of TRMM 3B42-v7 data to estimate rainfall erosivity using two adjusted equations for Pirassununga, SP resulted in useful estimates for annual rainfall erosivity values. Li et al. (2020), mapping rainfall erosivity with TRMM in China, found underestimations when precipitation data pointed to high rainfall erosivity, while overestimating when rain data pointed to the opposite (low rainfall erosivity). However, for tropical conditions, our results pointed to an opposite trend.

An innovation for the assessment of different methodologies was the usage of the Additive Main effects and Multiplicative Interaction (AMMI) model. This AMMI model is a hybrid analysis that incorporates both, the additive and multiplicative, components of the two-way data structure. Other studies have used other statistical methodologies to determine the accuracy of the estimates between methods: mean square root error, mean absolute percentage, correlation coefficient, or determination coefficient (Lee and Heo, 2011; Ma et al., 2014; Vantas et al., 2019; Li et al., 2020). The AMMI model allowed us to apply in tandem the ANOVA and PCA to the sums of squares allocated by the ANOVA to analyze the two factor interaction effects. This way we verified the efficiency of the methods, while statistically grouping them and identifying them as more or less reliable estimates of rainfall erosivity (R factor).

According to our results, the modified Fournier (MF) index was the closest estimate to rainfall erosivity. This is in accordance with those results of Oğuz (2019), while it opposes to what Angulo-Martínez and Beguería (2009) reported. Using the unit kinetic energy calculation of the RUSLE model, the MF index underestimated rainfall erosivity for the Ebro basin in Spain (Angulo-Martínez and Beguería, 2009). Nearing et al. (2017) compared three different methodologies (USLE, RUSLE and RUSLE2) to calculate the kinetic energy, and results showed the kinetic energy values determined by the RUSLE method were underestimating as compared to USLE and RUSLE2. Thus, it is possible that discordance with Angulo-Martínez and Beguería (2009) may be due to an embedded underestimation of the kinetic energy due to RUSLE methodology. Although there was still no test of the effectiveness of the modified Fournier index –until this study–, MF method has been used for Brazilian conditions as a rainfall erosivity estimator in several parts of the country, as the States of Santa Catarina (Back et al., 2018), Espírito Santo (Moreira et al., 2020), Tocantins (Avanzi et al., 2019), Mato Grosso (Di Raimo et al., 2018), São Paulo (Lombardi Neto, 1977), and Amazonas (Silva et al., 2020), along with large areas for regional studies (Mello et al., 2013, 2015; Oliveira et al., 2013).

Annual rainfall erosivity was overestimated by MF-Z (Zhang et al., 2002) and underestimated by MF-M (Men et al., 2008). These methods were developed for other climatic conditions, helping to explain such results. The other methods (MF, RD, TRMM-F, and TRMM-M) used local rain characteristics, improving the estimations. Our results agreed well with those of Ma et al. (2014), as they presented negative values of MSDE; nevertheless, MF-M had lower absolute MSDE and RMSE values than MF-Z.

Finally, usage of precipitation data obtained by TRMM proved to be a viable alternative to estimate annual rainfall erosivity. Our results were in accordance with those reported in other parts of the world (Fan et al., 2013; Vrieling et al., 2010). For African climatic conditions, the best performance was obtained using the MF index derived from monthly data from TRMM Multisatellite Precipitation Analysis (TMPA) 3B43 (Vrieling et al., 2010). In our work, usage of this product in an adjusted equation based on the MF was less accurate as an estimator (R-squared values around to 0.9), although it would be useful for locations with scarce or irregular pluviographic or pluviometric data. Thus, regions with small number of meteorological stations can very well use precipitation data obtained by TRMM as a viable alternative for R factor estimation.

5. Conclusions

The best tested method for rainfall erosivity estimation was the Modified Fournier Index, showing great potential to substitute the standard method in the absence of more detailed rainfall data.

For monthly and annual estimations, the methods modified Fournier by Men and modified Fournier by Zhang underestimated and overestimated the values of rainfall erosivity indexes in relation to the Wischmeier and Smith method (standard), respectively.

For locations without any on-site rainfall instrumentation, the rainfall data obtained through satellite (TRMM) may be a viable alternative, since its annual rainfall erosivity estimation was situated in the same statistical group as the standard method. Nevertheless, inaccuracy was observed for monthly estimates.

For the months of low rainfall erosivity (June to August) the methods of estimating rainfall erosivity were not different to the standard one, so any method could be potentially adopted.

Heterogeneous performance in the estimation of monthly rainfall erosivity was observed by the analyzed methods depending on the data associated to rainy or dry seasons.

References

- Alvares, C.A., Stape, J.L., Sentelhas, P.C., Gonçalves, J.L. de M., Sparovek, G., 2013. Köppen's climate classification map for Brazil. *Meteorol. Zeitschrift* 22, 711–728. <https://doi.org/10.1127/0941-2948/2013/0507>.
- AGÊNCIA NACIONAL DE ÁGUAS E SANEAMENTO BÁSICO - ANA (Brasil) 2019. **Sistema Nacional de Informações sobre Recursos Hídricos - SNIRH**. Módulo Hidroweb, Brasília: ANA, 2020. <http://www.snirh.gov.br/hidroweb/>. Accessed 01.04.2019.
- Angulo-Martínez, M., Beguería, S., 2009. Estimating rainfall erosivity from daily precipitation records: A comparison among methods using data from the Ebro Basin (NE Spain). *J. Hydrol.* 379, 111–121. <https://doi.org/10.1016/j.jhydrol.2009.09.051>.
- Arnoldus, H.M.J., 1980. An approximation of the rainfall factor in the Universal Soil Loss Equation. *An Approx. rainfall factor Univers. Soil Loss Equation.* 127–132.
- Avanzi, J.C., Viola, M.R., Mello, C.R. de, Giongo, M.V., Pontes, L.M., 2019. Modeling of the rainfall and R-Factor for Tocantins state, Brazil. *Rev. Bras. Ciência do Solo* 43, 1–14. <https://doi.org/10.1590/18069657rbcs20190047>.
- Back, Á.J., Alberton, J.V., Poletto, C., 2018. Erosivity index and characteristics of erosive rainfall from the far western region of Santa Catarina, Brazil. *J. Environ. Eng.* 144, 04018049. [https://doi.org/10.1061/\(ASCE\)EE.1943-7870.0001388](https://doi.org/10.1061/(ASCE)EE.1943-7870.0001388).
- Brown, L.C., Foster, G.R., 1987. Storm erosivity using idealized intensity distributions. *Trans. ASAE* 30, 379–386. <https://doi.org/10.13031/2013.31957>.
- Cardoso, D.P., Silva, E.M., Avanzi, J.C., Muniz, J.A., Ferreira, D.F., Silva, M.L.N., Acuña-Guzman, S.F., Curi, N., 2020. RainfallErosivityFactor: An R package for rainfall erosivity (R-factor) determination. *Catena* 189, 104509. <https://doi.org/10.1016/j.catena.2020.104509>.
- CENTRO NACIONAL DE MONITORAMENTO E ALERTAS DE DESASTRES NATURAIS - Cemaden 2019. Mapa Interativo. São José dos Campos: Cemaden, 2020. <http://www.cemaden.gov.br/mapainterativo/>. Accessed 01.04.2019.
- Crossa, J., 1990. Statistical Analyses of Multilocation Trials, in: *Advances in Agronomy*. pp. 55–85. [https://doi.org/10.1016/S0065-2113\(08\)60818-4](https://doi.org/10.1016/S0065-2113(08)60818-4).
- Di Raimo, L.A.D.L., Amorim, R.S.S., Couto, E.G., Nóbrega, R.L.B., Torres, G.N., Bocuti, E.D., Almeida, C.O.S., Rodrigues, R.V., 2018. Spatio-temporal variability of erosivity in Mato Grosso, Brazil. *Rev. Ambient. e Água* 13, e2276. <https://doi.org/10.4136/ambi-agua.2276>.
- Diodato, N., Bellocchi, G., 2010. MedREM, a rainfall erosivity model for the Mediterranean region. *J. Hydrol.* 387, 119–127. <https://doi.org/10.1016/j.jhydrol.2010.04.003>.
- Diodato, N., Borrelli, P., Fiener, P., Bellocchi, G., Romano, N., 2017. Discovering historical rainfall erosivity with a parsimonious approach: A case study in Western Germany. *J. Hydrol.* 544, 1–9. <https://doi.org/10.1016/j.jhydrol.2016.11.023>.
- Diodato, N., Knight, J., Bellocchi, G., 2013. Reduced complexity model for assessing patterns of rainfall erosivity in Africa. *Glob. Planet. Change* 100, 183–193. <https://doi.org/10.1016/j.gloplacha.2012.10.016>.

- Duarte, M.L., Silva Filho, E.P. da, 2019. Estimativa da erosividade da chuva na bacia hidrográfica do rio Juma com base em dados do satélite TRMM. *Cad. Geogr.* 29, 45–60. <https://doi.org/10.5752/p.2318-2962.2019v29n56p45>.
- ENVIRONMENTAL SYSTEMS RESEARCH INSTITUTE - ESRI, 2014. ArcGIS 10.3 software. <http://www.esri.com/software/arcgis>.
- Fan, J., Chen, Y., Yan, D., Guo, F., 2013. Characteristics of rainfall erosivity based on Tropical Rainfall Measuring Mission data in Tibet, China. *J. Mt. Sci.* 10, 1008–1017. <https://doi.org/10.1007/s11629-013-2378-1>.
- Ferreira, D.F., Zambalde, A.L., 1997. Simplificação das análises de algumas técnicas especiais da experimentação agropecuária no Mapgen e softwares correlatos, in: Congresso Da Sociedade Brasileira de Informática Aplicada à Agropecuária e Agroindústria. pp. 285–291.
- Fournier, F., 1960. *Climat et érosion: la relation entre l'érosion du sol par l'eau et les précipitations atmosphériques*, Presses universitaires de France, Paris, France.
- Galvão, J.M.F., Duarte, M.L., Castro, A.L. de, Silva, T.A. da, Valente, K.S., 2020. Statistical evaluation between the estimates of precipitation of the TRMM satellite and surface stations: An analysis to the Mesoregion sul Amazonense. *J. Hyperspectral Remote Sens.* 10, 108–116. <https://doi.org/10.29150/jhrs.v10.2.p108-116>.
- Hirai, W.Y., 2019. Caracterização da estrutura de interação genótipo e ambiente utilizando modelo AMMI e W-AMMI por meio de biplot. Doctoral dissertation. Universidade de São Paulo. 2019. 65p.
- INSTITUTO NACIONAL DE METEOROLOGIA - INMET 2019. Banco de Dados Meteorológicos para Ensino e Pesquisa-BDMEP. Brasília: INMET, 2020. <https://bdmep.inmet.gov.br/>. Accessed 01.04.2019.
- Lee, J.-H., Heo, J.-H., 2011. Evaluation of estimation methods for rainfall erosivity based on annual precipitation in Korea. *J. Hydrol.* 409, 30–48. <https://doi.org/10.1016/j.jhydrol.2011.07.031>.
- Li, X., Li, Z., Lin, Y., 2020. Suitability of TRMM Products with Different Temporal Resolution (3-Hourly, Daily, and Monthly) for Rainfall Erosivity Estimation. *Remote Sens.* 12, 3924. <https://doi.org/10.3390/rs12233924>.
- Lombardi Neto, F., 1977. Rainfall erosivity-its distribution and relationship with soil loss at Campinas, Brazil. Doctoral dissertation. West Lafayette, Purdue University, 1977. 53p.
- Ma, X., He, Y., Xu, J., van Noordwijk, M., Lu, X., 2014. Spatial and temporal variation in rainfall erosivity in a Himalayan watershed. *Catena* 121, 248–259. <https://doi.org/10.1016/j.catena.2014.05.017>.
- Mello, C.R., Viola, M.R., Beskow, S., Norton, L.D., 2013. Multivariate models for annual rainfall erosivity in Brazil. *Geoderma* 202–203, 88–102. <https://doi.org/10.1016/j.geoderma.2013.03.009>.
- Mello, C.R. de, Viola, M.R., Owens, P.R., Mello, J.M. de, Beskow, S., 2015. Interpolation methods for improving the RUSLE R-factor mapping in Brazil. *J. Soil Water Conserv.* 70, 182–197. <https://doi.org/10.2489/jswc.70.3.182>.
- Men, M., Yu, Z., Xu, H., 2008. Study on the spatial pattern of rainfall erosivity based on

- geostatistics in Hebei Province, China. *Front. Agric. China* 2, 281–289.
<https://doi.org/10.1007/s11703-008-0042-2>.
- Moraes, B.C., Sodré, G.R.C., Souza, E.B., Ribeiro, J., Meira Filho, L.G., Ferreira, D., 2015. Climatologia da precipitação na Amazônia. *Rev. Bras. Geogr. Física* 8, 1359–1373.
- Moreira, L.L., Novais, R.R., Schwambach, D., Carvalho Júnior, S.M. de, 2020. Spatial–temporal dynamics of rainfall erosivity in the state of Espírito Santo (Brazil) from remote sensing data. *World J. Sci. Technol. Sustain. Dev.* 17, 297–309.
<https://doi.org/10.1108/wjtsd-08-2019-0059>.
- NATIONAL AERONAUTICS AND SPACE ADMINISTRATION - NASA. Giovanni. TRMM 3B43_7. 2020. Data Tropical Rainfall Measuring Mission -TRMM. URL <https://giovanni.gsfc.nasa.gov/giovanni/>. Accessed 16.12.2020.
- Nearing, M.A., Yin, S., Borrelli, P., Polyakov, V.O., 2017. Rainfall erosivity: An historical review. *Catena* 157, 357–362. <https://doi.org/10.1016/j.catena.2017.06.004>.
- Oğuz, I., 2019. Rainfall erosivity in north-central Anatolia in Turkey. *Appl. Ecol. Environ. Res.* 17, 2719–2731. https://doi.org/10.15666/aer/1702_27192731.
- Oliveira, P.T.S., Wendland, E., Nearing, M.A., 2013. Rainfall erosivity in Brazil: A review. *Catena* 100, 139–147. <https://doi.org/10.1016/j.catena.2012.08.006>.
- Perkins, J.M., Jinks, J.L., 1968. Environmental and genotype-environmental components of variability: III. Multiple lines and crosses. *Heredity (Edinb)*. 23, 339–356.
<https://doi.org/10.1038/hdy.1969.11>.
- Porto, P., 2016. Exploring the effect of different time resolutions to calculate the rainfall erosivity factor R in Calabria, southern Italy. *Hydrol. Process.* 30, 1551–1562.
<https://doi.org/10.1002/hyp.10737>.
- R Core Team, 2020. R: A Language and Environment for Statistical Computing.
- Renard, K.G., Freimund, J.R., 1994. Using monthly precipitation data to estimate the R-factor in the revised USLE. *J. Hydrol.* 157, 287–306. [https://doi.org/10.1016/0022-1694\(94\)90110-4](https://doi.org/10.1016/0022-1694(94)90110-4).
- Sabaghpour, S.H., Razavi, F., Danyali, S.F., Tobe, D., Ebadi, A., 2012. Additive main effect and multiplicative interaction analysis for grain yield of Chickpea (*Cicer arietinum* L.) in Iran. *Int. Sch. Res. Netw.* 1–6. <https://doi.org/10.5402/2012/639381>.
- Scott, A.J., Knott, M., 1974. A cluster analysis method for grouping means in the analysis of variance. *Biometrics* 507–512.
- Silva, D.S. dos S., Blanco, C.J.C., Santos Junior, C.S. dos, Martins, W.L.D., 2020. Modeling of the spatial and temporal dynamics of erosivity in the Amazon. *Model. Earth Syst. Environ.* 6, 513–523. <https://doi.org/10.1007/s40808-019-00697-6>.
- Silveira, A.L.L. da, 2000. Equação para os coeficientes de desagregação de chuva. *Rev. Bras. Recur. Hídricos* 5, 143–147.
- Todisco, F., Vergni, L., Vinci, A., Pampalone, V., 2019. Practical thresholds to distinguish erosive and rill rainfall events. *J. Hydrol.* 579, 124173.
<https://doi.org/10.1016/j.jhydrol.2019.124173>.
- Trindade, A.L.F., Oliveira, P.T.S. de, Anache, J.A.A., Wendland, E., 2016. Variabilidade

espacial da erosividade das chuvas no Brasil. *Pesqui. Agropecuária Bras.* 51, 1918–1928. <https://doi.org/10.1590/s0100-204x2016001200002>.

USDA, 2020. World Agricultural Production.

Vantas, K., Sidiropoulos, E., Evangelides, C., 2019. Rainfall erosivity and its estimation: Conventional and machine learning methods, in: *Soil Erosion-Rainfall Erosivity and Risk Assessment*. IntechOpen. 19p.

Vrieling, A., Sterk, G., Jong, S.M. de, 2010. Satellite-based estimation of rainfall erosivity for Africa. *J. Hydrol.* 395, 235–241. <https://doi.org/10.1016/j.jhydrol.2010.10.035>.

Waltrick, P.C., Machado, M.A. de M., Dieckow, J., Oliveira, D. de, 2015. Estimativa da erosividade de chuvas no estado do Paraná pelo método da pluviometria: Atualização com dados de 1986 a 2008. *Rev. Bras. Cienc. do Solo* 39, 256–267. <https://doi.org/10.1590/01000683rbc20150147>.

Wischmeier, W.H., 1959. A rainfall erosion index for a Universal Soil-Loss Equation. *Soil Sci. Soc. Am. J.* 23, 246–249. <https://doi.org/10.2136/sssaj1959.03615995002300030027x>.

Wischmeier, W.H., Smith, D.D., 1978. Predicting rainfall erosion losses: A guide to conservation planning, *Agriculture Handbook Number 537*.

Wischmeier, W.H., Smith, D.D., 1958. Rainfall energy and its relationship to soil loss. *Trans. Am. Geophys. Union* 39, 285–291. <https://doi.org/10.1029/TR039i002p00285>.

Yue, T., Xie, Y., Yin, S., Yu, B., Miao, C., Wang, W., 2020. Effect of time resolution of rainfall measurements on the erosivity factor in the USLE in China. *Int. Soil Water Conserv. Res.* 8, 373–382. <https://doi.org/10.1016/j.iswcr.2020.06.001>.

Zhang, W.-B., Xie, Y., Liu, B.-Y., 2002. Rainfall erosivity estimation using daily rainfall amounts. *Sci. Geogr. Sin.* 22, 705–711.

**Article III - Machine Learning Assessment of the Soil Erosion Modeling using RUSLE:
A case study in a sub-basin on the Upper Tocantins River, Brazil**

(Article elaborated according to standards of the Journal Catena, ISSN: 0341-8162)

Abstract

Water erosion leads to removal of soil particles from a high positions in the landscape to low positions. The erosive process modify as land use and soil cover changes through conversion of forest to pasture and agricultural crops. The aim was to assess the soil losses and sediment export –considering land use in the chronological scenarios of 1990, 2000, 2010, and 2017– for the Peixe Angical Reservoir drainage basin on the Upper Tocantins River, Brazil; identify priority areas –considering soil losses– in need of soil and water conservation practices; and to apply a statistical analysis –using RF algorithm– to assess the contribution and importance of the RUSLE factors (R, K, LS, and C). To estimate soil losses the RUSLE model was coupled with GIS tools to calculate the product of factors R, K, LS, C (rasters of 90-m resolution), and P (equal to 1). Soil losses were then classified by erosion risk from very low (0 to 2.5 Mg ha⁻¹ yr⁻¹), to extremely high (greater than 100 Mg ha⁻¹ yr⁻¹). Assessment of the level of importance of each RUSLE factor was performed using a non-parametric machine learning algorithm Random Forest. Additionally, sediment exports values were also computed to identify areas where soil conservation practices were needed. The level of importance of RUSLE factors was assessed in the following order: C > K > LS > R. Water erosion in the Peixe Angical Reservoir drainage basin increased over the years due to changes in land use, although soil losses in the majority of the basin were classified as very low. Additionally, although in small proportion, a trend towards the reduction of sediment export was calculated as areas with null values of sediment increased through time in the basin. Soil conservation practices should be adopted to support the expansion of agricultural production in a sustainable manner to minimize the effects caused by changes in land use, and ensuring both the quantity and quality of water in the water ways, as well as natural and artificial reservoirs.

Keywords: Land use; soil losses; random forest; sediment export; land management.

1. Introduction

Water erosion is deleterious to the sustainability of agricultural systems. Detached soil particles are transported downstream together with nutrients, organic carbon, and agrochemical

compounds. This impacts negatively on crop production, and water quality. This also affects the service life of water reservoirs, including storage dams for hydroelectric power plants. The Peixe Angical Hydroelectric Power Plant (HPP) is on the Upper Tocantins River, extending through the states of Goiás and Tocantins, as well as the Distrito Federal (Figure 1). This HPP is preponderant for electricity production in the region, promoting socioeconomic development. To sustain reservoir hydroelectricity generation, the reservoir must be maintained in terms of stored water volume. Thus, monitoring silting rates is fundamental for the assessment of the service life of reservoirs.

Considering the consequences of water erosion, prevention is the first step. Therefore, different stakeholders must identify the most vulnerable to erosion areas, within regions of interest by monitoring ecosystem services, edaphic and climatic environments at different scales. Since monitoring areas, at basin or landscape scales, is laborious, expensive and time-consuming, modeling of soil erosion is a long used tool.

Various erosion prediction models have been used for environmental analysis. In Brazil, the Revised Universal Soil Loss Equation (RUSLE) (Renard et al., 1997) has been widely applied for over two decades (Angima et al., 2003; Fu et al., 2006; Ganasri and Ramesh, 2016; Ostovari et al., 2017). RUSLE considers input variables such as rainfall erosivity, soil erodibility, slope length, and steepness of the area, cover management, and support practices. It was been proved that RUSLE ran together with Geographic Information System (GIS), facilitates its applicability in large areas as basins, provinces, states, or countries (Barros et al., 2018; Cunha et al., 2017; Gomes et al., 2017). This integration allows localization of critical points in relation to the erosion processes, which can assist the decision making process regarding the need of soil and water conservation practices (Chen et al., 2019; Fayas et al., 2019; Vijith et al., 2018; Zerihun et al., 2018). Furthermore, although the Peixe Angical Reservoir drainage basin (PARDB) is inserted in the Cerrado biome, this area has not yet been studied.

Considering RUSLE takes into account several factors to predict and model soil erosion (R, K, LS, C, and P) (Renard et al., 1997), and the fact that transdisciplinary usage of machine learning statistical analysis are on the rise, the aim of this work is to assess the level of importance of these factors for modeling soil losses. We hypothesized that by modeling soil losses through RUSLE-GIS, we could apply the Random Forest (RF) algorithm –a non-parametric machine learning algorithm– (Liaw and Wiener, 2002; RColorBrewer and Liaw, 2018) to better understand the greater or lesser level of importance of each of the RUSLE

factors. This coupled approach can provide a better insight for soil and water conservation planning.

To achieve our objective, we estimated soil losses and sediment export –considering land use in the chronological scenarios of 1990, 2000, 2010, and 2017– for the Peixe Angical Reservoir drainage basin; we also identified priority areas –due to soil losses– in need of soil and water conservation practices; and we applied a statistical analysis –using RF algorithm– to assess the contribution and importance of the RUSLE factors (R, K, LS, and C).

2. Materials and Methods

2.1. Study area

The Peixe Angical Reservoir drainage basin (PARDB), formed by the Upper Tocantins River and its tributaries, composed by the rivers Palma, Paranã, Maranhão, and Almas, occupies an area of 125,776 km², with 0.62% in the Distrito Federal, 75.58% in the state of Goiás (West Central region of Brazil), and the remaining 23.80% in the state of Tocantins (North region of Brazil). The PARDB is located between the geographic coordinates 11° to 17° S and 46° to 51° W (Figure 1).

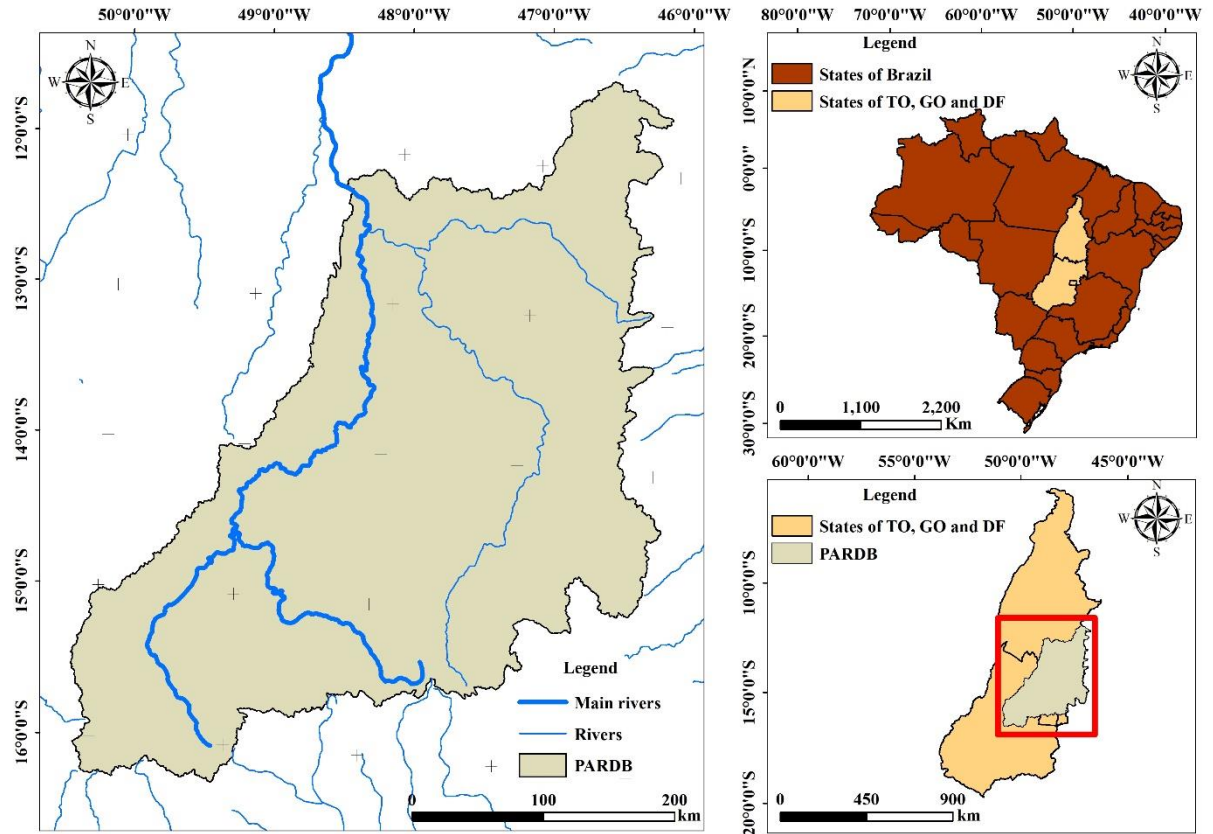


Fig. 1. Location of the Peixe Angical Reservoir drainage basin (PARDB).

The climate in the drainage basin, according to the Köppen climate classification, is Aw - tropical with dry winter (Alvares et al., 2013). The altitude ranges from 236 to 1,670 m, and the slope ranges from near zero to more than 75% (Figure 2).

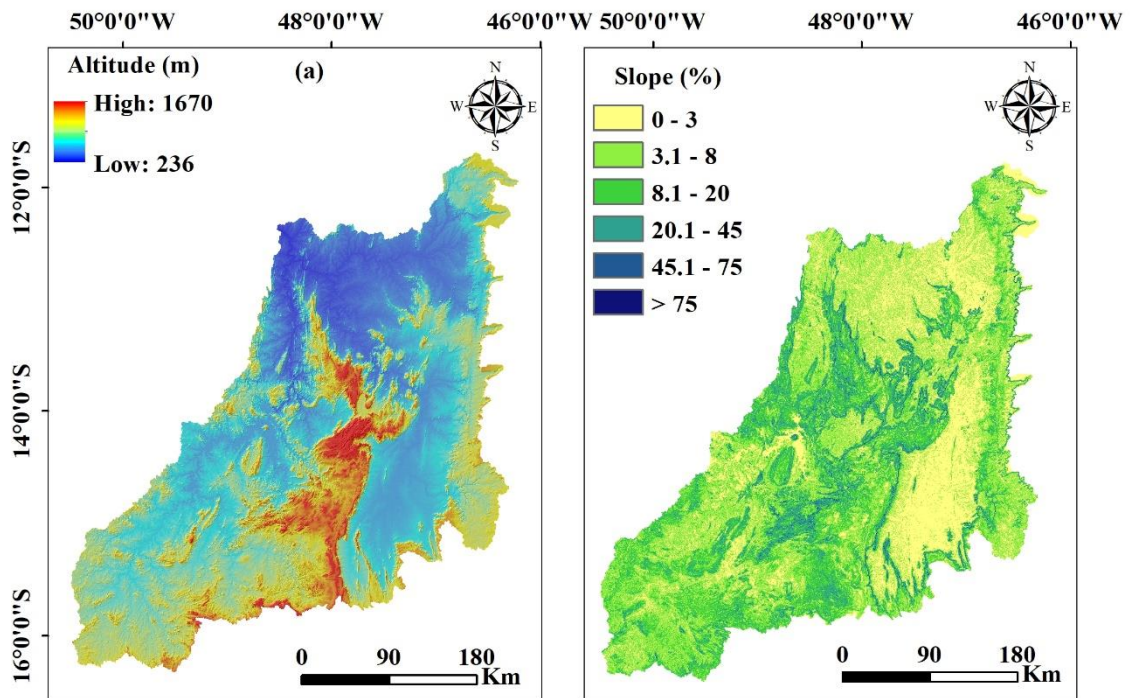


Fig. 2. Digital Elevation Model (a), and slope steepness categories (%) of the Tocantins River upstream from Peixe Angical Reservoir drainage basin (PARDB).

2.2. *RUSLE Model*

For modeling water erosion in the PARDB, the Revised Universal Soil Loss Equation (RUSLE) was used (Renard et al., 1997), described as follows:

$$A = R * K * LS * C * P \quad (1)$$

where A = annual soil loss, in $\text{Mg ha}^{-1} \text{ yr}^{-1}$; R = rainfall erosivity factor ($\text{MJ mm ha}^{-1} \text{ h}^{-1} \text{ yr}^{-1}$); K = soil erodibility factor ($\text{Mg ha h ha}^{-1} \text{ MJ}^{-1} \text{ mm}^{-1}$); LS = slope length and steepness factor (dimensionless); C = cover management factor (dimensionless), and P = support practices (dimensionless). The spatial resolution adopted in this modeling was 90 m.

2.2.1. *Rainfall erosivity factor (R factor)*

Historical rainfall data were obtained from Meteorological Database (BDMEP) from Meteorological Institute (INMET) and also from HidroWeb portal, a tool that is part of the National System of Information on Water Resources, coordinated by the National Water and Sanitation Agency (ANA). A total of 62 rainfall stations were selected (Figure 3), containing information corresponding to the period from 1990 to 2017.

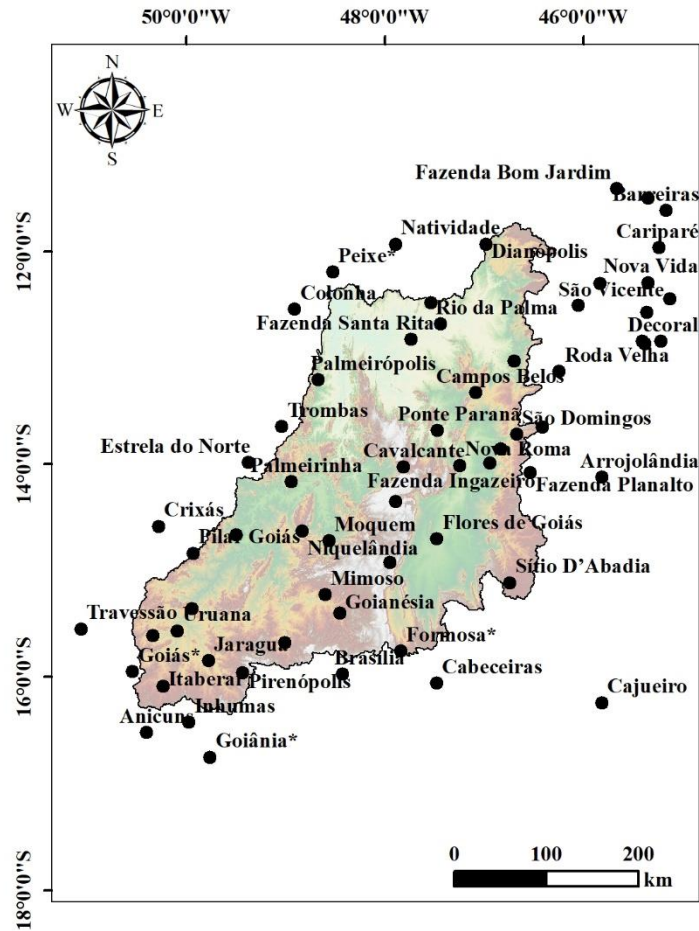


Fig. 3. Location of the gauging station inside and around the Peixe Angical Reservoir drainage basin (PARDB).

When data collection failed in the rain-gauge into the monthly rainfall data, the nearest-neighbor method was used to fill in these gaps. Then, the double mass curve method was applied to check the consistency of the data.

The method selected to estimate the rainfall erosivity was the Modified Fournier (MF) index, based on the results obtained in this thesis (Article II). Thus, rainfall erosivity factor for each rain-gauge was estimated by equations surrounding the PARDB that correlate the rainfall erosivity factor with the Modified Fournier Index (R_c) (Arnoldus, 1980). To define which equation for each one of the rain-gauge, the Thiessen Polygon was determined. Equations found in the neighboring area are: Canarana-MT, $EI_{30} = 317.397829 * R_c^{0.484654}$ (Almeida et al., 2012), Conceição do Araguaia-PA, $EI_{30} = 321.50 + 36.20 * R_c$ (Oliveira Junior, 1996), and Goiânia-GO, $EI_{30} = 215.33 + 30.23 * R_c$ (Silva et al., 1997). After defining, based on Thiessen Polygon, the MF equation to be used in each rain gauge, rainfall erosivity was estimated. Then, geostatistics technique was applied to obtain the rainfall erosivity spatial distribution.

Ordinary kriging was used to adjust the exponential semivariogram model. During kriging, cross validation was performed together with the process. Afterward, rainfall erosivity was mapped on the ArcGIS® software - version 10.3 (ESRI, 2014).

2.2.2. Soil erodibility factor (*K* factor)

The soil groups, according to (FAO, 2014), can be observed in the Table 1, as well as the corresponding K factor. The soil erodibility was selected from Brazilian studies available on the literature. However, when this factor was not found for some soil class, K factor was estimated by equation. Information of soil profile description contained on sheets SC. 22 Tocantins, SD. 22 Goiás, SD. 23 Brasília, and SE. 22 Goiânia of the RadamBrasil were used (RadamBrasil, 1983, 1982, 1981a, 1981b). In that case, soil erodibility was calculated based on the nomogram of Wischmeier and Smith (1978), using the following equation:

$$K = \frac{\{[(2.1) \cdot (10^{-4}) \cdot (M^{1.14}) \cdot (12 - O.M.)] + [3.25 \cdot (e - 2)] + [2.5 \cdot (p - 3)]\}}{100} \quad (2)$$

where K = soil erodibility factor (Mg acre h). Transformation to the International System of Units (SI) was through multiplication of the correction factor 0.1317, obtaining the value in Mg ha h ha⁻¹ MJ⁻¹ mm⁻¹; M = percentage of modified silt, i.e., percentage of silt plus very fine sand, in reference to the North American Classification System (USDA), which corresponds to the size fraction of 0.002-0.1 mm; O.M. = percent organic matter; e = code referring to soil structure; and p = code referring to soil permeability. The description of Marques et al. (1997) was used for these codifications for Brazilian soils.

Table 1. Soil classification according to the FAO-World Reference Base (WRB) and the Brazilian Soil Classification System (SiBCS), their respective geographical expression within the Peixe Angical Reservoir drainage basin (PARDB), and soil erodibility factor values.

Soil Groups	Soil Classes	Area	Soil erodibility	References
FAO-WRB	SiBCS	(%)	(Mg ha h ha ⁻¹ MJ ⁻¹ mm ⁻¹)	
Rhodic Acrisol	Red Argisol	3.66	0.0192	Di Raimo et al. (2019)
Lithic Leptosol	Litholic Neosol	26.87	0.0344	Calculated by the authors
Rhodic Ferralsol	Red Latosol	14.91	0.0032	Silva et al. (2009)
Dystric Cambisol	Haplic Cambisol	13.40	0.0355	Silva et al. (2009)
Haplic Plinthosol	Haplic Plinthosol	9.99	0.0170	Martins et al. (2011)
Chromic Acrisol	Red-Yellow Argisol	9.28	0.0106	Eduardo et al. (2013)
Haplic Ferralsol	Red-Yellow Latosol	7.01	0.0100	Silva et al. (2000)
Petric Plinthosol	Petric Plinthosol	4.57	0.0206	Calculated by the authors
Dystric Arenosol	Quartzarenic Neosol	4.37	0.0567	Castro et al. (2011)
Haplic Phaeozem	Argilluvic Chernosol	2.81	0.0316	Calculated by the authors
Xanthic Ferralsol	Yellow Latosol	1.92	0.0090	Silva et al. (2000)
Rhodic Nitisol	Red Nitisol	1.10	0.0138	Calculated by the authors
Dystric Gleysol	Haplic Gleysol	0.10	0.0180	Di Raimo et al. (2019)

WRB available in (FAO, 2014) and SiBCS (Santos et al., 2018)

2.2.3. Topographic factor (LS factor)

The LS factor represents the topographic factor that considers the slope and the contribution area of the basin, by which, soil loss is also influenced. For calculation of the LS factor, the Digital Elevation Model (DEM) from Shuttle Radar Topography Mission (SRTM) (Farr et al., 2007) was used, with 90 m-resolution (Jarvis et al., 2008). Preprocessing of the DEM-SRTM was performed to voids filling (Wang and Liu, 2006). Applying the Multiple Flow Direction algorithm proposed by Quinn et al. (1991), the drainage area of the basin was determined, then LS factor was figured out. The System for Automated Geoscientific Analyses – SAGA software (SAGA, 2013) was used for that determination, through the algorithm of Desmet and Govers (1996).

2.2.4. Cover management factor (C factor)

The land use maps in the years of 1990, 2000, 2010, and 2017 were obtained from the MapBiomass Project (Alencar et al., 2020; Souza Jr. et al., 2020) collection 4.1 (Projeto MapBiomass, 2020). Collection 4 presented accuracy assessment analysis based on acquisition of 100 thousand independent samples per year from 1985 to 2018 (Souza and Azevedo, 2017). The global accuracy for Cerrado Biome (collection 4.1) was 72.6%, with 21.7% of allocation disagreement and 5.7% of area disagreement.

All the maps were download from Projeto MapBiomass (2020). Then, the rasters for each year were projected for Albers (South America Albers Equal Area Conic). The maps were trimmed down according to the delimitation of the drainage basin and converted to a 90 m-resolution. Finally, C factor values were attributed, according to Table 2.

Table 2. Land use and the respective values for the C factor.

Land use	C factor	Reference
Forest Formation	0.001	Cunha et al. (2017)
Savanna Formation	0.013	Oliveira et al. (2015)
Forest Plantation	0.12	Silva et al. (2014)
Grassland	0.50	Cunha et al. (2017)
Pasture	0.22	Silva et al. (2014)
Agricultural Crops	0.13	Corrêa et al. (2016)
Urban Infrastructure	0	
Other Non Vegetated Area	0	
Mining*	0	
Water	0	

Source: Adapted from (Projeto MapBiomass, 2020). *It was considered that water erosion would be restricted to the created crater, without contributing to the study drainage basin.

2.2.5. Support practices factor (*P* factor)

Practices of soil conservation influence on a reduction of soil erosion processes. However, the study intends to ascertain the land use change. Thus, the entire area was considered without support practices of erosion control. Therefore, the value assigned to the *P* factor was 1.

2.3. Soil losses

The spatial distribution of soil losses in the PARDB was obtained using Equation (1), by multiplying the rasters of the *R*, *K*, *LS*, and *C* factors, with the assistance of ArcMap 10.3 (ESRI, The Redlands, CA, USA). Then, these losses were separated into erosion risk categories according to the classification proposed by Avanzi et al. (2013). In sequence, the *combine* function in ArcMap 10.3 (ESRI, The Redlands, CA, USA) was used for comparison among the years evaluated, thus obtaining information of changes in soil losses between the years 1990 to 2000, 2000 to 2010, and 2010 to 2017, besides the change for the entire period from 1990 to 2017.

2.4. Level of importance of each *RUSLE* factor

The level of importance of each *RUSLE* factor was assessed by extracting each pixel data using the SAGA-GIS software. Then the *randomForest* package (Liaw and Wiener, 2002; RColorBrewer and Liaw, 2018) was run in the R environment (R Core Team, 2020) to obtain the level of importance of each *RUSLE* factor to predict soil losses using the following parameters: number of trees of the model, $n_{\text{tree}}=1000$, number of variables in each node, $\text{nodesize}=4$, and number of variables used in each tree, $\text{mtry}=\text{one-third of the total number of predictor variables}$, as suggested by (Liaw and Wiener, 2002). During the adjustments of the RF models, the mean squared error (MSE_{OOB}) (Eq. 3) and the percent variance explained ($\% \text{Var}_{\text{ex}}$) (Eq. 4) were computed using the out-of-bag (OOB) methodology. In this method, for each interaction, only a few predictor variables are used to generate a tree based on a measure of their importance as predictor variables. Thus, the model is able to identify the informative variables and ignore noisy data (Liaw and Wiener, 2002); *i.e.* if one variable is removed from the model, resulting in a greater error and less prediction accuracy, the more important this variable is for the model.

$$\text{MSE}_{\text{OOB}} = \frac{1}{n} \sum_1^n [y_i - \hat{y}_i^{\text{OOB}}]^2 \quad (3)$$

$$\%Var_{ex} = 1 - \frac{MSE_{OOB}}{\hat{\sigma}_y^2} \quad (4)$$

where $n = n_{tree}$; y_i is the i th observed value; \hat{y}_i^{OOB} is the average of the OOB predictions for the i th observation; and $\hat{\sigma}_y^2$ is the variance computed with n as divisor, instead of $(n - 1)$.

2.5. Sediment analysis

2.5.1. Sediment Delivery Ratio (SDR)

The RUSLE model does not estimate the sediment delivery rate (SDR). Alternately, we used the InVEST sediment delivery ratio model (Hamel et al., 2015). According to (Cong et al., 2020) this model requires a smaller amount of input data, being adequate to estimate the SDR using the little available data for the Peixe Angical basin. Table 3 shows the essential input data for modeling with InVEST SDR.

Table 3. The input data, format, variation, spatial resolution (m) and references used in the InVEST SDR model, version 3.8.2.

Input	Format	Range	Resolution	Reference
Digital Elevation Model	Raster	(236-1670)	90	Jarvis et al. (2008)
Rainfall Erosivity Index (R)	Raster	(7047.64-11348.5)	90	/
Soil Erodibility	Raster	(0.0032-0.0567)	90	Vide Table 1
Land-Use/Land-Cover	Raster	(1-10)	90	Vide Table 2
Watersheds	Vector	/	/	/
Biophysical Table	Decimal	(1-0.5)	/	/
Threshold Flow Accumulation	Integer	1000	/	Luo et al. (2008)
Borselli K Parameter	Decimal	1	/	Vigiak et al. (2012)
Borselli ICo Parameter	Decimal	0.5	/	Vigiak et al. (2012)
Max SDR Value	Decimal	0.2	/	Vigiak et al. (2012)

Spatial resolution in meters (m).

The sediment delivery ratio for the i th pixel is derived from the connectivity index IC using a sigmoid function (Vigiak et al., 2012):

$$SDR_i = \frac{SDR_{max}}{1 + \exp\left(\frac{IC_o - IC_i}{K}\right)} \quad (5)$$

where:

SDR_i = sediment delivery ratio for a pixel i ;

SDR_{max} = maximum theoretical sediment delivery ratio; and

IC_o and K = are model calibration parameters.

2.5.2. Sediment Export

The sediment export from a given pixel, is the amount of sediment eroded from that pixel that actually reaches the stream (Sharp et al., 2014). Sediment export is given by:

$$E_i = A_{RUSLEi} * SDR_i \quad (6)$$

where:

E_i = sediment exported from a given pixel i ($Mg\ ha^{-1}\ ano^{-1}$);

A_{RUSLEi} = soil losses from a given pixel i ($Mg\ ha^{-1}\ ano^{-1}$), estimated by RUSLE model; and

SDR_i = sediment delivery ratio from a given pixel i , estimated by InVEST SDR.

2.6. Calibration and Validation of the models

For the calibration and validation of the RUSLE and InVEST SDR models, the exported sediment obtained by the product of the soil loss estimated by RUSLE and the InVEST SDR was used. However, the observed sediment was provided by Enerpeixe S.A., using data from the Station (code 21660000) HPP Peixe Angical Farm Visão do Santana. In sedimentometric monitoring (Posse Junior and Manz, 2020), at least four measurements are made throughout the year to define and update, in this case, the solid discharge curve.

Part of the data observed from 2011 to 2018 (70%) was used for calibration. The parameters PBIAS were obtained using the hydroGOF package (Zambrano-Bigiarini, 2020), utilizing exclusively 30% of the data points for validation purposes.

3. Results

3.1. Soil erosion factors

The values of rainfall erosivity in the PARDB exhibited minimum values of 7,047.64 MJ mm ha⁻¹ h⁻¹ yr⁻¹ (east and west part) and maximum values of 11,348.5 MJ mm ha⁻¹ h⁻¹ yr⁻¹ (north part). These classes occupy 7.84%, 82.01%, and 10.15% of the total area of the drainage basin in reference to the moderate to strong class, strong class, and very strong class, respectively. Considering the entire PARDB, mean annual erosivity was 9,198.07 MJ mm ha⁻¹ h⁻¹ yr⁻¹ (Figure 4).

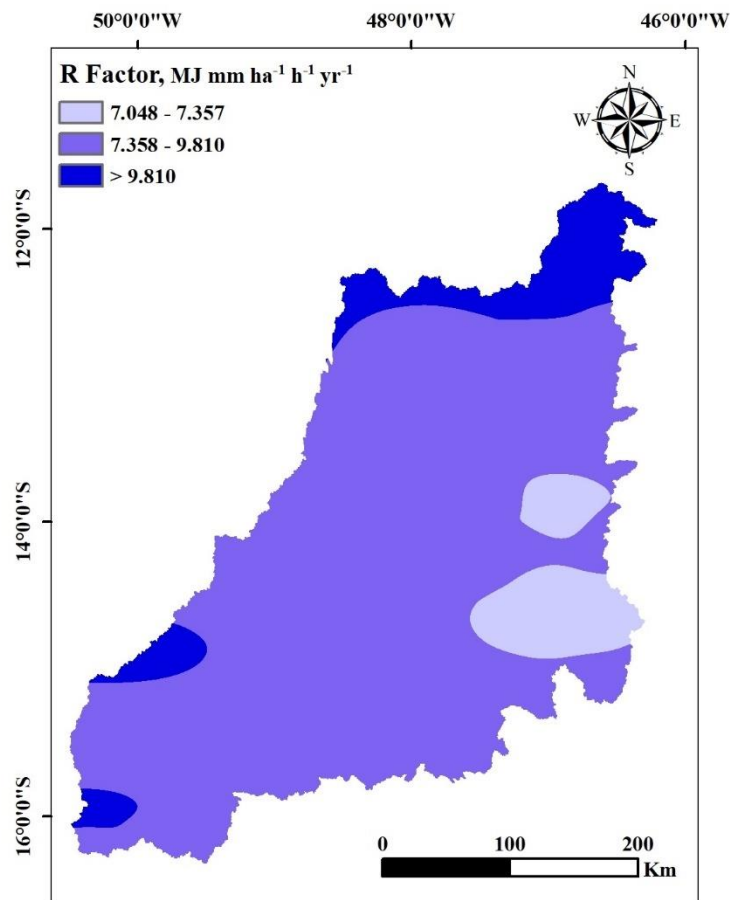


Fig. 4. Annual average rainfall erosivity (MJ mm ha⁻¹ h⁻¹ yr⁻¹) from 1990 to 2017 in the Peixe Angical Reservoir drainage basin (PARDB).

The Dystric Arenosol had the highest values of soil erodibility, 0.0567 Mg ha h ha⁻¹ MJ⁻¹ mm⁻¹ (Table 1), occupying an area of 4.37% (Figure 5). In contrast, the lowest value of erodibility was 0.032 Mg ha h ha⁻¹ MJ⁻¹ mm⁻¹ (Table 1) for Rhodic Ferralsol, which represents 14.91% of the area. Lithic Leptosol is the dominant soil class occupying 26.87% of the area of the PARDB, besides it presents high erodibility value (0.0344 Mg ha h ha⁻¹ MJ⁻¹ mm⁻¹).

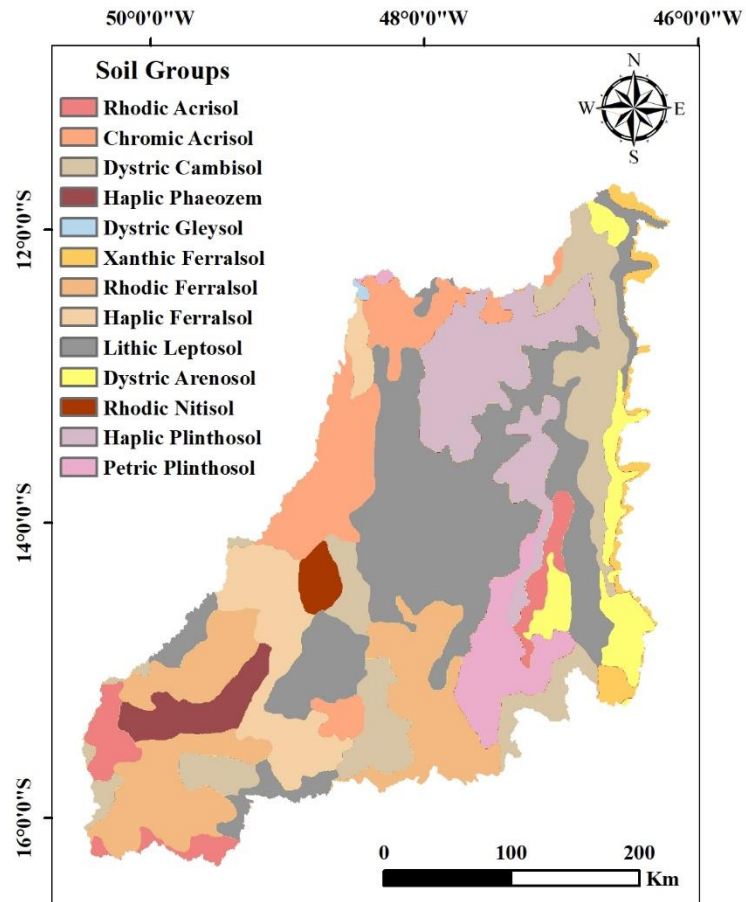


Fig. 5. Soil classes distribution in the Peixe Angical Reservoir drainage basin (PARDB).

The values for the LS factor were separated into 8 classes (Figure 6). Thus, as expressed in the topographic factor, most of the area (87.05%) will not increase soil losses. However, 0.41% of the area leaves the drainage basin more vulnerable to erosion processes, as it exhibits LS values higher than 20.

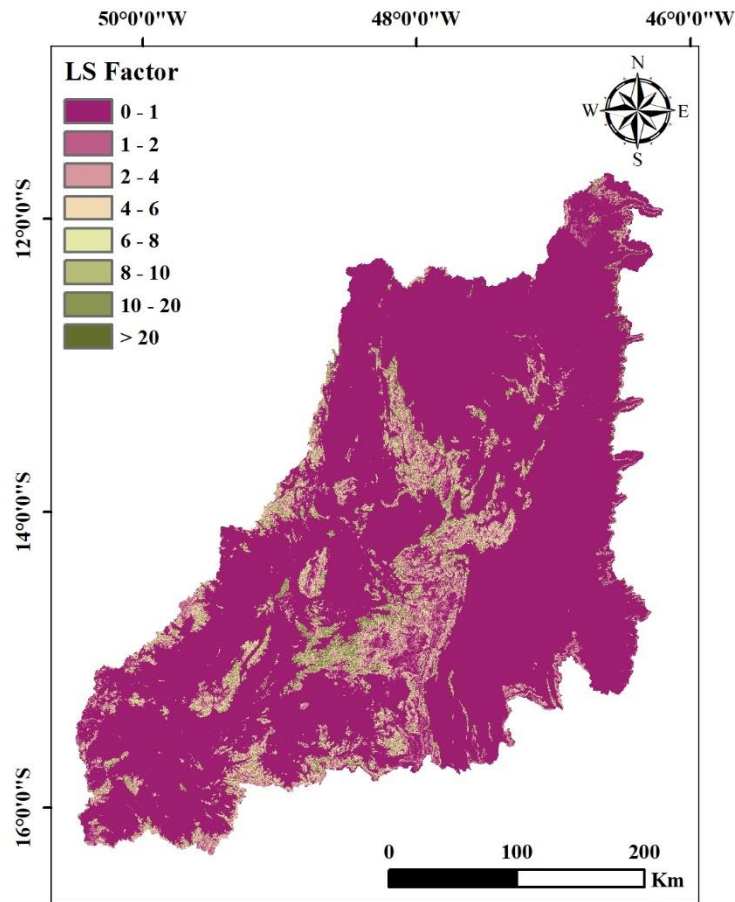


Fig. 6. Spatial distribution of topographic factor - LS (dimensionless) in the Peixe Angical Reservoir drainage basin (PARDB).

The vegetated areas in the PARDB (Figure 7) are represented by forests, non-forest natural formations, crops, and livestock systems. Forest cover (Figure 7) comprises forest formation, savanna formation, and forest plantation, which represented 60.61% in 1990, 54.56% in 2000, 51.21% in 2010, and 48.70% in 2017 of the total PARDB area. The savanna formation was the most extensive over years.

The area percentage occupied by the grassland (Figure 7), showed reduction for each analyzed time scenario, occupying an area of 11.69%, 10.76%, 10.24%, and 8.97% in 1990, 2000, 2010, and 2017, respectively. In the case of crop and livestock operations (pasture and agricultural crops), the opposite occurred: an increase in the area was observed as the years went by (Figure 7), showing the advance of crop and livestock systems in this region.

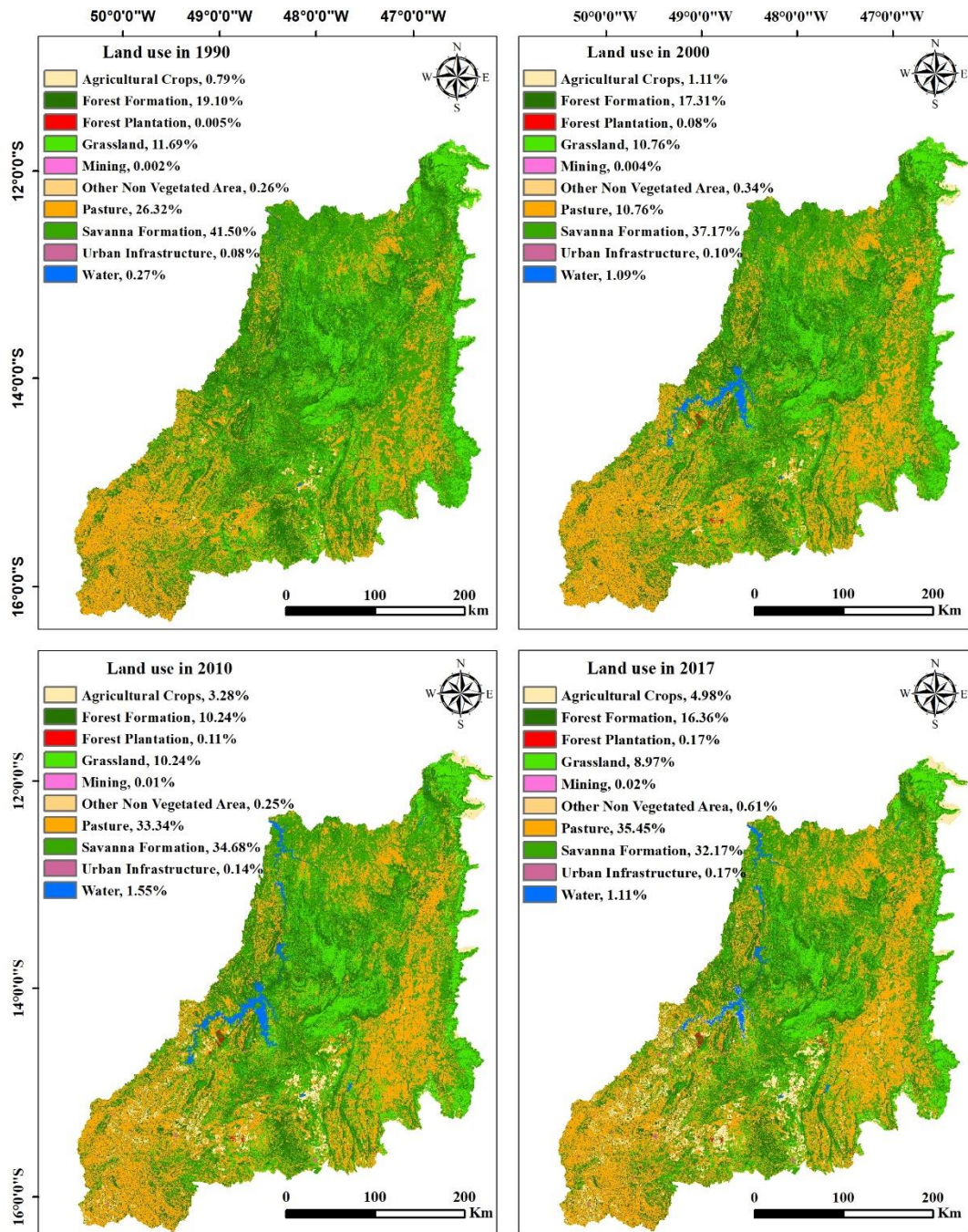


Fig. 7. Map of land use for the Peixe Angical Reservoir drainage basin (PARDB) in the years of 1990, 2000, 2010, and 2017. (Adapted from MapBiomias).

Although most of the area of the PARDB is occupied by native forest, there are still soil losses in these environments. Other important land uses in the PARDB are Brazilian savanna formation and forest plantation, however, they present a low plant cover index (Table 2).

As previously mentioned, the PARDB revealed an increase in the crop and livestock area (Figure 7), advancing across 13.32%. Nearly in the same proportion was reduction of 12.07% and 2.72% in the areas of native forest and non-forest formations (Figure 7), respectively.

3.2. Soil loss potential

After mapping each factor separately –R, K, LS, and C factors– soil losses were calculated via RUSLE coupled to GIS for spatial distribution at the PARDB (Figure 8).

High soil losses were predicted for central and northeast regions, though in lower amount for the latter. Small areas occupying the highest level of soil loss class were also observed in the eastern, southern, and western parts at the edges of the drainage basin (Figure 8).

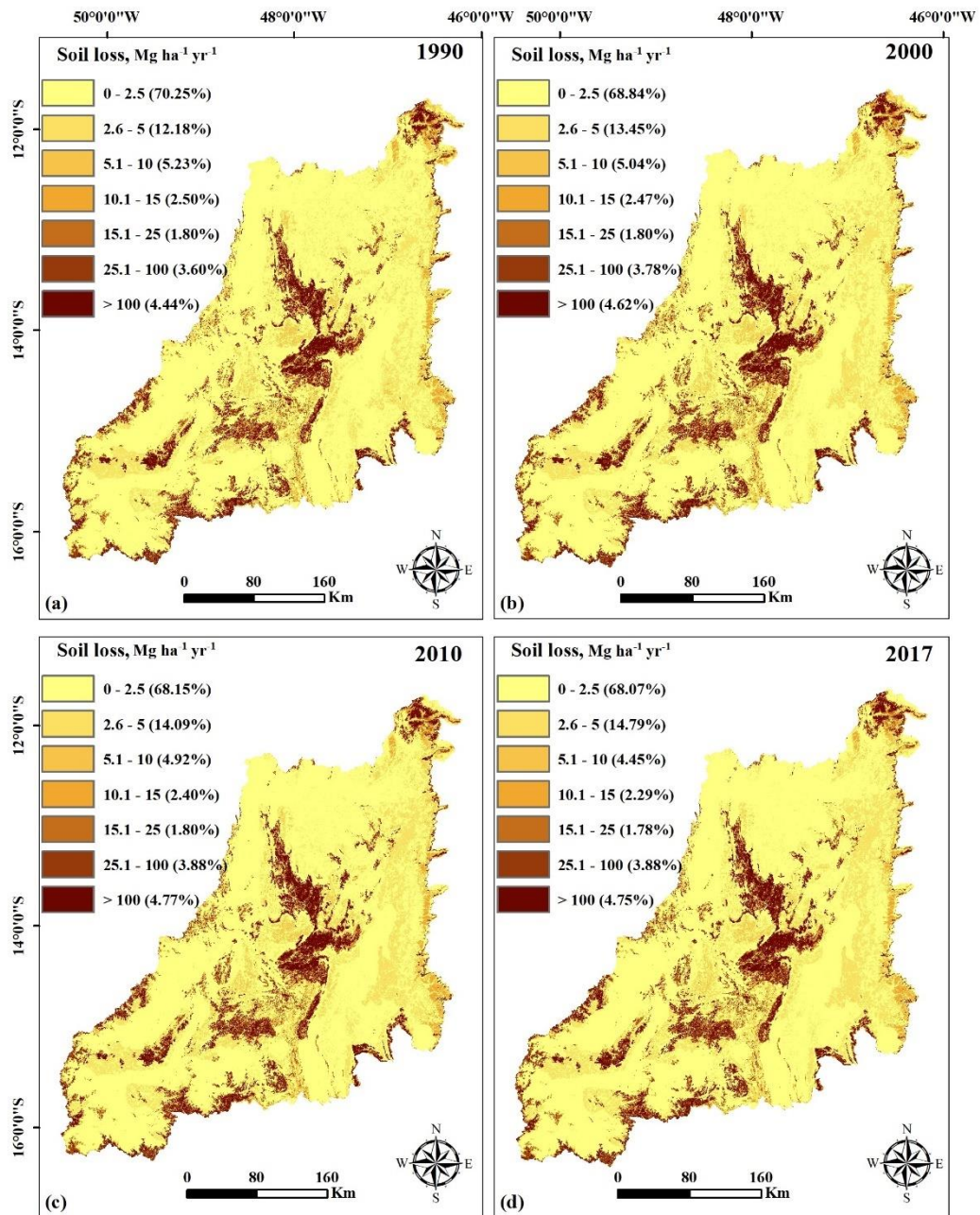


Fig. 8. Map of soil loss rate (Mg ha⁻¹ yr⁻¹) for the Peixe Angical Reservoir drainage basin (PARDB) in the years of 1990, 2000, 2010, and 2017.

3.3. Analysis of soil erosion risk

In general, from 1990 to 2000 (Table 4), inside the erosion class –line of the table–, a reduction of the erosion risk has been verified for all the classes. However, for the first class –very low erosion risk– showed an increase of the percentage of erosion risk. For the next two

decades, from year 2000 to 2010 and from 2010 to 2017, the changes in soil loss were like the previous decade (Table 4).

Table 4. Change in the percentage of erosion risk classes from 1990 to 2000, from 2000 to 2010, and from 2010 to 2017, which corresponds to the complete chronological scenario, in a time span of 28 years.

Classes	1	2	3	4	5	6	7	Erosion risk class	
								Increase	Reduce
1990-2000									
1	65.89	3.16	0.50	0.17	0.13	0.26	0.14	4.36	0.00
2	2.11	9.63	0.21	0.02	0.00	0.12	0.08	0.43	2.11
3	0.41	0.46	4.17	0.01	0.01	0.03	0.14	0.19	0.87
4	0.11	0.08	0.03	2.20	0.01	0.01	0.08	0.09	0.21
5	0.08	0.02	0.04	0.01	1.56	0.01	0.09	0.10	0.14
6	0.13	0.07	0.03	0.02	0.03	3.21	0.12	0.12	0.28
7	0.11	0.04	0.07	0.04	0.06	0.14	3.88	0.00	0.46
Total area	68.84	13.45	5.04	2.47	1.80	3.78	4.62		
2000-2010									
1	65.24	2.63	0.39	0.14	0.11	0.21	0.14	3.60	0.00
2	2.10	10.86	0.29	0.01	0.00	0.12	0.06	0.49	2.10
3	0.42	0.38	4.06	0.01	0.01	0.04	0.11	0.17	0.81
4	0.10	0.09	0.04	2.16	0.00	0.01	0.07	0.08	0.23
5	0.07	0.02	0.03	0.02	1.56	0.02	0.08	0.10	0.14
6	0.12	0.07	0.03	0.02	0.05	3.35	0.13	0.13	0.30
7	0.09	0.04	0.07	0.04	0.05	0.15	4.18	0.00	0.44
Total area	68.15	14.09	4.92	2.40	1.80	3.88	4.77		
2010-2017									
1	65.54	2.07	0.21	0.06	0.06	0.12	0.09	2.61	0.00
2	1.79	12.02	0.15	0.01	0.00	0.07	0.04	0.28	1.79
3	0.34	0.53	3.93	0.01	0.01	0.02	0.07	0.12	0.87
4	0.10	0.07	0.05	2.13	0.01	0.01	0.04	0.06	0.22
5	0.07	0.01	0.02	0.02	1.61	0.02	0.05	0.07	0.12
6	0.12	0.06	0.02	0.01	0.05	3.50	0.11	0.11	0.27
7	0.11	0.03	0.06	0.04	0.05	0.14	4.34	0.00	0.43
Total area	68.07	14.79	4.45	2.29	1.78	3.88	4.75		

Erosion risk classes: 1 – very low (0 - 2.5 Mg ha⁻¹ yr⁻¹); 2 – low (2.6 – 5.0 Mg ha⁻¹ yr⁻¹); 3 – moderate (5.1 – 10.0 Mg ha⁻¹ yr⁻¹); 4 - moderate high (10.1 – 15.0 Mg ha⁻¹ yr⁻¹); 5 – high (15.1 – 25.0 Mg ha⁻¹ yr⁻¹); 6 – very high (25.1 – 100.0 Mg ha⁻¹ yr⁻¹); and 7 – extremely high (> 100.0 Mg ha⁻¹ yr⁻¹).

3.4. Evaluation of the R, K, LS, and C factors, through Random Forest

Through Random Forest analysis (Figure 9), the importance of the factors for soil loss was determined by analyzing the increases in the mean square error for each factor when

excluded from the model. Therefore, the most important variables for the prediction of soil losses using RUSLE were the C and K factors (Figure 9).

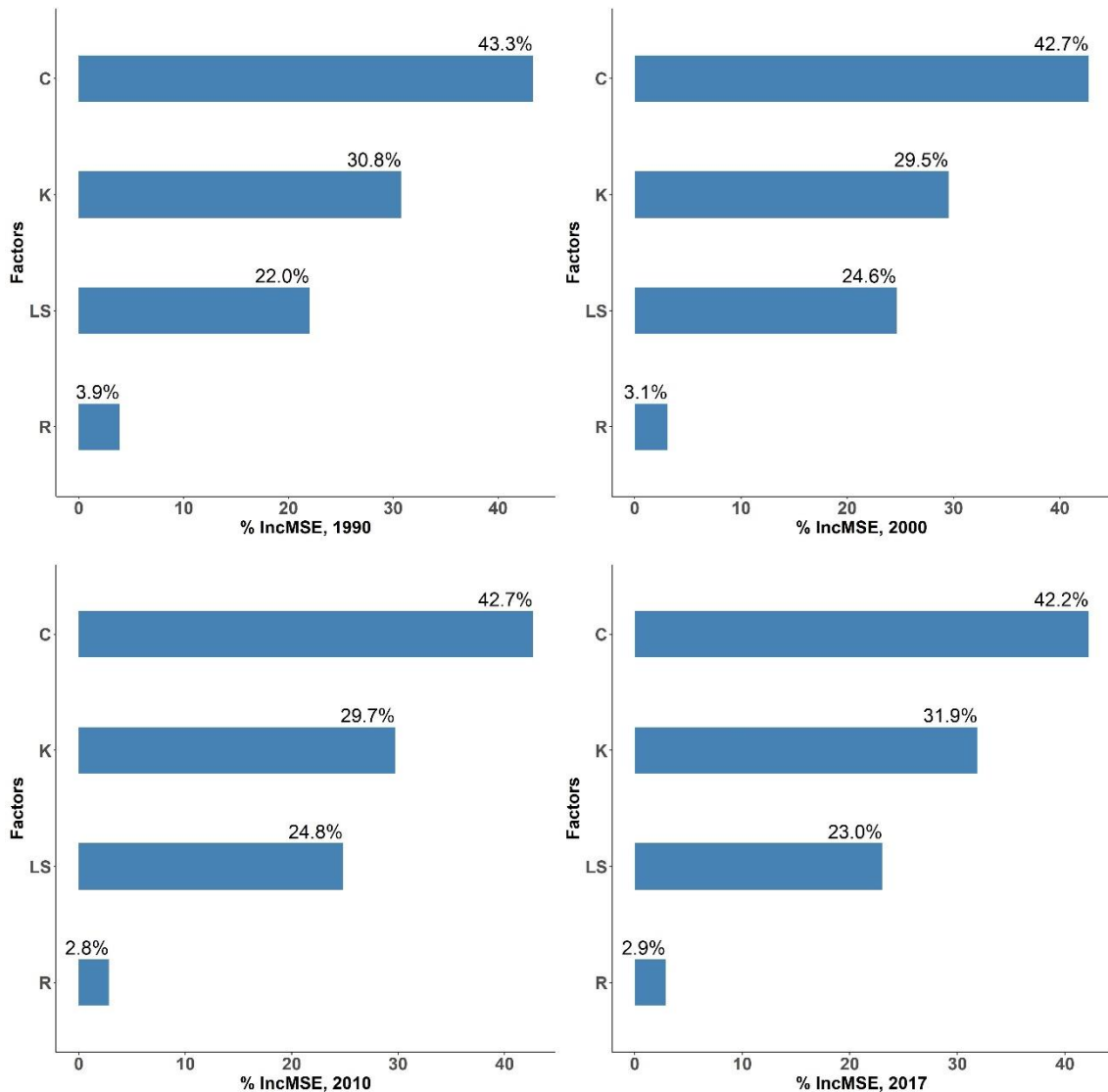


Fig. 9. Identification of explanatory variables of soil losses by Random Forest algorithm. Factors C and K were assessed as the most important variables for soil loss prediction using RUSLE at the Peixe Angical Reservoir drainage basin (PARDB) in the years of 1990, 2000, 2010, and 2017.

High values of percent increase in mean square error (MSE_{OOB}) mean high explanatory value. Thus, the level of importance of RUSLE factors was assessed—considering all scenarios—in the following order: $C > K > LS > R$. The observed MSE_{OOB} were 42.73% (C factor), 30.48% (K factor), 23.62% (LS factor), and 3.16% (R factor) (Figure 9).

3.5. Sediment export

The estimation of the sediment export from a catchment is particularly important, especially those with reservoirs, since retained sediments (sedimentation) can reduce the service life span of the reservoir.

Sediment export was computed spatially with values ranging from 0 to more than 3.30 Mg ha⁻¹ year⁻¹. Areas with null values corresponded to an average of 5.2% of the total area of the basin considering the different time scenarios (1990, 2000, 2010 and 2017). Likewise, areas ranging from 0.01 to 1.1 Mg ha⁻¹ year⁻¹ occupied 93.5% of the basin. Furthermore, areas with sediment export values from 1.11 to 3.29 Mg ha⁻¹ year⁻¹ represented 0.9% of the total area. Finally, only 0.38% of the total area presented values above 3.30 Mg ha⁻¹ year⁻¹. Although in small proportion, a trend towards the reduction of sediment export was calculated. Areas with null values of sediment export corresponded to 4.58%, 5.16%, 5.50%, and 5.53%, for 1990, 2000, 2010, and 2017, respectively.

The areas with the highest values of sediment export added up to less than 0.40% of the total area of the basin and are associated to the class of high soil loss. Even though these areas are covered with native grasslands, its main phytophysiognomic have land cover of less than 5%. Sano and Almeida (1998) reported specific characteristics for similar regions within the Cerrado biome where land cover were less than 1%. Thus, these phytophysiognomies offer little soil cover to raindrop impact, and consequently erosion processes are accentuated.

To evaluate the sediment export model, the trend percentage (PBIAS) was applied. Thus, for calibration and validation, the PBIAS values were -34.9% and -24.8%, respectively.

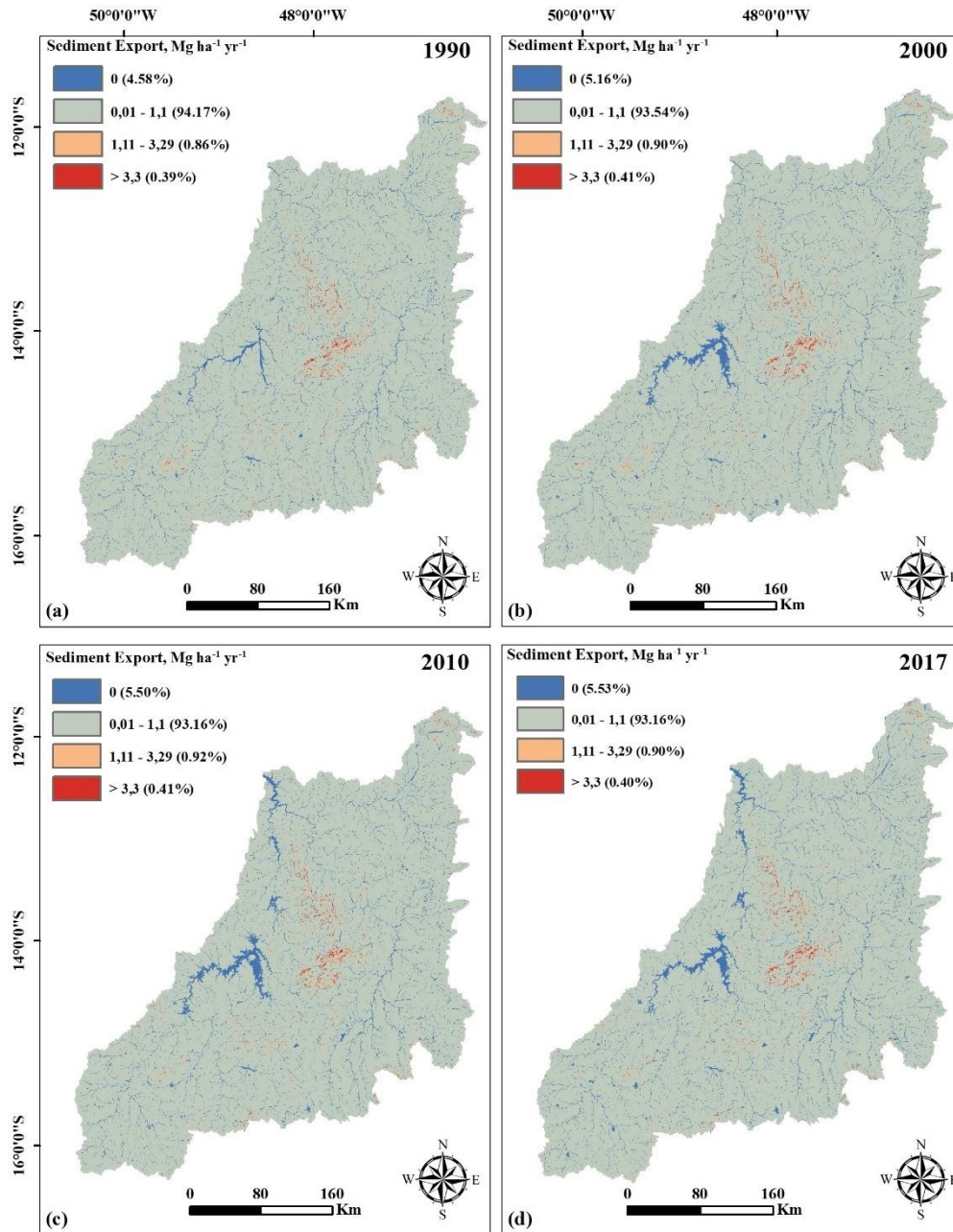


Fig. 10. Spatial distribution of exported sediments (Mg ha⁻¹ year⁻¹) and percentage classification for the Peixe Angical Reservoir drainage basin (PARDB).

4. Discussion

The computed rainfall erosivity values were classified, according to Foster et al. (1981), as moderate to strong (4,905 to 7,357 MJ mm ha⁻¹ h⁻¹ yr⁻¹), strong (7,357 to 9,810 MJ mm ha⁻¹ h⁻¹ yr⁻¹), and very strong (greater than 9,810 MJ mm ha⁻¹ h⁻¹ yr⁻¹) (Figure 4). Previous studies in the surroundings of, or proximal to, the area of study reported rainfall erosivity values

ranging from 8,000 to 12,000 MJ mm ha⁻¹ h⁻¹ yr⁻¹ (Mello et al., 2013; Oliveira et al., 2012). Meanwhile, according to Avanzi et al. (2019) rainfall erosivity values ranged from 4,905.1 to 9,810.0 MJ mm ha⁻¹ h⁻¹ yr⁻¹ in Tocantins, Brazil. This discordance in values is what Nearing et al. (2017) reported regarding how short time series influence calculation of rainfall erosivity due to significantly wetter or drier periods (outliers). Since 28 consecutive years of rainfall observations were used in our work, the mean value of rainfall erosivity for the area of study can be considered reliable for this time span.

Vegetation cover protects the soil surface from direct impact of raindrops, impeding or reducing the beginning of erosion processes. To achieve more efficient cover protection, it is preponderant that areas under permanent preservation remain protected. This way, rain drop impact and soil disaggregation can be ameliorated, consequently reducing the overall sediment dispersion, transportation, and deposition. Since there are areas already endangered due to anthropogenic activities such as the expansion of crop production and livestock pastures, replacing native vegetation in the Brazilian Savanna (Cerrado), adoption of soil and water conservation practices are of paramount importance to support sustainable agroecosystems within this region, pointed out as the last Brazilian agricultural frontier, where crop and livestock systems currently occupy 40.43% (Figure 7) of the total area.

The values of soil losses were classified in classes of soil loss, as proposed by Avanzi et al. (2013). It should be noted that, the PARDB presented spots with high soil losses, even in small areas (Figure 8). These places require adequate land management and soil conservation practices. Thus, these areas should be a top priority for preventive and corrective actions to stop the further evolution of erosion processes.

According to the edaphic and climatic characteristics of each drainage basin, there are (large or small) areas prone to extreme soil losses. For the area of study, results of soil losses above 100 Mg ha⁻¹ yr⁻¹ corresponded to 4.44% and 4.75% of the basin, for years 1990 and 2017, respectively.

Other studies in Brazil reported soil loss classes considered very high (> 100 Mg ha⁻¹ yr⁻¹), values of 2.2% in the Amazon biome (Cruz et al., 2019), from 0,66% (Gomes et al., 2017) to 6% (Salis et al., 2019), in the Cerrado biome. Considering degraded pasture scenario, Galdino et al. (2016) reported 3.04% of the area. In the Atlantic Forest biome considering soil losses greater than 200 Mg ha⁻¹ yr⁻¹, this corresponded to 0.10% of the total area (Oliveira and Vieira, 2017). For the Pampa biome, the percentage of the area with losses above 100 Mg ha⁻¹ yr⁻¹ ranged from 1.5% (Steinmetz et al. 2018) to 2.60% (Nachtigall et al., 2020).

Studies in other parts of the world also reported small areas of the drainage basin with extreme soil losses in tropical or subtropical regions. In India, for the Nethravath drainage basin, Ganasri and Ramesh (2016) reported that for the very high erosion category, soil losses were $25.63 \text{ Mg ha}^{-1} \text{ yr}^{-1}$, occupying 4.4% of the total area. For the Baram River drainage basin (Malaysia), the erosion value higher than $50 \text{ Mg ha}^{-1} \text{ yr}^{-1}$ represented 8.3% of the total area of that drainage basin (Vijith et al., 2018). Fayas et al. (2019) found that approximately 1% of the total area of the Kelani River drainage basin in Sri Lanka occupied the extremely-vulnerable-to-erosion class. For the upper Blue Nile drainage basin (Ethiopia), the values of soil loss greater than $50 \text{ Mg ha}^{-1} \text{ yr}^{-1}$ corresponded to 0.9% (Zerihun et al., 2018). Conversely, some drainage basins may be very susceptible to erosion, as noted for 23.7% of the area of the Koga River drainage basin (South Africa) with soil losses greater than $60 \text{ Mg ha}^{-1} \text{ yr}^{-1}$ (Gelagay and Minale, 2016).

The soil erodibility (K factor) did not exhibit significant alteration over the years; however, there are regions within the basin where the predominant soil class is Lithic Leptosol, prone to high erodibility values. The topographic factor did not alter much over the analyzed time span. A synergistic effect of these two factors aggravated the soil erosion vulnerability of areas as observed in maps of K factor, LS factor and soil losses (Figures 5, 6, and 8).

Regarding the C factor, the highest soil losses occurred in grassland areas (Figure 8). This phytophysiology of the Cerrado biome is characterized as having low plant density per area, which help explain soil losses, due to little soil cover. Contrarily, the phytophysiology of the Tall Woodland –including native perennial vegetation with tree coverage of 50% to 90%– was the land use that offered most efficient soil cover and consequently lowest soil losses.

According to the chronological scenario a reduction in the erosion risk within each class was computed. Nevertheless, each time the values of erosion risk were estimated, this percentage of the area was somehow redistributed to the upper classes (very high and extremely high erosion risk) (Table 4). Therefore, from 1990 to 2017 there was a reduction of the percentage of areas where soil losses corresponded to the first erosion risk class, meanwhile an increase of the percentage of areas associated to the highest risk classes was observed (Figure 8 and Table 4). Thus, it is of paramount importance to consider that land use conversion – specially for regions within endangered biomes susceptible for agricultural expansion– must include soil and water conservation practices as part of the regional management planning to ameliorate anthropogenic impacts to the environment.

Considering the level of importance of the four RUSLE factors ($C > K > LS > R$), our results are in accordance with Paul et al. (2019). They reported the C factor as the most

important variable for explanation of soil loss in 2010 for the Kiskatinaw River drainage basin in Canada. Similarly, Estrada-Carmona et al. (2017) also found that the C factor was the top explanatory variable for various areas of Austria, Estonia, Italy, Latvia, the Netherlands, Slovenia, Costa Rica, and the United States. Therefore, different stakeholders should be aware of the preponderance of plant cover for the control of water erosion; *i.e.* soil conservation practices for vulnerable soils –such as Lithic Leptosol –should be adopted in these areas to improve soil cover. In this soil class, the predominant vegetation cover over the years was the savanna formation.

The generated sediments, which can impact water ways and the Peixe Angical hydroelectric reservoir, showed little connectivity index between the points of soil disaggregation and deposition. Within the basin, the maximum sediment delivery rate corresponds to 20% of the total soil losses. This is associated to a large percentage (66.2%) of gentle slopes and a considerable area (36.4% from 1990-2017) of savanna formation within the area of study.

In other regions of the world where the InVEST SDR model was utilized, divergent estimates were computed (Aneseyee et al., 2020; Dias et al., 2019; Zhou et al., 2019; Bouguerra and Jebari, 2017). This relates to the inputs needed: soil erodibility, rainfall erosivity, soil cover, conservation practices, digital elevation model, and connectivity index. All these inputs correspond to specific characteristics of the basin, influencing the maximum rate of sediment delivery. Therefore, the higher the rate of sediment delivery, the greater the sediment export values. For a similar period of our work, Aneseyee et al. (2020) evaluated the sediment export in the Omo Gibe basin (Ethiopia) –for 30 years– focusing on the effects of changes in land use and occupation. They determined a maximum sediment export of $5.35 \text{ Mg ha}^{-1} \text{ year}^{-1}$ for year 1998, and $5.42 \text{ Mg ha}^{-1} \text{ year}^{-1}$ for 2018. In the Peixe Angical basin, the maximum sediment export value was about 52 times higher than those reported by Aneseyee et al. (2020). Other work in the Qiantang River basin in China reported a reduction in sediment export values from $1.69 \text{ Mg ha}^{-1} \text{ year}^{-1}$ (1990) to $1.22 \text{ Mg ha}^{-1} \text{ year}^{-1}$ (2015) (Zhou et al., 2019). Thus, comparisons of this methodology can be furthered studied for regions within Brazil, a country of continental proportions and diverse environmental conditions.

Furthermore, negative values meant overestimation of the model, *i.e.* the estimated values were higher than those observed. These results prove the sampling methodology –carried out by Enerpeixe SA Company–, as described in the Technical Report No. 4 (Posse Junior and Manz, 2020), only considered suspended sediments, while the deposited sediment was quantified in terms of the texture of the material. According to Yang (1996), bottom drag

sediments can be equivalent to up to 25% of suspended sediments. Thus, it is plausible that deposited sediments were not fully quantified.

According to Moriasi et al. (2007), the performance evaluation of the model was classified as good in relation to sediments, as the values –during validation– were $\geq 15\%$ and $\leq 30\%$. The values obtained from PBIAS indicate the adequacy of the RUSLE and InVEST SDR models to estimate the sediment export values for the Peixe Angical basin. Therefore, changes in land use and occupation over the analyzed time span were satisfactorily estimated by the models.

Finally, other soil conservation practices –in a regional scale– should be adopted to support the expansion of agricultural production in a sustainable manner minimizing the impacts caused by changes in land use, and ensuring both the quantity and quality of water in the water ways, and natural and artificial reservoirs.

5. Conclusions

Application of RF algorithm proved to be useful for the assessment of the level of importance in the RUSLE model. The most explanatory variable for soil losses in the study case of the Peixe Angical Reservoir drainage basin was land cover (C factor), followed by soil erodibility (K factor).

Water erosion in the Peixe Angical Reservoir drainage basin increased over the years due to changes in land use, although soil losses in the majority of the basin were classified as very low. Additionally, although in small proportion, a trend towards the reduction of sediment export was calculated as areas with null values of sediment increased through time in the basin.

The expansion of agricultural activity in this watershed should include best management practices for soil and water conservation. Further research studies are also required to prevent endangerment of waterways and reservoirs, as well as to assure agroecosystems sustainability.

References

- Alencar, A., Shimbo, J.Z., Lenti, F., Marques, C.B., Zimbres, B., Rosa, M., Arruda, V., Castro, I., Ribeiro, J.P.F.M., Varela, V., Alencar, I., Piontekowski, V., Ribeiro, V., Bustamante, M.M.C., Sano, E.E., Barroso, M., 2020. Mapping Three Decades of Changes in the Brazilian Savanna Native Vegetation Using Landsat Data Processed in the Google Earth Engine Platform. *Remote Sens.* 12, 1–23. <https://doi.org/10.3390/rs12060924>.
- Almeida, C.O.S., Amorim, R.S.S., Eltz, F.L.F., Couto, E.G., Jordani, S.A., 2012. Erosividade da chuva em municípios do Mato Grosso: distribuição sazonal e correlações com dados

- pluviométricos. *Rev. Bras. Eng. Agrícola e Ambient.* 16, 142–152. <https://doi.org/10.1590/S1415-43662012000200003>.
- Alvares, C.A., Stape, J.L., Sentelhas, P.C., Gonçalves, J.L. de M., Sparovek, G., 2013. Köppen's climate classification map for Brazil. *Meteorol. Zeitschrift* 22, 711–728. <https://doi.org/10.1127/0941-2948/2013/0507>.
- Aneseyee, A.B., Elias, E., Soromessa, T., Feyisa, G.L., 2020. Land use/land cover change effect on soil erosion and sediment delivery in the Winike watershed, Omo Gibe Basin, Ethiopia. *Sci. Total Environ.* 728, 1–16. <https://doi.org/10.1016/j.scitotenv.2020.138776>.
- Angima, S.D., Stott, D.E., O'Neill, M.K., Ong, C.K., Weesies, G.A., 2003. Soil erosion prediction using RUSLE for central Kenyan highland conditions. *Agric. Ecosyst. Environ.* 97, 295–308. [https://doi.org/10.1016/S0167-8809\(03\)00011-2](https://doi.org/10.1016/S0167-8809(03)00011-2).
- Arnoldus, H.M.J., 1980. An approximation of the rainfall factor in the Universal Soil Loss Equation. An Approx. rainfall factor Univers. Soil Loss Equation. 127–132.
- Avanzi, J.C., Silva, M.L.N., Curi, N., Norton, L.D., Beskow, S., Martins, S.G., 2013. Spatial distribution of water erosion risk in a watershed with eucalyptus and Atlantic Forest. *Ciência e Agrotecnologia* 37, 427–434. <https://doi.org/10.1590/S1413-70542013000500006>.
- Avanzi, J.C., Viola, M.R., Mello, C.R. de, Giongo, M.V., Pontes, L.M., 2019. Modeling of the rainfall and R-Factor for Tocantins state, Brazil. *Rev. Bras. Ciência do Solo* 43, 1–14. <https://doi.org/10.1590/18069657rbcs20190047>.
- Barros, E.N. de S., Viola, M.R., Rodrigues, J.A.M., Mello, C.R. de, Avanzi, J.C., Giongo, M., 2018. Modelagem da erosão hídrica nas bacias hidrográficas dos rios Lontra e Manoel Alves Pequeno, Tocantins. *Rev. Bras. Ciências Agrárias* 13, 1–9. <https://doi.org/10.5039/agraria.v13i1a5509>.
- Bouguerra, S., Jebari, S., 2017. Identification and prioritization of sub-watersheds for land and water management using InVEST SDR model: Rmelriver basin, Tunisia. *Arab. J. Geosci.* 10, 1–9. <https://doi.org/10.1007/s12517-017-3104-z>.
- Castro, W.J. de, Lemke-de-Castro, M.L., Lima, J. de O., Oliveira, L.F.C. de, Rodrigues, C., Figueiredo, C.C. de, 2011. Erodibilidade de solos do cerrado Goiano. *Rev. em Agronegócio e Meio Ambient.* 4, 305–320.
- Chen, S., Zha, X., Bai, Y., Wang, L., 2019. Evaluation of soil erosion vulnerability on the basis of exposure, sensitivity, and adaptive capacity: A case study in the Zhuxi watershed, Changting, Fujian Province, Southern China. *Catena* 177, 57–69. <https://doi.org/10.1016/j.catena.2019.01.036>.
- Cong, W., Sun, X., Guo, H., Shan, R., 2020. Comparison of the SWAT and InVEST models to determine hydrological ecosystem service spatial patterns, priorities and trade-offs in a complex basin. *Ecol. Indic.* 112, 106089. <https://doi.org/10.1016/j.ecolind.2020.106089>.
- Corrêa, E.A., Moraes, I.C., Pinto, S. dos A.F., Lupinacci, C.M., 2016. Perdas de solo, razão de perdas de solo e fator cobertura e manejo da cultura de cana-de-açúcar: Primeira aproximação. *Rev. do Dep. Geogr.* 32, 72–87. <https://doi.org/10.11606/rdg.v2i0.116671>.
- Cruz, D.C. da, Benayas, J.M.R., Ferreira, G.C., Monteiro, A.L., Schwartz, G., 2019. Evaluation of soil erosion process and conservation practices in the Paragominas-Pa municipality (Brazil). *Geogr. Tech.* 14, 14–35. <https://doi.org/10.21163/GT>.

- Cunha, E.R. da, Bacani, V.M., Panachuki, E., 2017. Modeling soil erosion using RUSLE and GIS in a watershed occupied by rural settlement in the Brazilian Cerrado. *Nat. Hazards* 85, 851–868. <https://doi.org/10.1007/s11069-016-2607-3>.
- Desmet, P.J.J., Govers, G., 1996. A GIS procedure for automatically calculating the USLE LS factor on topographically complex landscape units. *J. Soil Water Conserv.* 51, 427–433.
- Di Raimo, L.A.D.L., Amorim, R.S.S., Torres, G.N., Bocuti, E.D., Couto, E.G., 2019. Variabilidade espacial da erodibilidade no estado de Mato Grosso, Brasil Spatial variability of erodibility in Mato Grosso State, Brazil. *Rev. Ciências Agrárias* 42, 55–67. <https://doi.org/10.19084/RCA18122>.
- Dias, B.A.R.H., Udayakumara, E.P.N., Jayawardana, J.M.C.K., Malavipathirana, S., Dissanayake, D.A.T.W.K., 2019. Assessment of soil erosion in Uma Oya catchment, Sri Lanka. *J. Environ. Prof. Sri Lanka* 8, 39–51. <https://doi.org/10.4038/jepsl.v8i1.7875>.
- Eduardo, E.N., de Carvalho, D.F., Machado, R.L., Soares, P.F.C., de Almeida, W.S., 2013. Erodibilidade, fatores cobertura e manejo e práticas conservacionistas em argissolo vermelho-amarelo, sob condições de chuva natural. *Rev. Bras. Cienc. do Solo* 37, 796–803. <https://doi.org/10.1590/S0100-068320130003000026>.
- ENVIRONMENTAL SYSTEMS RESEARCH INSTITUTE - ESRI, 2014. ArcGIS 10.3 software. <http://www.esri.com/software/arcgis>.
- Estrada-Carmona, N., Harper, E.B., DeClerck, F., Fremier, A.K., 2017. Quantifying model uncertainty to improve watershed-level ecosystem service quantification: A global sensitivity analysis of the RUSLE. *Int. J. Biodivers. Sci. Ecosyst. Serv. Manag.* 13, 40–50. <https://doi.org/10.1080/21513732.2016.1237383>.
- FAO, 2014. World reference base for soil resources 2014. International soil classification system for naming soils and creating legends for soil maps, World Soil Resources Reports No. 106.
- Farr, T.G., Rosen, P.A., Caro, E., Crippen, R., Duren, R., Hensley, S., Kobrick, M., Paller, M., Rodriguez, E., Roth, L., Seal, D., Shaffer, S., Shimada, J., Umland, J., Werner, M., Oskin, M., Burbank, D., Alsdorf, D.E., 2007. The shuttle radar topography mission: *Reviews of Geophys.*, 45. RG2004 45, 1–13. <https://doi.org/https://doi.org/10.1029/2005RG000183>.
- Fayas, C.M., Abeysingha, N.S., Nirmanee, K.G.S., Samaratunga, D., Mallawatantri, A., 2019. Soil loss estimation using rusle model to prioritize erosion control in KELANI river basin in Sri Lanka. *Int. Soil Water Conserv. Res.* 7, 130–137. <https://doi.org/10.1016/j.iswcr.2019.01.003>.
- Foster, G.R., McCool, D.K., Renard, K.G., Moldenhauer, W.C., 1981. Conversion of the universal soil loss equation to SI metric units. *J. Soil. Water Conserv.* 36, 355–359.
- Fu, G., Chen, S., McCool, D.K., 2006. Modeling the impacts of no-till practice on soil erosion and sediment yield with RUSLE, SEDD, and ArcView GIS. *Soil Tillage Res.* 85, 38–49. <https://doi.org/10.1016/j.still.2004.11.009>.
- Galdino, S., Sano, E.E., Andrade, R.G., Grego, C.R., Nogueira, S.F., Bragantini, C., Flosi, A.H.G., 2016. Large-scale modeling of soil erosion with RUSLE for conservationist planning of degraded cultivated Brazilian Pastures. *L. Degrad. Dev.* 27, 773–784. <https://doi.org/10.1002/ldr.2414>.

- Ganasri, B.P., Ramesh, H., 2016. Assessment of soil erosion by RUSLE model using remote sensing and GIS - A case study of Nethravathi Basin. *Geosci. Front.* 7, 953–961. <https://doi.org/10.1016/j.gsf.2015.10.007>.
- Gelagay, H.S., Minale, A.S., 2016. Soil loss estimation using GIS and remote sensing techniques: A case of Koga watershed, Northwestern Ethiopia. *Int. Soil Water Conserv. Res.* 4, 126–136. <https://doi.org/10.1016/j.iswcr.2016.01.002>.
- Gomes, L., Simões, S.J.C., Forti, M.C., Ometto, J.P.H.B., Nora, E.L.D., 2017. Using geotechnology to estimate annual soil loss rate in the Brazilian Cerrado. *J. Geogr. Inf. Syst.* 9, 420–439. <https://doi.org/10.4236/jgis.2017.94026>.
- Hamel, P., Chaplin-Kramer, R., Sim, S., Mueller, C., 2015. A new approach to modeling the sediment retention service (InVEST 3.0): Case study of the Cape Fear catchment, North Carolina, USA. *Sci. Total Environ.* 524–525, 166–177. <https://doi.org/10.1016/j.scitotenv.2015.04.027>.
- Jarvis, A., Reuter, H.I., Nelson, A., Guevara, E., others, 2008. Hole-filled SRTM for the globe Version 4, available from the CGIAR-CSI SRTM 90 m Database: <http://srtm.csi.cgiar.org>.
- RColorBrewer, S., Liaw, M.A., 2018. Package ‘randomForest.’ Univ. California, Berkeley Berkeley, CA, USA.
- Liaw, A., Wiener, M., 2002. Classification and Regression by randomForest. *R News* 2, 18–22.
- Luo, M., Tang, G., Dong, Y., 2008. Uncertainty of flow accumulation threshold influence in hydrology modeling-A case study in Qinling Mountain SRTM3 DEM based, in: *International Workshop on Education Technology and Training & International Workshop on Geoscience and Remote Sensing*. pp. 219–222.
- Souza, C., Azevedo, T., 2017. MapBiomass General “Handbook”: Algorithm: Theoretical Basis Document (ATBD).
- Marques, J., Curi, N., Ferreira, M.M., Lima, J.M., Silva, M., Carolino, M., 1997. Adequação de métodos indiretos para estimativa da erodibilidade de solos com horizonte B textural no Brasil. *Rev. Bras. Ciência do Solo* 21, 447–456. <https://doi.org/10.1590/S0100-06831997000300014>.
- Martins, S.G., Avanzi, C., Silva, M.L.N., Curi, N., Fonseca, S., 2011. Erodibilidade do solo nos Tabuleiros costeiros. *Pesqui. Agropecu. Trop.* 41, 322–327. <https://doi.org/10.5216/pat.v41i3.9604>.
- Mello, C.R., Viola, M.R., Beskow, S., Norton, L.D., 2013. Multivariate models for annual rainfall erosivity in Brazil. *Geoderma* 202–203, 88–102. <https://doi.org/10.1016/j.geoderma.2013.03.009>.
- Moriasi, D.N., Arnold, J.G., Liew, M.W. V., Bingner, R.L., Harmel, R.D., Veith, T.L., 2007. Model evaluation guidelines for systematic quantification of accuracy in watershed simulations. *Am. Soc. Agric. Biol. Eng.* 50, 885–900.
- Nachtigall, S.D., Nunes, M.C.M., Moura-Bueno, J.M., Lima, C.L.R. de, Miguel, P., Beskow, S., Silva, T.P., 2020. Modelagem espacial da erosão hídrica do solo associada à sazonalidade agroclimática na região sul do Rio Grande do Sul, Brasil. *Eng. Sanitária e Ambient.* 25, 933–946. <https://doi.org/10.1590/s1413-4152202020190136>.

- Nearing, M.A., Yin, S., Borrelli, P., Polyakov, V.O., 2017. Rainfall erosivity: an historical review. *Catena* 157, 357–362. <https://doi.org/10.1016/j.catena.2017.06.004>.
- Oliveira Junior, R.C. de, 1996. Índice de erosividade das chuvas na região de Conceição do Araguaia, Pará, EMBRAPA-CPATU. Boletim de Pesquisa, Número 165. Empresa Brasileira de Pesquisa Agropecuária. Centro de Pesquisa Agroflorestal da Amazônia Oriental. Ministério da Agricultura e do Abastecimento.
- Oliveira, N.G., Vieira, C. V., 2017. Soil loss estimate in the Cubatão do norte river hydrographic basin , northeast of Santa Catarina , Brazil. *Int. J. Dev. Res.* 07, 13887–13895.
- Oliveira, P.T.S., Nearing, M.A., Wendland, E., 2015. Orders of magnitude increase in soil erosion associated with land use change from native to cultivated vegetation in a Brazilian savannah environment. *Earth Surf. Process. Landforms* 40, 1524–1532. <https://doi.org/10.1002/esp.3738>.
- Oliveira, P.T.S., Wendland, E., Nearing, M.A., 2012. Rainfall erosivity in Brazil: A review. *Catena* 100, 139–147. <https://doi.org/10.1016/j.catena.2012.08.006>.
- Ostovari, Y., Ghorbani-Dashtaki, S., Bahrami, H.-A., Naderi, M., Dematte, J.A.M., 2017. Soil loss estimation using RUSLE model, GIS and remote sensing techniques: A case study from the Dembecha watershed, Northwestern Ethiopia. *Geoderma Reg.* 11, 28–36. <https://doi.org/10.1016/j.geodrs.2017.06.003>.
- Paul, S.S., Li, J., Li, Y., Shen, L., 2019. Assessing land use–land cover change and soil erosion potential using a combined approach through remote sensing, RUSLE and random forest algorithm. *Geocarto Int.* 1–15. <https://doi.org/10.1080/10106049.2019.1614099>.
- Posse Junior, E., Manz, R.E., 2020. Relatório de operação das estações Hidrométricas da 1ª campanha de campo de 2020 UHE Peixe Angical - TO.
- Projeto MapBiomass, 2020. Coleção 4.1 da Série Anual de Mapas de Cobertura e Uso de Solo do Brasil. Proj. MapBiomass.
- Quinn, P., Beven, K., Chevallier, P., Planchon, O., 1991. The prediction of hillslope flow paths for distributed hydrological modelling using digital terrain models. *Hydrol. Process.* 5, 59–79. <https://doi.org/10.1002/hyp.3360050106>.
- R Core Team, 2020. R: A language and environment for statistical computing.
- RadamBrasil, P., 1983. Folha SE. 22 Goiânia, Rio de Janeiro: Ministério das Minas e Energia. 768p.
- RadamBrasil, P., 1982. Folha SD. 23: Brasília, Rio de Janeiro: Ministério das Minas e Energia. 660p.
- RadamBrasil, P., 1981a. Folha SC. 22 Tocantins, Rio de Janeiro: Ministério das Minas e Energia. 524p.
- RadamBrasil, P., 1981b. FOLHA SD. 22 Goiás, Rio de Janeiro: Ministério das Minas e Energia. 640p.
- Renard, K.G., Foster, G.R., Weesies, G.A., McCool, D.K., Yoder, D.C., 1997. Predicting soil erosion by water: A guide to conservation planning with the Revised Universal Soil Loss Equation (RUSLE), Agriculture Handbook Number 703.

- SAGA, G.I.S., 2013. System for automated geoscientific analyses. Available www.saga-gis.org/en/index.html.
- Salis, H.H.C. de, Costa, A.M. da, Viana, J.H.M., 2019. Estimativa da perda anual de solos na bacia hidrográfica do córrego Marinheiro, Sete Lagoas – MG, por meio da RUSLE. *Bol. Geogr.* 37, 101–115. <https://doi.org/10.4025/bolgeogr.v37i1.37213>.
- Sano, S.M., Almeida, S.P. de, 1998. Cerrado: ambiente e flora.
- Santos, H.G. dos, Jacomine, P.K.T., Dos Anjos, L.H.C., De Oliveira, V.A., Lumbrreras, J.F., Coelho, M.R., Almeida, J.A. de, Araujo Filho, J.C. de, Oliveira, J.B. de, Cunha, T.J.F., 2018. Sistema brasileiro de classificação de solos. Brasília, DF: Embrapa, 2018.
- Sharp, R., Tallis, H.T., Ricketts, T., Guerry, A.D., Wood, S.A., Chaplin-Kramer, R., Nelson, E., Ennaanay, D., Wolny, S., Olwero, N., others, 2014. InVEST user's guide. Nat. Cap. Proj. Stanford.
- Silva, A.M. da, Silva, M.L.N., Curi, N., Avanzi, J.C., Ferreira, M.M., 2009. Erosividade da chuva e erodibilidade de Cambissolo e Latossolo na região de Lavras, sul de Minas Gerais. *Rev. Bras. Ciência do Solo* 33, 1811–1820. <https://doi.org/10.1590/S0100-06832009000600029>.
- Silva, M.A. da, Silva, M.L.N., Curi, N., Oliveira, A.H., Avanzi, J.C., Norton, L.D., 2014. Water erosion risk prediction in eucalyptus plantations. *Ciência e Agrotecnologia* 38, 160–172. <https://doi.org/10.1590/S1413-70542014000200007>.
- Silva, M.L.N., Curi, N., Lima, J.M. de, Ferreora, M.M., 2000. Avaliação de métodos indiretos de determinação da erodibilidade de Latossolos brasileiros. *Pesqui. Agropecuária Bras.* 35, 1207–1220. <https://doi.org/10.1590/S0100-204X2000000600018>.
- Silva, M.L.N., Freitas, P.L., Blancaneaux, P., Curi, N., Lima, J.M., 1997. Relação entre parâmetros da chuva e perdas de solo e determinação da erodibilidade de um Latossolo Vermelho-Escuro em Goiânia (GO). *Rev. Bras. Ciência do Solo* 21, 131–137.
- Souza Jr., C.M., Shimbo, J.Z., Rosa, M.R., Parente, L.L., Alencar, A.A., Rudorff, B.F.T., Hasenack, H., Matsumoto, M., Ferreira, L.G., Souza-Filho, P.W.M., Oliveira, S.W. de, Rocha, W.F., Fonseca, A. V., Marques, C.B., Diniz, C.G., Costa, D., Monteiro, D., Rosa, E.R., Vélez-Martin, E., Weber, E.J., Lenti, F.E.B., Paternost, F.F., Pareyn, F.G.C., Siqueira, J. V., Viera, J.L., Ferreira Neto, L.C., Saraiva, M.M., Sales, M.H., Salgado, M.P.G., Vasconcelos, R., Galano, S., Mesquita, V. V., Azevedo, T., 2020. Reconstructing three decades of land use and land cover changes in Brazilian Biomes with landsat archive and Earth Engine. *Remote Sens.* 12, 2735. <https://doi.org/10.3390/RS12172735>.
- Steinmetz, A.A., Cassalho, F., Caldeira, T.L., Oliveira, V.A. de, Beskow, S., Timm, L.C., 2018. Assessment of soil loss vulnerability in data-scarce watersheds in southern Brazil. *Ciência & Agrotecnologia* 42, 575–587. <https://doi.org/10.1590/1413-70542018426022818>.
- Vigiak, O., Borselli, L., Newham, L.T.H., McInnes, J., Roberts, A.M., 2012. Comparison of conceptual landscape metrics to define hillslope-scale sediment delivery ratio. *Geomorphology* 138, 74–88. <https://doi.org/10.1016/j.geomorph.2011.08.026>.
- Vijith, H., Hurmain, A., Dodge-Wan, D., 2018. Impacts of land use changes and land cover alteration on soil erosion rates and vulnerability of tropical mountain ranges in Borneo.

- Remote Sens. Appl. Soc. Environ. 12, 57–69.
<https://doi.org/10.1016/j.rsase.2018.09.003>.
- Wang, L., Liu, H., 2006. An efficient method for identifying and filling surface depressions in digital elevation models for hydrologic analysis and modelling. *Int. J. Geogr. Inf. Sci.* 20, 193–213. <https://doi.org/10.1080/13658810500433453>.
- Wischmeier, W.H., Smith, D.D., 1978. Predicting rainfall erosion losses: A guide to conservation planning, Agriculture Handbook Number 537.
- Zambrano-Bigiarini, M., 2020. Package ‘hydroGOF.’
- Zerihun, M., Mohammedyasin, M.S., Sewnet, D., Adem, A.A., Lakew, M., 2018. Assessment of soil erosion using RUSLE, GIS and remote sensing in NW Ethiopia. *Geoderma Reg.* 12, 83–90. <https://doi.org/10.1016/j.geodrs.2018.01.002>.
- Zhou, M., Deng, J., Lin, Y., Belete, M., Wang, K., Comber, A., Huang, L., Gan, M., 2019. Identifying the effects of land use change on sediment export: Integrating sediment source and sediment delivery in the Qiantang River Basin, China. *Sci. Total Environ.* 686, 38–49. <https://doi.org/10.1016/j.scitotenv.2019.05.336>.

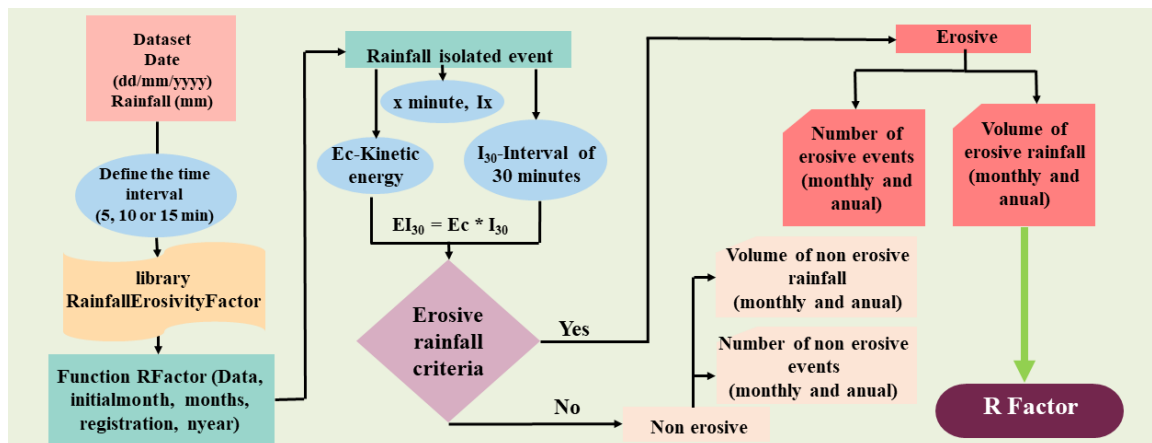
APPENDICES

Article I

Highlights

- Rainfall erosivity is used worldwide for estimating soil erosion rates.
- Rainfall data analysis for environmental modeling requires up-to-date tools.
- An R package, available at CRAN, was developed to compute rainfall erosivity.
- Monthly, annual, and average rainfall erosivity are presented as outputs.
- This user-friendly package is an advance in the area of soil conservation.

Graphical abstract

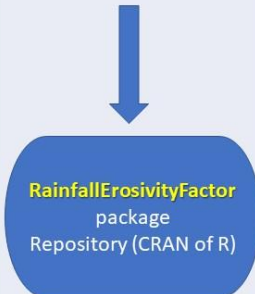


Article II

Highlights

- The rainfall erosivity is the product of the kinetic energy of rainfall by its maximum intensity in 30 minutes.
- Select a method identical to the Wischmeier and Smith, when rainfall data obtained by pluviographs are not available.
- An innovative technique in soil science to compare rain erosivity results called AMMI
- The methods evaluated showed similar behavior to the standard method of the Wischmeier and Smith.

Graphical abstract

E ₃₀ or R Factor			
Determination Methods	Estimation Methods	Application	Conclusion
<p>1. WS (Wischmeier and Smith, 1978)</p>  <p>RainfallErosivityFactor package Repository (CRAN of R)</p>	<p>2. MF (Arnoldus, 1980)</p> <p>3. MF-Z (Zhang et al., 2002)</p> <p>4. MF-M (Men et al., 2008)</p> <p>5. RD (Silveira, 2000)</p> <p>6. TRMM-F (Equation adjusted for Pirassununga-SP, Pm)</p> <p>7. TRMM-M (Equation adjusted for Pirassununga-SP, p)</p>	<p>1° - AMMI model (Innovation in Soil Science) Stability Program</p> <p>2° - Groupings (Scott & Knott, 1974) Mapgen program (Ferreira and Zambalde, 1997)</p>	<p>WS ≈ MF</p> <p>MF-M (underestimated)</p> <p>MF-Z (overestimated)</p> <p>Viable alternatives for locations without a weather station TRMM-F and TRMM-M</p>

Article III

Highlights

- Soil erosion and sediment exports threaten waterways and reservoirs.
- Soil erosion modelling was achieved via RUSLE, and spatially analyzed using GIS.
- Machine learning algorithm, Random Forest, was used to assess RUSLE factors.
- The level of importance of RUSLE factors was $C > K > LS > R$.
- Erosion in the basin increased over the years as changes in land use occurred.

Graphical abstract

